***Modeling Field-level Irrigation Demands with Changing Weather and Crop Choices***

By



Babak Mardan Doost

Submitted to the graduate degree program in Civil & Environmental and Architectural Engineering and the Graduate Faculty of the University of Kansas in partial fulfillment of the requirements for the degree of Master of Science

_____

Chairperson: Belinda S.M. Sturm

_____

Andrea E. Brookfield

_____

C. Bryan Young

Date Defended: January 30 2015

The Thesis Committee for Babak Mardan Doost

certifies that this is the approved version of the following thesis:

***Modeling Field-level Irrigation Demands with Changing Weather and Crop Choices***

_____

Chairperson: Belinda S.M. Sturm

Date approved: January 30 2015

## Abstract

The Kansas economy and way of life depend on groundwater reservoirs, specifically the High Plains Aquifer. However, long-term economic stability of the state will be jeopardized by unsustainable water withdraws. Modeling water demand is vital to developing sustainable water use policies that will be robust to water scarcity and climatic fluctuations. Additionally, developing a reliable water demand prediction model is a precursor for an integrated sustainable water resource management plan. The presented water budget model is capable of estimate daily water demand over space and time under predicted climate and land-use change. The model-predicted irrigation demand was developed based on crop-specific evapotranspiration, weather data, and with 2007 State-Wide Land Use and Land Cover data. In addition, two coupled sub-models have been developed: 1) a global climate change sub-model, and 2) a feasible pumping rate sub-model, which considers the spatial dynamics of the saturated thickness of the High Plains Aquifer.

The water budget model was calibrated to 1217 fields with reported water use extracted from the Kansas Water Right System (WRIS). In the 4544 water groups, predicted water use matched historic reported water use with a slope of 0.79 and $r^2$ value of 0.55.

The decadal-averaged monthly output of 21 global climate change models (Intergovernmental Panel on Climate Change AB1 scenario) was examined for south west Kansas. It was shown that the growthing season decreases by 20, 25, 30 days for sorghum, soybean, and winter wheat, respectively. Also, it was shown that evapotranspiration from soybean and sorghum fields will increase by .5 and 1.5 mm per day in peak time, whereas it will decrease by 1.5 mm less water for winter wheat per day in peak time between 2090 and 2100.

*To my wife, and beloved daughter*

**Acknowledgements**

This research is a part of the Kansas EPSCoR team Biofuels and Climate Change: Farmers' Land Use Decision (BAAC:FLUD) and was funded in part by the National Science Foundation EPSCoR grant #09030806: PI Dr. Dietrich Earnhart.

I would like to acknowledge Dr. Belinda Sturm, for introducing me this topic, being very encouraging and a wonderful support all throughout the duration of my graduate studies and dissertation work; Dr. Johnnes Feddema, for his water budget model; Dr. Andrea Brookfield, for providing excellent knowledge and extending great support during my research; and Dr. Bryan Young, for his instruction in water hydrology throughout my time at KU.

Also I would like to thank Reuben Dermyer, for his previous work with the water budget model; Brownie Wilson, for helping understanding the WIMAS database , training me on his water right grouping tool, and extending help whenever needed during the course of this research. I thank Dr. Jude Kanstan, Dana Peterson, Kevin Dobs, Chiris Bishop, and Vijay Bravo for processing the extensive data layers needed in the research. Finally, thank you to Dr. Jason Bergtold, for converting the Water Budget spreadsheet to the Matlab code.

The Civil, Environmental & Architectural Engineering Department of the University of Kansas awarded me two scholarships that helped me and my family remain financially stable – thank you.

Gene Tuel, thank you for being my first & best international friend in the United States, making my stay at KU memorable and being a wonderful support.

# TABLE OF CONTENTS

Abstract ..... iii

Acknowledgements ..... v

Chapter 1 : Introduction ..... 1

Chapter 2 Background ..... 3

2-1 Purpose of Project and Approach ..... 3

2-2 Geographic Setting ..... 5

2-3 General Climate ..... 6

2-4 Kansas Water Law and Water Use Reporting in Kansas ..... 7

2-5 The High Plains Aquifer and Kansas ..... 8

Chapter 3 Water Budget Model and Data Collection Methodology ..... 14

3-1 The Water Budget Model ..... 14

3-2 Calculation of Yield for High Plains Wells (pumping rate) ..... 22

3-3 Input Data ..... 26

3-4 Output of The Model ..... 30

3-5 Simulating Future Climate Change Projections ..... 32

3-6 Data Sources and Collection Methodology ..... 35

Chapter 4 : Model Validation ..... 47

4-1 Accuracy and Robustness of The Water Budget Model (Sensitivity analysis) ..... 47

4-2 Model Calibration and Validation ..... 49

4-3 Model Performance ..... 52

4-4 Coupling Water Budget with Climate Change Effect ..... 60

4-5 Discussion of Results ..... 69

4-6 Recommendations ..... 76

Appendix ..... 84

Appendix A: Weather Datasets Comparisons ..... 85

Appendix B: Seasonal Trends in Air Temperature and Precipitation in IPCC AR4 GCM Output for Kansas ..... 90

Appendix C Weather Extraction R Code: ..... 93

Appendix D Schematic of data preparation by water grouping tool ..... 96

# List of Tables

Table 3-1 Crops' base, and peck temperatures growth stages based on growing degree day ..... 20

Table 3-2 Polynomial equation of scaled crop coefficient ..... 21

Table 3-3 Number of fields based on geographic distribution and number per crop- KARS LULC training dataset ..... 40

Table 4-1 Initial and final values of the calibration parameters, plus possible ranges Where applicable ..... 48

Table 4-2 Effect of puming rate on the mean ratio( performance ratio) of GMDs. Averages and Standard Deviations (STD) are shown for all counties within each GMD..... 60

# List of Figures

Figure 2-1 Factors driving irrigation (Peterson, 2014) ..... 4

Figure 2-2 The state of Kansas and USDA NASS Agricultural Statistics District (ASD) boundary map along with its county boundaries with lighter color (Brian D Wardlow, 2007) ..... 6

Figure 2-3 Normal Annual Precipitation (Douglas G. Goodin, 1995) ..... 7

Figure 2-4 The High Plains aquifer cumulative depletion between 1900 and 2008 (Konikow, 2013) ..... 10

Figure 2-5 Water level changes in High Plains Aquifer from predevelopment through 2007 (Konikow, 2013) ..... 11

Figure 2-6 High Plains Aquifer and Groundwater Management Districts (GMDs) (Perry, 2006) ..... 12

Figure 3-1 Model Diagram ..... 15

Figure 3-4 Relationship between Well Yield and Saturated Thickness for Two Hydraulic Conductivity Values..... 25

Figure 3-5 Spatial Coverage of HPRCC stations, NARR, PRISM grid ..... 27

Figure 3-6 Probability distribution functions (PDF) of maximum and minimum temperature for PRISM, NARR, and HPRCC datasets for Ellis ..... 28

Figure 3-7 Hydrological Soil Group Map (Bruce M. McEnroe, 2003) ..... 37

Figure 3-8 Percentage of water from ground or surface water sources by county in 2000 (Sophocleous et al., 2000c) ..... 41

Figure 3-9 Percentage of water-use for each county in 2007; larger circles mean a larger quantity of water- use (Dermyer, 2011) ..... 41

Figure 3-10 Location of Wizard Wells ..... 44

Figure 3-11 Pumping rates based on the BACC:FLUD Survey Result ..... 46

Figure 4-1 Sensitivity Analysis of selected parameter for ASD 2010 Corn Fields ..... 49

Figure 4-2 Crop-specific Performance Ratios distribution for each crop ..... 52

Figure 4-3 Correlation of Predicted Irrigation Demand to Actual Demand at the Field- ..... **Error! Bookmark not defined.**

Figure 4-4 Predicted to Actual Irrigation Ratio for corn-planted fields for each irrigation system (Ratio< 5) ..... 55

Figure 4-5 Predicted to Actual Irrigation Ratio for sorghum-planted fields for each irrigation system (Ratio< 5) ..... 55

Figure 4-6 Predicted to Actual Irrigation Ratio for Soybean-planted fields for each irrigation system (Ratio< 5) ..... 56

Figure 4-7 Predicted to Actual Irrigation Ratio for Winter Wheat-planted fields for each irrigation system (Ratio< 5) ..... 57

Figure 4-8 Predicted to Actual Irrigation Ratio for Alfalfa-planted fields for each irrigation system (Ratio< 5) ..... 57

Figure 4-9 Calculated Predicted to Actual Irrigation Ratios (using a fixed pumping rate of 600 GPM) ..... 59

Figure 4-10 Calculated Predicted to Actual Irrigation Ratios (using a 10-year mean allowable pumping rate) ..... 59

Figure 4-11 GMD boundary ..... 60

Figure 4-12 Probability distribution functions (PDF) of maximum and minimum temperature and precipitation for 10 synthetic time series generated from Lakin HPRCC weather station (Historical weather data) ..... 62
Figure 4-13 Effect of Climate change on the daily evapotranspiration, A1b IPCC Scenario (2090-2100) ..... 64
Figure 4-14 Change in the monthly reference evapotranspiration, using the A1b IPCC Scenario ..... 64
Figure 4-15 Potential Evapotranspiration of Sorghum for two weather datastes for Lakin, KS: A baseline average weather data from 1980 to 1990 and a climate change scenario for 2090 to 2100 ..... 66
Figure 4-16 Instantaneous Irrigation of Sorghum of Sorghum for two weather datastes for Lakin, KS: A baseline average weather data from 1980 to 1990 and a climate change scenario for 2090 to 2100 ..... 66
Figure 4-17 Potential Evapotranspiration of Soybean for two weather datastes for Lakin, KS: A baseline average weather data from 1980 to 1990 and a climate change scenario for 2090 to 2100 ..... 67
Figure 4-18 Instantaneous Irrigation of Soybean for two weather datastes for Lakin, KS: A baseline average weather data from 1980 to 1990 and a climate change scenario for 2090 to 2100 ..... 67
Figure 4-19 Potential Evapotranspiration of Winter Wheat for two weather datastes for Lakin, KS: A baseline average weather data from 1980 to 1990 and a climate change scenario for 2090 to 2100 ..... 68

Figure 4-20 Instantaneous Irrigation of Winter Wheat for two weather datastes for Lakin, KS: A baseline average weather data from 1980 to 1990 and a climate change scenario for 2090 to 2100 ..... 68

# Chapter 1 : Introduction

The goal of this study is to predict irrigation demands of primary crops for Kansas. A soil-water balance model, often referred to as water budget (WB), was developed to estimate the spatial and temporal irrigation demands of main crops for Kansas by incorporating a typical center pivot irrigation system module. The first version of the model was developed by Professor Johannes Feddema (University of Kansas) using the Hamon, Hargreaves-Samani, and Thornthwaite evapotranspiration equations for reference crops. A revised model was developed and calibrated by Reuben Dermyer (MS Civil Engineering 2012, University of Kansas). The revised model utilized the Hargreaves-Samani, Penman-Monteith evapotranspiration models and crop coefficients for 5 major Kansas crops: corn, soybean, winter wheat, sorghum, and alfalfa. However, the revised model required Microsoft Excel to run and was computationally limited for geospatial application. In this study, the model is expanded to consider the process of precipitation, surface runoff, soil-moisture storage, snowmelt, and evapotranspiration through use of GIS inputs into a combination of Matlab and R codes. The model is deterministic, one dimensional, and physically based.

Given the above context, the objective of this study is to test and validate a WB framework for predicting irrigation water demand in Kansas. The model is used to determine irrigation demands of the five major crops for the period of 2000 through 2010 for the study region (Kansas). These results are compared to historical irrigation records for model validation.

To determine what effect future climate change will have on irrigation demand in western Kansas, the model was run using select Intergovernmental Panel on Climate Change ’s (IPCC)

(2007) temperature and precipitation projections for the period 2010 through 2099 from the A1B scenario, mean multi-model ensembles for Kansas.

Before the results of model validation and climate change irrigation prediction are described, the literature background of the study will be presented in the context of groundwater resource vulnerability. The study was directed at improving the ability to predict the effect of various land-use and climate conditions on the water balance and water budget.

# Chapter 2 Background

## 2-1 Purpose of Project and Approach

The NSF-funded "Biofuels and Climate Change: Farmers' Land Use Decisions" (BACC: FLUD) project focused on Kansas farmers' decisions regarding crop production, and it studied farmers' responses and adaptations to climate change. A key priority for the project was developing a unified set of cross-disciplinary methods, qualitative and quantitative, for identifying the factors driving farmers' decisions (IPSR, 2012) (Mair et al., 2013).

Land use change often has been seen as a function of a selection of socioeconomic and biophysical variables that act as the so-called 'driving forces'(Verburg et al., 2004a). In agricultural economics, which deals with land usage, driving forces are divided into three groups: socio-economic, environmental drivers and proximate causes (land management variables such as distance to the market, as a proxy for transportation costs, and agro-climatic potential) (Brown et al., 2004; Serneels et al., 2001). Frequently, environmental factors do not 'drive' land use change directly. However, they can cause changes in crop productivity (e.g. through climate change), and they impact land use allocation choices (e.g. soil quality, water availability) (Verburg et al., 2004b). In the agricultural sector, irrigation is a very important factor that depends on many factors. Previous studies show that driving forces on irrigation are weather, irrigation technology, market incentives, policy incentives, and water availability (Dridi et al., 2005; Fraser et al., 2009; Peterson, 2014; White et al., 2013). The interplay of these factors in farmer irrigation choices is illustrated in Figure 2-1 (Peterson, 2014).

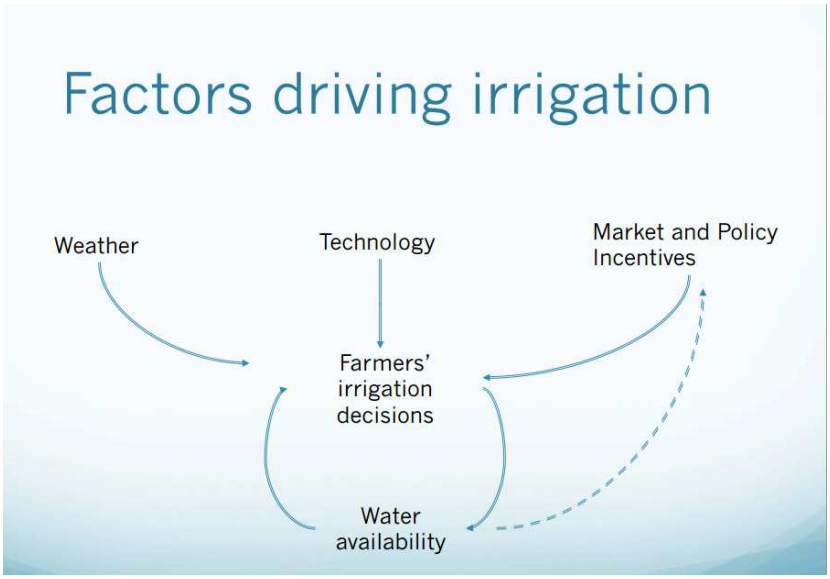


**Figure 2-1 Factors driving irrigation (Peterson, 2014)**

While some of these factors are beyond the control of the farmers, farmers can maximize the profit attainable from irrigated crops through manipulating irrigation systems, irrigation time, and amount of water used. Agricultural economists have typically captured the change in revenue by quantifying how crop yield responds to water use (Peterson et al., 2005). In order to estimate a production function, a crop yield is expressed as a function of total irrigation water used, actual or potential evapotranspiration, and soil deficit during the growing season (Hargreaves et al., 1984; Peterson & Ding, 2005). Likewise, understanding the interaction of climate, land use, and water availability in supporting responsible stewardship of natural resources will be valuable. The agricultural sector has already been confronted with manifold challenges of climate, population increase and bio-energy feedstock competition. Biofuel feedstock production in arable land competes with food production. Climate change imposes risk on agricultural production. Such a complex issue should be addressed by integrating future climate change into agriculture decision-making (Sik et al., 2014).

Models simulating plant-water-soil systems, such as the developed model and methodology described in this thesis, are a beneficial means to observe and understand the interrelationship between environmental and economic factors.

## 2-2 Geographic Setting

Kansas is located in the center of the continental United States and has a total area of 213,096 $km^2$. Kansas is located between the 37° to 40° north latitude and the 94°35′ to 102°3′ west longitude. The altitude varies from 207 meters to 1232 meters with a mean of 610 meters. The state is divided into 105 counties, and 9 agricultural districts (Brian D Wardlow, 2007). Figure 2-2 shows agricultural districts and counties (Brian D Wardlow, 2007).

The State is one of the nation's most productive agricultural states. It ranks first in the nation for wheat (*Triticum aestivum*) and sorghum grain (*Sorghum bicolor*) production. It ranks third regarding total land acreage in farms with 10.7 million hectares (ha), or 26.5 million acres equal to 46.9% of its total area (Brian D Wardlow, 2007). In addition to the state's best-known crops, a significant fraction of its cropland is planted to other summer crops including corn (*Zea mays*), soybeans (*Glycine max*), and alfalfa (*Medicago sativa*) (Brian D Wardlow, 2007; White & Selfa, 2013).

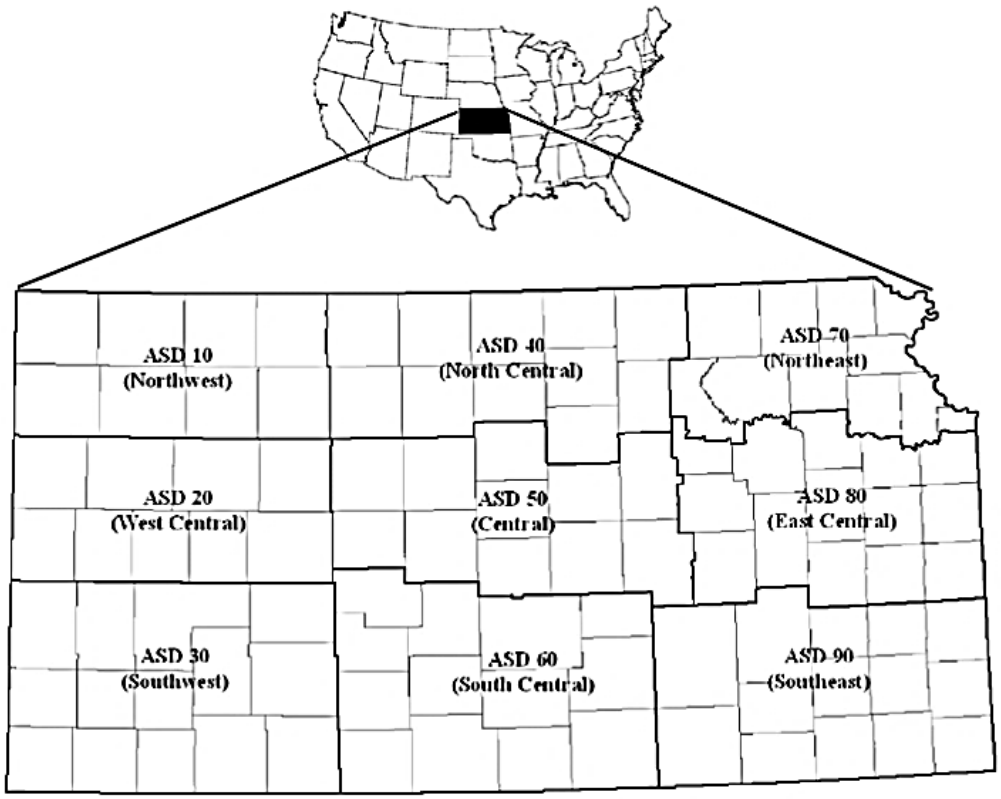


**Figure 2-2 The state of Kansas and USDA NASS Agricultural Statistics District (ASD) boundary map along with its county boundaries with lighter color (Brian D Wardlow, 2007)**

## 2-3 General Climate

The state has a noticeable east-west precipitation gradient. Temperate eastern Kansas receives approximately 1016 millimeters annual precipitation (40 inches) , wheras semi-arid western Kansas receives less than 508 millimeters (20 inches) per year (Brian D. Wardlow, 2006). Due to a transitional climate between the humid east and the semiarid and arid western portion of the continent, annual precipitation amounts along the western boundary are only one-third of those in the Southeast corner of the state. This precipitation variation is typical for the Great Plains region of central North America (Brian D. Wardlow, 2006; Douglas G. Goodin, 1995). The normal annual precipitation from 1961 to 1991 has been shown in Figure 2-3.

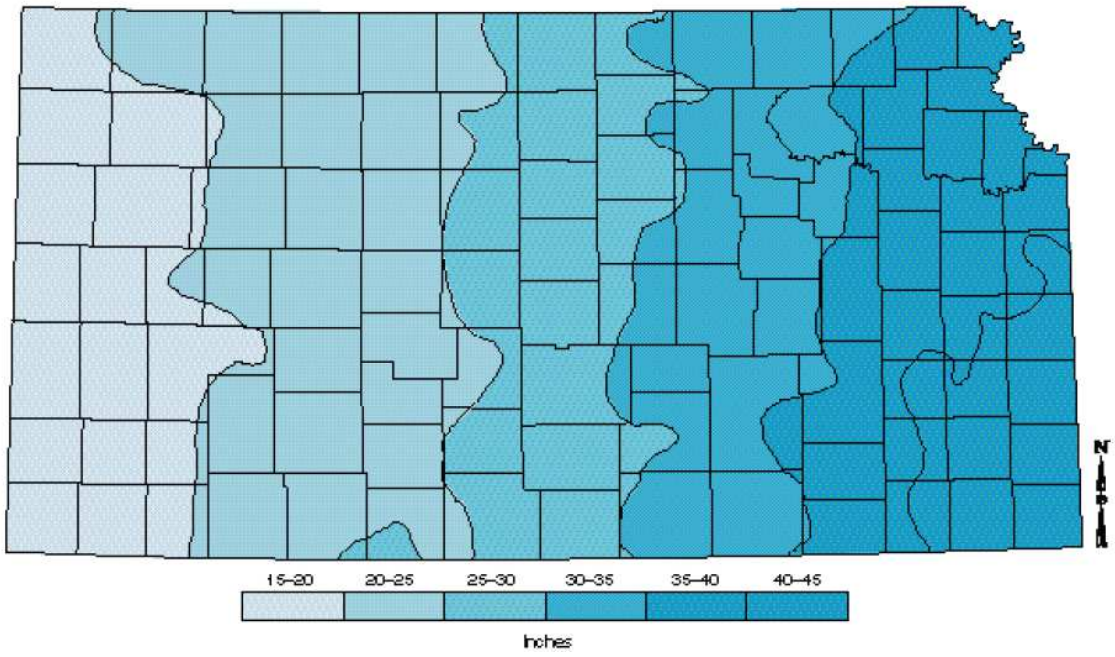


**Figure 2-3 Normal Annual Precipitation (Douglas G. Goodin, 1995)**

In addition to precipitation, temperature varies considerably over the course of a year. The annual mean temperature ranges from 58° F along the south-central and southeastern border to 52° F in the northwest. The coldest and hottest months of the year are January and July, with a mean of 30° F and 79° F, respectively. On average, the eastern and western counties have maximum daily temperatures equal or above 100° F for ten days each summer. In the central counties, the number of days with a maximum daily temperature equal or above 100° F on average is fifteen days per year (Flora, 1988).

## 2-4 Kansas Water Law and Water Use Reporting in Kansas

Detailed records regarding water rights and annual reported water use in Kansas are accessible to the public through the Water Information Management and Analysis System (WIMAS). Each year, the annual water use report is reviewed by the Division of Water Resources (DWR−the water rights regulatory organization in Kansas) and the Kansas Water

Office (KWO−the water planning organization in Kansas). Then, the reviewed report is jointly published. Using the WIMAS data set to compare allocated water to utilized water requires in-depth understanding of water law of Kansas because of the complexity in the definition of water rights in the state.

Generally, individual American states control the water resources in the interior of state borders (Peck, 2002). The arid conditions in Kansas resulted in a method of water allocation known as the *prior appropriation* doctrine, which was distinctive from the traditional *riparian* doctrine. From the time of the water law inception (1868) to now (2014), many aspects of Kansas water law have been modified (Danny H. Rogers, 2013). In chapter 3, more detail will be provided about how the WIMAS data set has been used.

## 2-5 The High Plains Aquifer and Kansas

In Kansas, irrigation, making up 79% of the total water-use annually, is supplied mostly from groundwater. Between Eastern and Western Kansas, the West depends largely on groundwater, due to lack of surface water resources and the semiarid climate (Sophocleous, 2005). West of the 25-inch precipitation line (Figure 2-3), surface water is often inadequate for irrigation supply, hence using irrigation systems that withdraw groundwater essential to plant grain crops (Douglas G. Goodin, 1995).The High Plains Aquifer (HPA) is the primary source of fresh water in the west and south-central part of Kansas (Buchanan et al., 2009; Sophocleous, 2005).

The HPA is the major freshwater aquifer in the USA and underlies portions of eight states from South Dakota to Texas (Dennehy et al., 2000; Gutentag et al., 1984). The Miocene–Pliocene Ogallala Formation, well-known as the Ogallala aquifer is the most widespread unit of

the HPA system (Sophocleous, 2005). Due to economic values of irrigated agriculture in the region, the Aquifer is an important regional economic driver (Dennehy et al., 2002). Roughly 30% of the irrigation-based groundwater uses withdraws from the HPA in the country (Sophocleous, 2005). 95% of the land lying on top of the aquifer is used for crop production or rangeland (U.S. Geological Survey, 2010). In total, the aquifer supports production of 15 percent of all grain crops in the USA including corn, wheat, cotton, and and 20 percent of cattle (Dennehy & US Geological Survey, 2000).

Due to using widespread large-scale irrigation systems through the region, water level in the HPA started declining around 1950 (McGuire, 2007, 2009), but the most dramatic depletion happened between 2001 and 2008. In a study conducted by USGS, it has been shown that 'the depletion during the last 8 years of record (2001–2008, inclusive) is about 32 percent of the cumulative depletion in this aquifer during the entire 20th century' (Konikow, 2013). The HPA's cumulative depletion between 1900 and 2008 is shown in **Error! Reference source not found.** (Konikow, 2013).

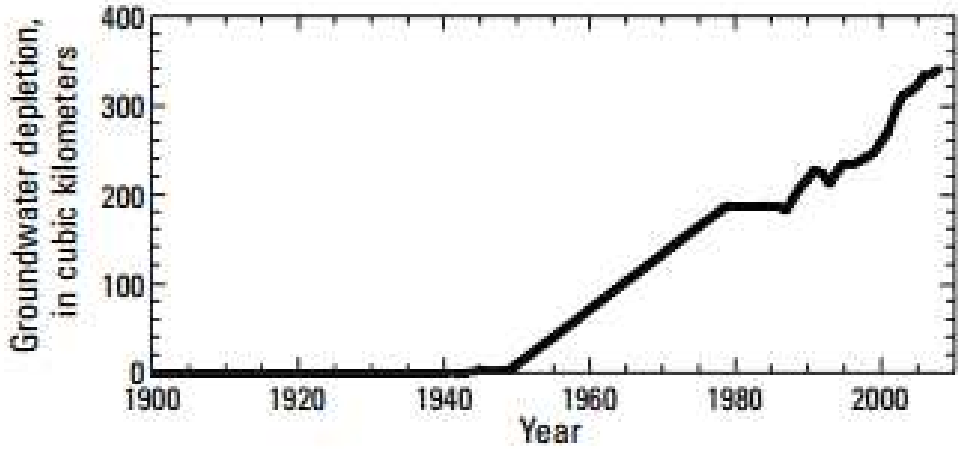


**Figure 2-4 The High Plains aquifer cumulative depletion between 1900 and 2008 (Konikow, 2013)**

In this study, the period prior to 1950 is called "predevelopment". Whereas severe drop in the water table has been seen in much of the aquifer, parts of Texas and Kansas have experienced the hardest impact (Buchanan et al., 2009). In Kansas, the most significant water loss has been in the Southwest corner with over a one hundred foot a drop in the water level (Buchanan et al., 2009). **Error! Reference source not found.Error! Reference source not found.** shows the HPA along with the change in water surface elevation from predevelopment through 2007 (Buchanan et al., 2009; McGuire, 2007, 2009).

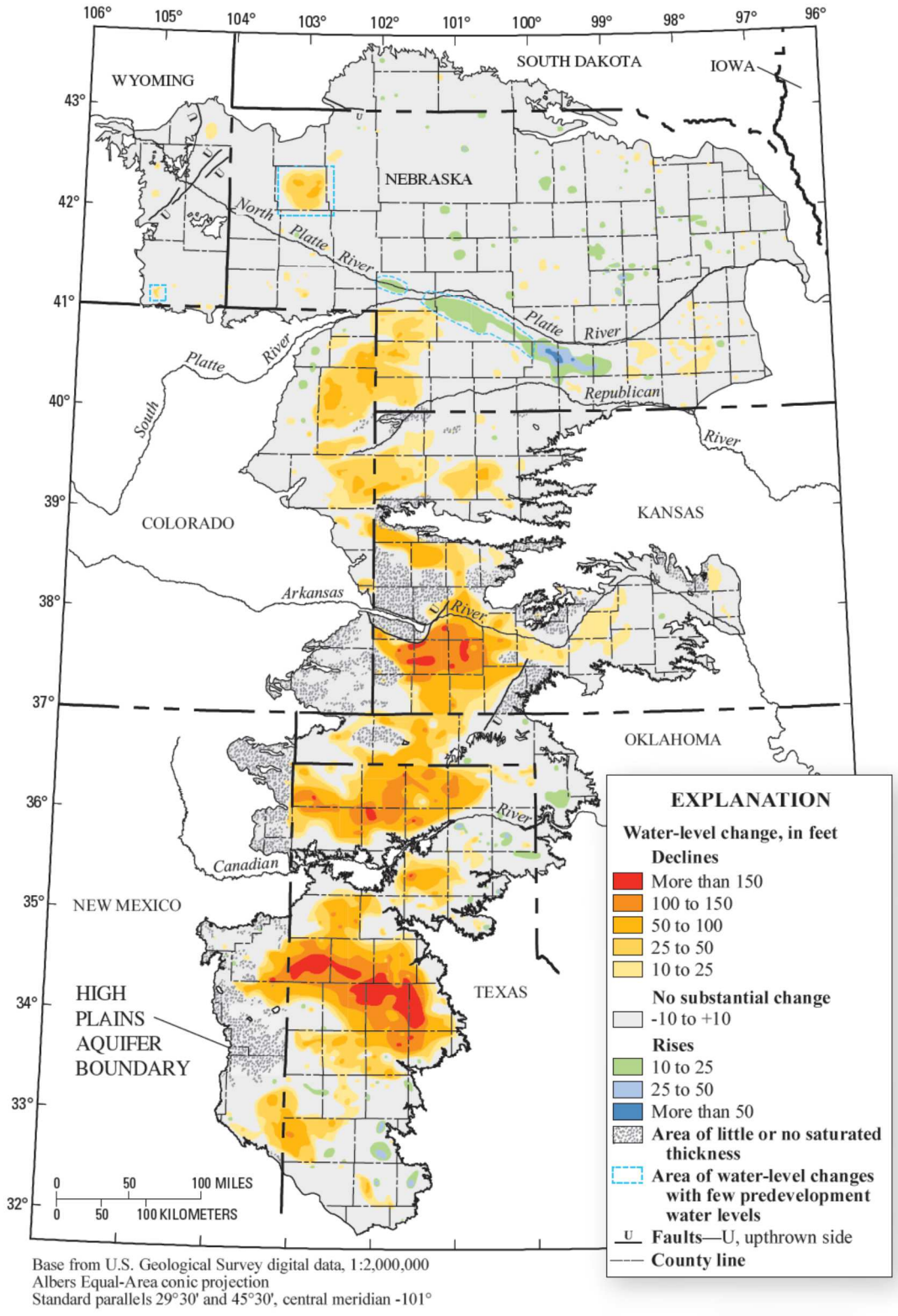


**Figure 2-5 Water level changes in High Plains Aquifer from predevelopment through 2007 (Konikow, 2013)**

Due to construction of too many wells between the 60's and 70's, and significant declines in the water table, a number of water management programs were announced in Kansas. The main objective of those water management programs was conserving the High Plain Aquifer water resource (Perry, 2006). Among them, the Groundwater Management District (GMD) Act was enacted by the Kansas legislature in 1970s (Perry, 2006). As a result of the GMD act, five GMDs covering most of the High Plains Aquifer in Kansas were established (Perry, 2006). In Figure 2-6, the High Plains aquifer, and Groundwater Management Districts (GMDs) are shown.

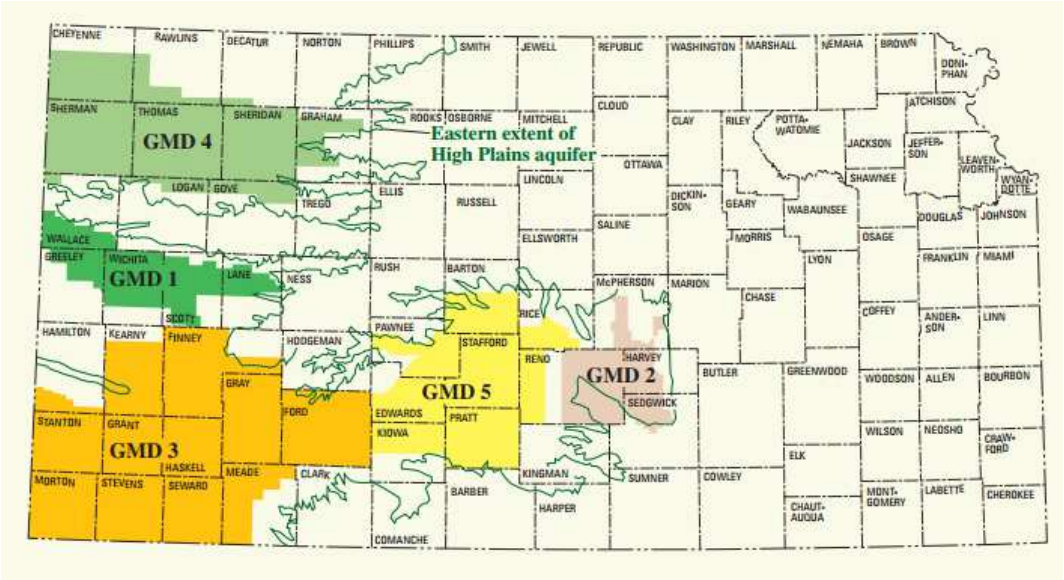


**Figure 2-6 High Plains Aquifer and Groundwater Management Districts (GMDs) (Perry, 2006)**

Because of the noticeable east-west precipitation gradient and rainfall variation discussed earlier, recharge rates of the Aquifer are limited to an inch or less each year in the western part of Kansas (Buchanan et al., 2009; Gutentag et al., 1984; Hansen, 1991; Sophocleous et al., 2000b). By definition, in any sustainable groundwater system, the discharge rate should be equal to the recharge rate. If the pumping volume of water (discharge) continuously surpasses the total amount recharged, the system in not sustainable and balanced.

Many studies have attempted to predict the usable life of the aquifer. In a recent study, the aquifer was predicted to be depleted by an estimated 69 percent by 2060 (Steward et al., 2013); however, the effect of excessive water withdrawals from the aquifer is not uniform. Based on another study conducted by KGS, parts of the southwest within GMD 3 boundary have enough irrigation water for another 50 to100 years, if water will be withdrawn with the current discharge rate. Whereas GMD 3 is stable, most parts of the GMD 1 aquifer, including Greely, Lane, Scott, and Wichita counties, will be depleted in less than 25 years (Buchanan et al., 2009). Tracking irrigation water demand spatially and temporally is critical.

# Chapter 3 Water Budget Model and Data Collection Methodology

## 3-1 The Water Budget Model

Water budget models were developed and used in 1957 by Thornthwaite and Mather in order to determine groundwater recharge (Alley, 1984). The original Thornthwaite-Mather model required minimal input parameters. A water budget used in this project was created by Dr. Johannes Feddema of the University of Kansas by incorporating Soil Conservation Service-Natural Resources Conservation Service (SCS-NRCS) surface runoff parameterization methodology, which is descried in the 3-1-1 section .

Theoretically, water in the system can be traced where the difference between the outflow and inflow is equal to change in storage. Inputs comprise precipitation, surface water inflow, and groundwater inflow. Outputs consist of evapotranspiration, runoff of surface water, groundwater withdrawals, and groundwater outflow. By breaking down into the most important terms, a mathematical form of the model can be described as:

$$\Delta S = P + I - ET - R$$

Where $\Delta S$ is change in soil storage is,$P$ is precipitation, $I$ is irrigation water,$ET$ is evapotranspiration and $R$ is runoff plus infiltration and groundwater recharge ($G_r$):

$$R = Runoff + Infilteration + G_r$$

The temporal scale of the model can vary from daily to multi-year scenarios, but it has been shown that a daily time step produces more accurate results (Allen, 2005). It has also been shown that a time step greater than 10 days produces large errors due to sensitivity of runoff and

infiltration to the antecedent soil moisture condition (Sophocleous et al., 2000a; Westenbroek et al., 2012). Therefore, daily time step has been chosen for the developed model. This model needs climate, land use, and soil input to calculate output variables. Based on the climate and land use a crop coefficient is calculated. The water balance estimates runoff and infiltration along with the snow/rain partition. In addition, the water balance also calculates soil moisture level, daily soil moisture deficit and surplus. Figure 3-1 shows model diagram.

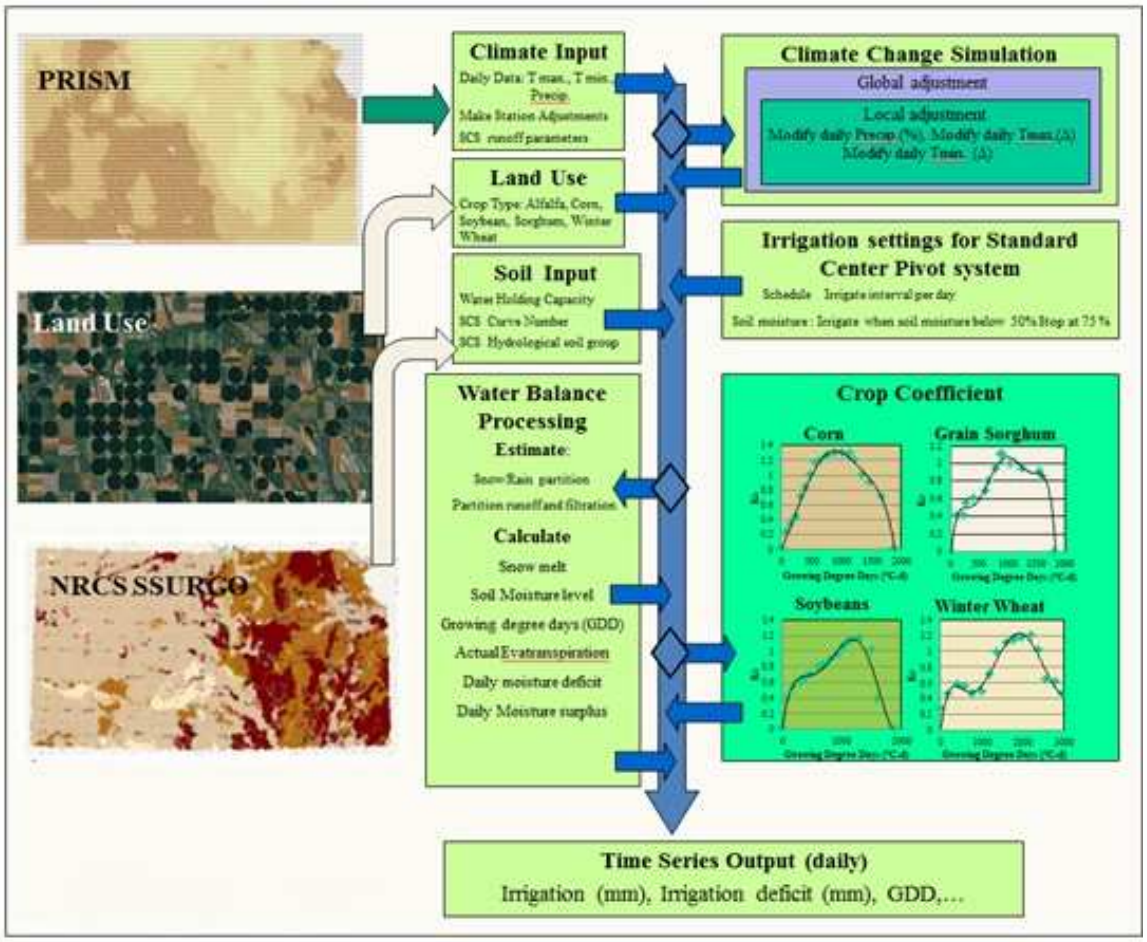


**Figure 3-1 Model Diagram**

In the following sections, the calculations illustrated in Figure 3-1will be fully described.

### 3-1-1 Snowmelt, Infiltration and Runoff

The form of precipitation, rain or snow, is defined by temperature data. A temperature-index approach is able to model daily accumulations of snow on the ground and snowmelt (Hock, 2003) .

Surface runoff is calculated for each snowmelt and precipitation according to the SCS-NRCS curve number approach (USDA-NRCS, 1986). In the SCS-NRCS curve number method, daily runoff is a function of the soil's infiltration capacity, antecedent soil moisture, and the land cover/usage. A soil's infiltration capacity is determined by the hydrologic soil group classification (A, B, C, and D), provided by the Soil Survey Geographic (SSURGO) Database. The antecedent soil moisture condition is a baseline for soil moisture. Pre-storm soil moisture has a large effect on runoff volume and rate. Antecedent soil moisture condition is defined based on total precipitation of the last five days before the rainfall event classified in three conditions; I, II, and III. According to the SCS-NRCS curve number method dry soil (above wilting point) is classified condition I whereas saturated soil is classified condition III. The condition II is for average condition. Runoff curve number values are for condition II. Given soil type and vegetation cover/land use, the equivalent curve number (condition II) is determined by tables provided by NRCS. According to land cover/usage, curve number 61, 73, 81, and 84 have been chosen for classes A, B, C, and D, respectively (USDA-NRCS, 1986).

In any precipitation event, surface runoff and infiltration are separated. Infiltration could partially or completely satisfy the maximum water holding capacity, whereas runoff exits the model domain. The maximum soil moisture is a function of water holding capacity and land cover for land soil type. In addition, the amount of groundwater recharge is calculated based on

retained water in the soil over the time step. The model only calculates recharge from precipitation events and not from surface water bodies.

The following formula shows the runoff calculation, where precipitation $P$ is in mm, $CN$ is the SCS curve number, $S$ is the potential maximum retention after runoff begins , and $I_a$ is the initial abstraction in mm

$$Runoff = \begin{cases} 0, & P \leq I_a \\ \frac{(P-I_a)^2}{P-I_a+S} & , P > I_a \end{cases}, I_a = .2S \ , S = \frac{1000}{CN} - 10$$

### 3-1-2 Evapotranspiration

Irrigation demand is a function of crop evapotranspiration. In order to calculate crop evapotranspiration, two key factors must be calculated: reference evapotranspiration and a crop-specific scaling factor. Several methods have been developed to convert reference evapotranspiration to actual evapotranspiration ($ET_C$) (Allen et al., 1998). The crop coefficient approach is one of them, and is used in this study.

Mathematically, crop evapotranspiration could be described as in the formula below, where $ET_0$ is potential evapotranspiration, and $K_c$ is a crop specific coefficient based on the growth stage of the crop (Allen, 2005; Allen et al., 1998; Piccinni et al., 2007).

$$ET_c = K_C * ET_0$$

### 3-1-3 Reference Evapotranspiration

Many methods have been developed for determining reference evapotranspiration, and they are classified in four groups: mass transfer (e.g. Harbeck, 1962), temperature-based

(Hamon,1963; Hargreaves and Sammani, 1982; Thronthwaite, 1957; Blaney and Criddle) , radiation-based (e.g. Priestly & Taylor, 1972), and combination type (e.g. Penman-Monteith, 1998) (Allen, 2005; Hamon, 1963; Howell et al., 2004; Jensen et al., 1990; Thornthwaite, 1948).

Among these methods, the Penman-Monteith method is widely used because of its comprehensive theoretical base and its accommodation of small time steps. However, the method needs many input data including air temperature, wind speed, relative humidity, and net radiations. On the other hand, the Hargreaves-Samani method uses a simpler approach and relies on fewer input data (minimum and maximum temperature, precipitation, latitude of location). The method determines reference evapotranspiration for a grass. The Hargreaves-Samani formula is shown below (Samani, 2000). $ET_0$ is reference evapotranspiration in mm/day, $T_{max}$ and $T_{min}$ are maximum and minimum daily temperatures in °C, and $R_\alpha$is extraterrestrial radiation in $MJ/m^2\ day$ or equivalent evaporated water depth (mm/day).

$$ET_0 = 0.0023(T_{max} - T_{min})^2\ (T_{mean} + 17.8)R_\alpha$$

Extraterrestrial radiation is a function of geographical latitude and day of the year.

$$R_\alpha = \frac{24}{\pi} 4.92 \left(1 + 0.033 \cos\frac{2\pi J}{365}\right)(\omega_s \sin\varphi \sin\delta + \cos\varphi \cos\delta \sin\omega_S)$$

$$\delta = 0.409\ sin\left(\frac{2\pi J}{365} - 1.39\right)$$

$$\omega_s = cos^{-1}(-tan\varphi\ tan\delta)$$

### 3-1-4 Crop Coefficient

In this study, the specific value of $K_c$ changed with the growth stage of the crop, which was quantified with the cumulative growing degree days (GDD) (Colaizzi et al., 2009; McMaster et al., 1997). In this method, crop maturation and harvesting time are determined by a certain accumulated GDDs. The mathematical formulation of daily GDD is shown below, where $i$ is day of year, $T_{Base}$ is the base temperature, which is a crop-specific number, $T_{Peak}$ is an upper limit for temperature for each crop. $T_{max,i}$ , and $T_{min,i}$ are the maximum and minimum daily temperatures.

$$GDD_i = \begin{cases} \dfrac{T_{max,i} + T_{min,i}}{2} - T_{base} & \begin{cases} if\ \dfrac{T_{max,i} + T_{min,i}}{2} > T_{base} \\ And\ T_{peak} > T_{max,i} \end{cases} \\ \dfrac{T_{peak} + T_{min,i}}{2} - T_{base} & \begin{cases} if\ \dfrac{T_{max,i} + T_{min,i}}{2} > T_{base} \\ And\ T_{peak} < T_{max,i} \end{cases} \\ 0 & if\ \dfrac{T_{max,i} + T_{min,i}}{2} < T_{base} \end{cases}$$

For any day with an average temperature less than $T_{Base}$, the daily GDD is zero, and no growing degree day accumulates. Also, any temperature above $T_{Peak}$ does not have any effect on crop maturation (McMaster & Wilhelm, 1997).

Table 3-1 shows $T_{Peak}$, $T_{Base}$, and minimum cumulative GDD at which irrigation is assumed to stop and harvesting can begin for all of the main crops in this study (Colaizzi et al., 2009). At minimum cumulative GDD, the crop is mature enough to harvest and irrigation is not needed after this point. All values have been taken from the previous study Dermyer (2011).

**Table 3-1 Crops' base, and peck temperatures growth stages based on growing degree day**

| | Corn | Sorghum | Soy | Winter Wheat | Alfalfa |
|---|---|---|---|---|---|
| **Start of Growing Season (Julian day of the year)** | April 10 (100) | April 25 (115) | May 5 (125) | September 15 (258) | April 10 (100) |
| **End of Growing Season (Julian day of the year)** | November 5 (304) | November 10 (309) | November 5 (304) | July 10 (191) | November 5 (300) |
| **Base Temperature, C ($T_{base}$)** | 10.0 | 10.0 | 7.8 | 0 | 4.4 |
| **Peak Temperature , C ($T_{peak}$)** | 30.0 | 37.8 | 30.0 | 26.1 | 25.0 |
| **GDD at termination of Irrigation** | 1530 | 1230 | 1780 | 2470 | 3120 |
| **GDD at harvest** | 1890 | 1830 | 1890 | 2970 | 3120 |

In order to estimate the crop coefficient as a function of growing degree day in the growing season, a polynomial equation of scaled crop coefficient was established in the previous study in the project, showed in Table 3-2 (Dermyer, 2011). To establish these equations, primary data of crop coefficients of three crops (corn, sorghum, and soybean) were obtained from the Bushland, Texas High Plains Evaporation network (Colaizzi et al., 2009) and scaled to the shorter growing season of Kansas. For alfalfa and winter wheat the primary data of crop coefficients were obtained from High Plain Reginal Climate Center (HPRCC). It should be noted that the equation for alfalfa is created for one cutting cycle, but it is very usual to cut alfalfa two or three times per growing season. In the model, the curve is repeated for two cycles. Because the crop coefficient of wheat and alfalfa were not available for a grass-based reference ET, they were scaled based on the following formula (Dermyer, 2011).

$$ET_c = K_r K_{C(alfalfa)} ET_0$$

Two coefficients, $K_{C(alfalfa)}$ , and $K_r$, should be used for converting alfalfa-reference to grass-reference. For winter wheat, $K_{C(alfalfa)}$ is 1.4 (Dermyer, 2011). The $K_r$ value varies between 1 and 1.5 based on location, time, and method. In this study, 1.35 for the growing season has been selected, based on previous studies (Dermyer, 2011).

Evaporation is a natural phenomenon, which is always occurring from all surfaces. In order to estimate evaporation from bare ground in the pre/post growing seasons, the reference ET was multiplied by 0.18, according to (Allen, 2000).

**Table 3-2 Polynomial equation of scaled crop coefficient**

| Crop | Equation ($K_{c,i}$) | $R^2$ |
|---|---|---|
| **Corn** | -1E-18 $GDD_i^6$+4E-15 $GDD_i^5$ -6E-12 $GDD_i^4$ +2E-08 $GDD_i^3$ +7E-08 $GDD_i^2$ +.002 $GDD_i$ | 0.9921 |
| **Sorghum** | -7E-18 $GDD_i^6$+4E-14 $GDD_i^5$ -7E-11 $GDD_i^4$ +7E-08 $GDD_i^3$ -3E-05 $GDD_i^2$ +.0064 $GDD_i$ | 0.9816 |
| **Soy** | -3E-15 $GDD_i^5$-1E-11 $GDD_i^4$ +2E-8 $GDD_i^3$ -2E-05 $GDD_i^2$ +.0054 $GDD_i$ | 0.9508 |
| **Winter Wheat** | 1E-18 $GDD_i^6$+4E-15 $GDD_i^5$ -6E-12 $GDD_i^4$ +2E-08 $GDD_i^3$ +7E-08 $GDD_i^2$ +.002 $GDD_i$ | 0.9159 |
| **Alfalfa** | -1E-19 $GDD_i^6$+1E-15 $GDD_i^5$ -6E-12 $GDD_i^4$ +1E-08 $GDD_i^3$ +1E-05 $GDD_i^2$ +.0042 $GDD_i$ | 0.9886 |

### 3-1-5 Irrigation Module:

The revised water budget model is capable of scheduling irrigation inputs based on soil moisture conditions. A maximum and feasible irrigation amount to be applied to the model domain (depth per time) can be determined by dividing pumping rate (volume per time) by the irrigated area (area). Center pivot irrigation is the dominant irrigation system in Kansas, comprising over 90 percent of all systems (Rogers et al., 2011). A typical center pivot system

can cover between 125 and 160 acres (Kranz et al., 2008; Rogers et al., 1997). In irrigation practice, only a fraction of the field's water holding capacity is allowed to deplete. This fraction can be described as an allowable range, so two input values are added to model: minimum and maximum soil moisture. The minimum value is a guide for when to irrigate, whereas the maximum value is when irrigation needs to stop. The specific values for minimum and maximum soil moisture were defined during model calibration. The final minimum and maximum soil moisture values are selected as 60 and 95 percent respectively. In addition, 600 gallons per minute is used as the pumping capacity.

If the daily irrigation demand is higher than the maximum irrigation rate calculated based on pump capacity, the maximum rate is applied as irrigated water. In Kansas, this is often the case during the peak of the summer, when the ET demand of a crop surpasses the ability to meet that demand. The model also is capable of simulating irrigation demand as needed, known here as "instantaneous irrigation.

## 3-2 Calculation of Yield for High Plains Wells (pumping rate)

The amount of water that can be withdrawn from a well per unit of time is known as 'well yield' (Hecox et al., 2002), and is a function of saturated thickness and hydraulic conductivity of the aquifer. Saturated thickness is defined as the difference between the bedrock of an aquifer and the water table elevation. The saturated thickness needed to sustain in a given pump rate is dependent upon geophysical properties, well construction and the local aquifer characteristics (e.g. transmissibility, and specific yield). In order to calculate the maximum well yield from a HPA irrigation well with a known saturated thickness, methodology is consistent with Hecox et al. (2002), who used (Hecox et al., 2002).

Drawdown for a single well can be calculated using the Cooper-Jacob (1946) equation, shown below:

$$S_{Aquifer} = \frac{Q}{4\pi T}\left[-.0572 - ln\left(\frac{r^2 S}{4Tt}\right)\right]$$

Where $S_{Aquifer}$ is aquifer drawdown, $T$ is transmissivity in $\frac{\text{ft}^2}{\text{day}}$, $Q$ is pumping rate in $Gpm$, $t$ is time of pumping in days, $S$ is specific yield, $r$ is effective well radius in $feet$.

When many wells are in close vicinity to each other, calculating well drawdown considering the effect of the other wells can be possible using a polynomial approximation. The following formula shows how calculation of yield could be possible:

$$u = \left(\frac{r^2 S}{4Tt}\right)$$

$$S_{Aquifer} = \frac{Q}{4\pi T}\begin{bmatrix} -.0572 - \ln(u) + 0.99999u - 0.24991055u^2 \\ +0.05519968u^3 - 0.00976004u^4 + 0.00107657u^5 \end{bmatrix}$$

Where u is Theis well function. Transmissivity is multiplcation of the hydraulic conductivity, $K$, in $\frac{ft}{day}$ , and saturated thickness, *B,* in foot. In order to determine pumping rate, two procedures have been developed. First, a polynomial equation that defines the relationship between saturated thickness and pumping rate has been for each county. Then, mean values of saturated thickness of the HPA have been calculated for each county within aquifer boundary between 2000 and 2010. Well yield is then calculated by applying the county-base mean values of saturated

thickness to the polynomial equations. The resultant mean values of allowable pumping rates (well yields) have been input into the water budget model.

### 3-2-1 Defining Relationship between Saturated Thickness And Pumping Rate:

For this project, aquifer physical properties including hydraulic conductivity and specific yield were calculated as a spatially-weighted county-level average using the ArcGIS zonal statistics toolbox. The distances to neighboring pumping wells and time of pumping were assumed to be 2500 feet and 90 days, respectively consistent with Hecox et al. (2002). For the drawdown calculation, it was assumed that a central well would be surrounded by 4 similar wells at an equal distance, also consistent with Hecox et al. (2002). By applying a range of pumping rates, aquifer drawdown has been calculated for each case. Then a polynomial equation, representative of the relationship between saturated thickness and the maximum allowable pumping rate w regressed for each county above the HPA. In the Figure 3-2, the relationship between saturated thickness and maximum allowable pumping rate (or well yield) for two hydraulic conductivities is shown.

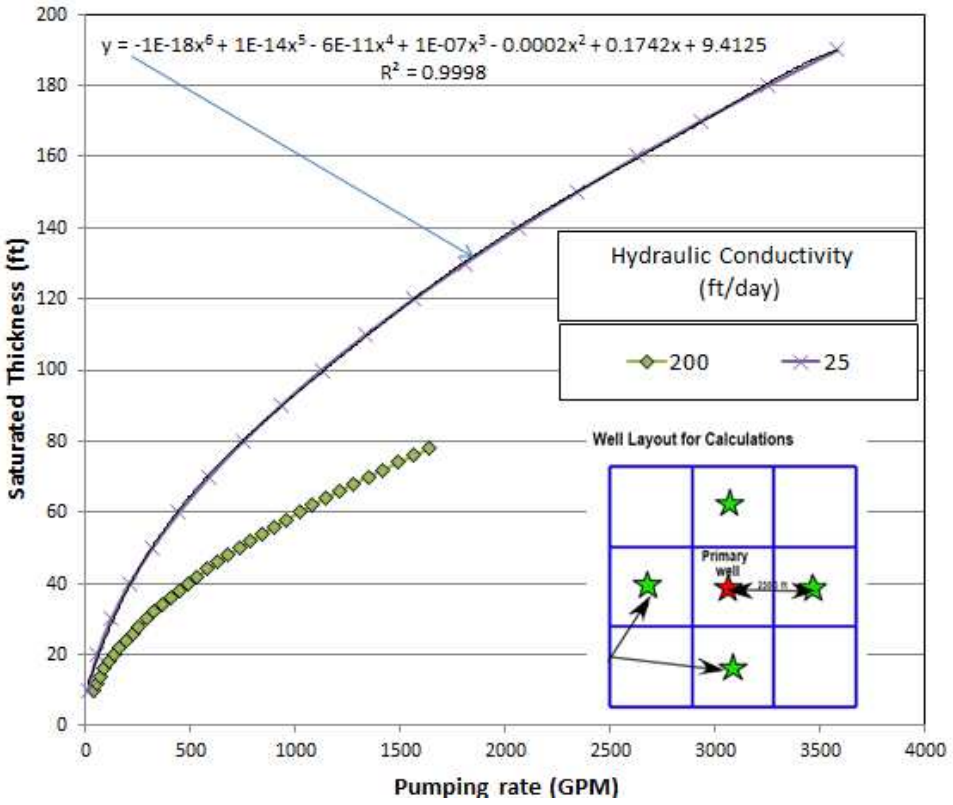


**Figure 3-2 Relationship between Well Yield and Saturated Thickness for Two Hydraulic Conductivity Values**

### 3-2-2 Calculation of Saturated Thickness:

The High Plain Aquifer bedrock and its physical properties was obtained from USGS. In order to calculate water table elevations, the Wizard database has been used. More detail about physical properties of High Plain Aquifer and Wizard database can be found in the data sources and collection methodology section (Section 3-6).

For each well in the Wizard database, the elevation of the local bedrock and ground surface elevation was extracted by the ArcGIS get elevation (getZ) function and the difference between bedrock and ground surface elevation was calculated. In order to calculate the saturated

thickness of each well, the depth of water in the well was subtracted from the above value. The mean average of the well saturated thicknesses for each county was then calculated. These calculations were repeated for each year.

## 3-3 Input Data

The Water Budget Model has been coded as a user-defined MATLAB function. The function needs nine input data to calculate output variables. The input data include latitude, min and max daily temperature, daily precipitation, soil hydrological group equivalent number (SCS curve number), soil water holding capacity of the root zone, crop type, and pumping rate.

### 3-3-1 Meteorological Data

In order to obtain Meteorological data, two sets of data have been evaluated with High Plains Regional Climate Center (HPRCC) weather stations. HPRCC stations coverage being sparse for a statewide study. Therefore, two raster-based meteorological data sets were evaluated at the HPRCC station sites, in order to determine which dataset is more accurate for this project. The two datasets were North American Regional Reanalysis (NARR) and the monthly Parameter-elevation Relationships on Independent Slopes Model (PRISM). More detail about two dataset can be found in the data collection methodology section. In order to have a visual idea of the data coverage statewide, the spatial coverage has been presented in the Figure 3-3

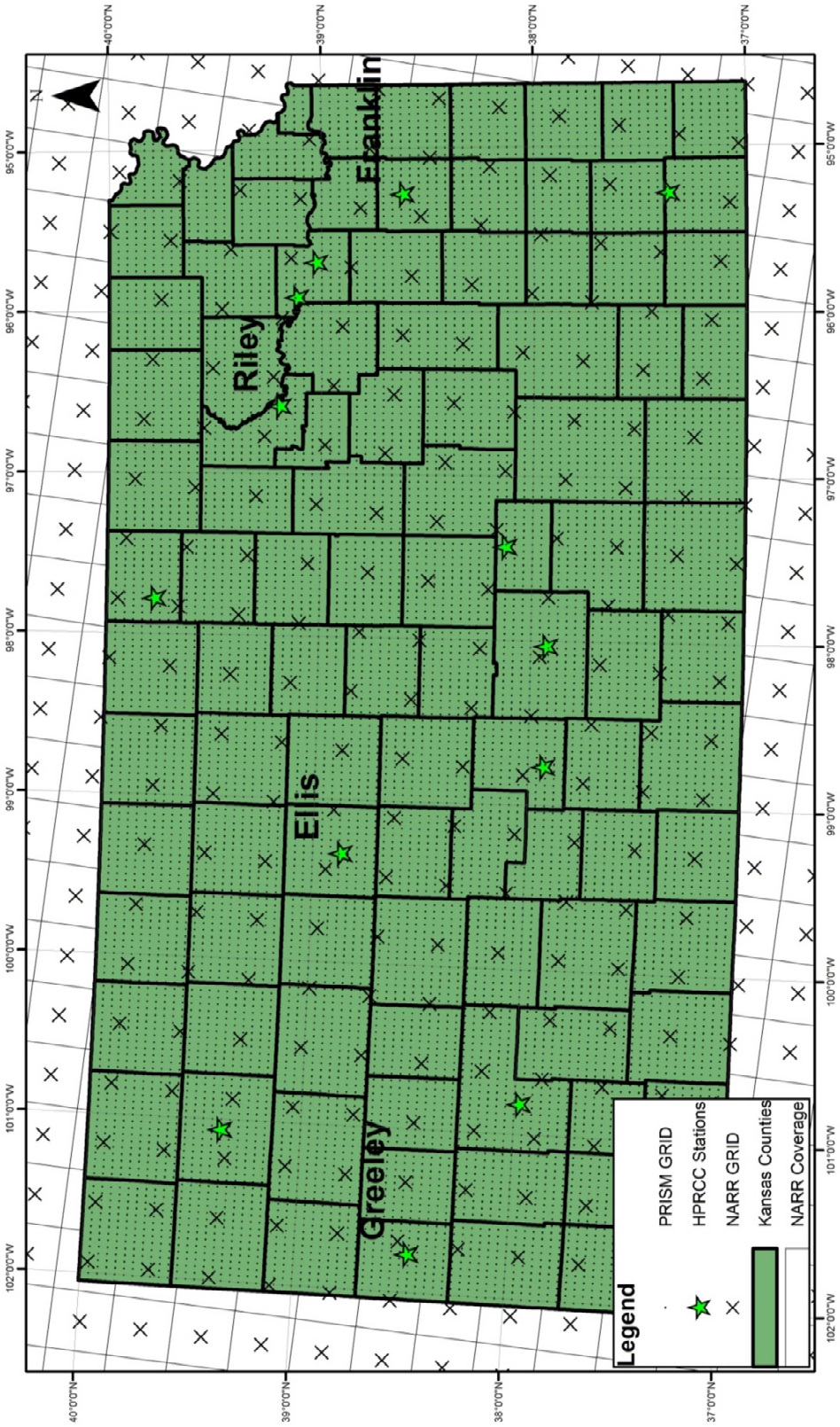


**Figure 3-3 Spatial Coverage of HPRCC stations, NARR, PRISM grid**

In order to compare datasets, a probability distribution function (PDF) of each variable was produced for five HPRCC stations between 1975 and 2010. Figure 3-4 shows PDFs of maximum and minimum temperature for PRISM, NARR, and HPRCC datasets for Ellis. The distributions of maximum and minimum temperature for Ellis HPRCC weather station are mostly overlapped by the PRISM PDFs. In Ellis, the PRISM-base maximum and minimum temperatures distributions are closer to the HPRCC station data in comparison to the NARR dataset.

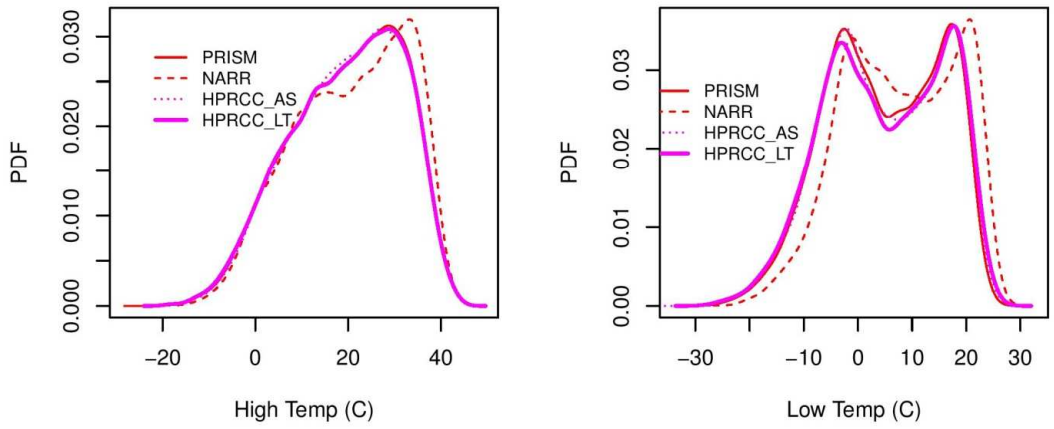


**Figure 3-4 Probability distribution functions (PDF) of maximum and minimum temperature for PRISM, NARR, and HPRCC datasets for Ellis**

As a result of the comparison, the PRISM data set has been selected as the Meteorological data set. PDFs of weather datasets for four HPRCC weather stations are attached in Appendix A.

With a set of GIS and R codes, the nearest grid cell of PRISM to the centroid of any geographical boundary is found, based on its latitude and longitude. The R code of weather dataset extraction is shown in appendix C. The temporal range for the county-level study is 1975 to 2010. The temporal range for the field-level study is 2005 to 2007.

### 3-3-2 Land Cover Code or Crop Code for Main Crops of Study

The crop code is a number representing crops studied: (1) corn, (2) sorghum, (3) soybean, (4) winter wheat, and (5) alfalfa.

### 3-3-3 Soil Properties

Representative soil properties of any geographical boundary such as field boundary, including water holding capacity of the root zone (WHC) and hydrological soil group (HSG) have been used as data input. More detail about WHC and HSG is provided in the data sources and collection methodology section. Hydrological soil group or SCS curve number has been used in the runoff process, whereas WHC has been used for determining the maximum water content of the root zone of soil. The total depth of water that soil can absorb above the wilting point aggregated over the specific soil depth is named water holding capacity. In order to match the root zone of crops with the soil depth, the depth of 100 cm was chosen (NRCS, 2004; Rogers, 1995). More detail about the two soil parameters can be found in the data sources and collection methodology.

In order to capture needed soil properties of any geometric boundary (such as field level) the ArcGIS zonal statistic toolbox was used. With the Zonal Statistics tool, spatially-weighted average value is calculated for each geometric boundary, excluding non-data cells. This process, aggregates data at the pixel level to a more coarse level. Two raster layers have been used as a

base of soil properties. One layer is a statewide representation of WHC values, and the other layer is a statewide representation of HSG values.

For field-level study, the boundary of selected fields, defined in vector-based Land Cover/Land Use layer (LCLU) has been used as an input into ArcGIS zonal statistics toolbox. County‘s boundaries are overlaid by the WIMAS Place of Use Layer (PLU) and are used for county-level studies. More detail about LCLU and PLU is provided in the data sources and collection methodology section.

### 3-3-4 Pumping Rate:

The amount of water that flows into the well from surrounding rock or soil in a given amount of time are defined as well yield. Pump capacity is defined as the maximum water discharge rate of the pump. The minimum of well yield and pump capacity was chosen as the pump rate. Well yield is calculated based on local saturated thickness of aquifer, which has been discussed in the section 3-2.

## 3-4 Output of The Model

This section outlines the terms calculated by the water budget model. Some terms are intermediate variables, while some are final calculations that are coded as outputs.

### 3-4-1 Actual Evapotranspiration (AET)

Actual evapotranspiration (AET) is defined as is the quantity of water that is actually removed from a surface due to the processes of evaporation and transpiration (Allen, 2005) The value is dependent on the previous day’s soil moisture content, the WHC of the soil, and the potential evapotranspiration (which is previously calculated using the Hargreaves Samani

equation and crop coefficient scaling factor). The mathematical formulation of AET calculation is shown below, where $ST_{i-1}$ is a previous day's soil moisture content in mm of water:

$$AE_i = \frac{ST_{i-1}}{WHC} * PE$$

### 3-4-2 Soil Moisture Content (ST):

Soil moisture content is equal to the total amount of water, stored in the crop root zone. The maximum value of the soil moisture content is defined as the water holding capacity of the soil, which was discussed earlier as a property of the soil type.

### 3-4-3 Runoff:

The following formula shows the daily runoff calculation, where $P$ precipitation is in mm, $CN$ is SCS curve number, $S$ potential maximum retention after runoff begins , and $I_a$ initial abstraction are in mm.

$$Runoff = \begin{cases} 0, & P \leq I_a \\ \frac{(P-I_a)^2}{P-I_a+S} & , P > I_a \end{cases}, I_a = .2S \ , S = \frac{1000}{CN} - 10$$

### 3-4-3 Deficit:

When the irrigation demand (potential evapotranspiration) exceeds the amount of actual evapotranspiration, a soil deficit developed. Soil deficit is calculated by subtracting potential evapotranspiration from the actual evapotranspiration.

### 3-4-4 Surplus and Groundwater Recharge:

Surplus is calculated by subtracting actual evapotranspiration and runoff from precipitation. A positive value is surplus when is an indication of groundwater recharge, if the soil moisture capacity reaches the field's WHC .

## 3-5 Simulating Future Climate Change Projections

To investigate the potential impacts of climate change, the result of one regional study, focusing on the Intergovernmental Panel on Climate Change (IPCC) fourth Assessment Report (AR4) projections -A1B scenario among of Emissions Scenarios has been used (Brunsell et al., 2010)

According to the IPCC AB1 scenario, economic growth likely will be very rapid with the introduction of new and more efficient technologies. In this scenario, the total worldwide energy consumption will not rely primarily on fossil energy but on a mix of energy sources. In the Brunsell et al. (2010) studies, decadal-averaged monthly output of 21 global climate change models were examined for six grid cells representing Kansas. The result of multi-model ensemble projections for the region for the period 2010–2100 indicates that temperatures will probably increases in all seasons. The largest seasonal trend in air temperature is likely to be 0.04 °C/year in summer and fall. Rainfall is predicted to decrease in fall and summer, but increase slightly in winter. In Appendix B, the linear precipitation and temperature trends used in this study are shown.

Scenarios of climate change have been described by global circulation models (GCM) for which temporal and spatial resolution is too coarse for this work (typically 200km). They are useful for

describing the global climate statistics, but they are not a good representative of the local climate. For this work GCM results must be linked to the local climate.

In order to calculate irrigation demand for the AB1 climate change scenario, the mean climate data must be translated to daily weather data. To do this, weather datasets are constructed. To construct projected weather datasets, seasonal trends could be applied to historical records or synthetics weather dataset.

The purpose of making projected weather dataset is capturing the mean state of the changed weather (GCMs results) and not projected changes in climate variability.

### 3-5-1 Weather Generation

Using observed daily ground-based meteorological data in agricultural, ecosystem or climate change simulations is very common. However, obtaining adequate meteorological data is difficult due to inadequate length, completeness, and spatial coverage (Wilks et al., 1999). In order to solve that issues, specific statistical models, termed stochastic weather generators, have been developed to fill in missing data or create synthetic meteorological records. In order to assess regional climate change impacts, it is assumed that the statistical relationship between large scale predictors and local predictors is constant. Stochastic weather generation methods can produce daily weather series. Their performance has been measured by their ability to capture realistic inter-annual and seasonal variability along with the mean states of regional climate.

In this study, a weather generator, developed in the National Center for Atmospheric Research (Furrer et al., 2007), was used. The model is a Generalized Linear Model (GLM) allowing for direct assimilation of annual cycles and other covariates, including the El Niño-Southern Oscillation (ENSO) and the Pacific Decadal Oscillation (PDO). In the model,

precipitation is generated using a first-order Markov chain-gamma model, while daily maximum and minimum temperatures are modeled using separate first order autoregressive processes.

## 3-6 Data Sources and Collection Methodology

### 3-6-1 Weather

The "North American Regional Reanalysis (NARR) is a long-term, dynamically consistent, high-resolution, high-frequency, atmospheric and land surface hydrology dataset for the North American domain"(Mesinger et al., 2006). NARR has been developed by the National Centers for Environmental Prediction division (NCEP) of the National Oceanic and Atmospheric Administration NOAA. The original data had a 32 km scale with data including minimum and maximum temperature, and precipitation at 3-hour intervals. The NARR model combines the very high resolution NCEP ETA Model (32km/45 layers) with the Regional Data Assimilation System (RDAS). The data was aggregated to the daily level by Dr. Dave Mechem (Department of Geography and Atmospheric Sciences, University of Kansas) and was converted from the netCDF format to an excel format by Dr. Jude Kastens (Kansas Applied Remote Sensing, Kansas Biological Survey), specifically for this project.

The monthly Parameter-elevation Relationships on Independent Slopes Model or PRISM dataset is single-event gridded data that has been created by the PRISM climate change group at Oregon State University (http://oldprism.nacse.org/ ). The objective of the PRISM group is to represent complex climate regimes associated with many factors such as orography, rain shadows, temperature inversions, slope aspect, and coastal proximity. PRISM is the USDA's official spatial climatological data. A daily PRISM dataset was obtained from Dr. Wolfram Schlenker (Columbia University) and Dr. Micheal Roberts (North Carolina State University). In order to create the daily PRISM dataset, they used a monthly PRISM dataset with 2.5 arcmin spatial scale including minimum, maximum temperature, and precipitation along with daily

records of weather stations. Monthly averages at each PRISM grid were regressed with monthly averages at the seven closest weather stations. Then, by relating monthly PRISM averages to weather stations, regression estimates were applied to the daily weather data at the stations (Schlenker, 2014) . Since the initiation of this project, the PRISM group has released daily PRISM data, which can be downloaded at http://prism.oregonstate.edu

### 3-6-2 Soil

Soil information, including the water holding capacity of the root zone and hydrological soil group, was obtained from the United State Department of Agriculture-Natural Resource Conservation Services (USDA-NRCS) Soil Survey Geographic (gridded SSURGO) dataset (http://datagateway.nrcs.usda.gov/) (FY2012 official release). SSURGO is the most detailed level of soil properties in the USA. It was collected at scales ranging from 1:12,000 to 1:24,000 and is maintained by NRCS. The representative field for the WHC of 100 cm root zone is aws0100 field in SSURGO. In addition, the representative field for the hydrological soil group is HSG field in SSURGO this has been used in this study. In the Figure 3-5, distribution of hydrological soil Groups is showed.

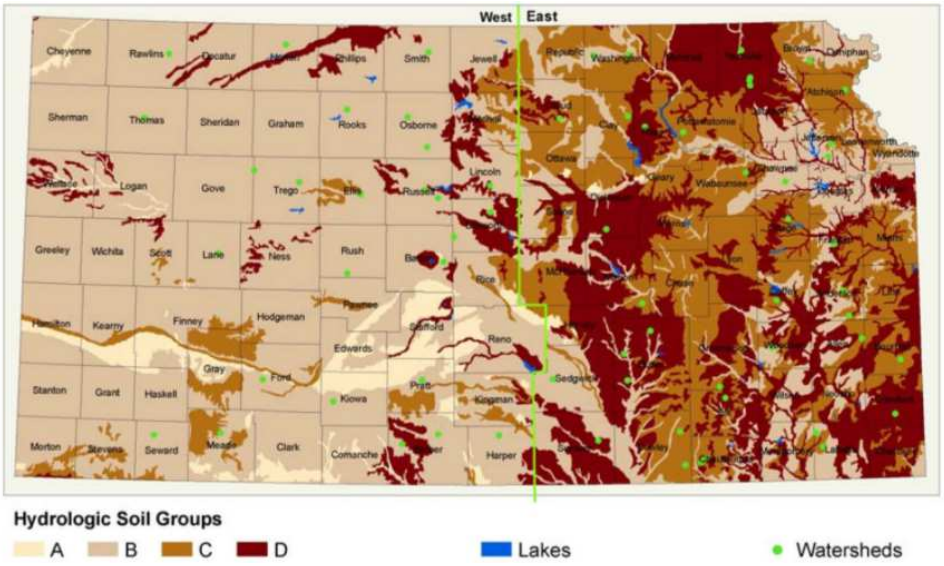


**Figure 3-5 Hydrological Soil Group Map (Bruce M. McEnroe, 2003)**

### 3-6-3 Land Use and Land Cover Data

In order to evaluate the irrigation demand, irrigated acreage, crop type is needed at the field level. The water budget model outputs mm water for a point. In order to determine the total volume of water needed for each field, the mm water output is multiplied by the acreage of the field. This way, the acre-ft of water that is predicted as an irrigation demand for a field (termed "Predicted" in the results section) can be compared to the actual acre ft pumped to that feld from a point of diversion.

For the county-level analysis irrigated crop data was obtained from USDA's National Agricultural Statistics Service (NASS). For the field-level analysis, the data has been obtained from Kansas Applied Remote Sensing Program (KARS).The NASS data is reported based on Kansas counties for each year. For each county, the total acreage of each crop is reported. Therefore for each county at each year crop type acreages are avaiable. But the number of fields in the field scale analysis are much more higher than county-level anlysis. Statiscially, more data

are avaliable for field level analysis.Each dataset is described more fully in below (Section 3-6-4 and 3-6-5).

### 3-6-4 NASS Data Set.

The USDA's National Agricultural Statistics Service (NASS) provides reports and statictics about U.S. agriculture products through many surveys each year. Quick Stats 2.0 is the most comprehensive tool for accessing agricultural data published by NASS (http://www.nass.usda.gov/Quick_Stats/) . Irrigated acreage of crops can be retrieved from Quick stats at 5 year intervals; years 2000 to 2010 were used in this study. In order to validate the water budget model at the county level, one data set of NASS statistics has been obtained from Dr. Jason Bergtold of Kansas State University. The Dataset was downloaded at 10/8/2012. In order to fill years without any data for Alfalfa (2000-2001,2003-2006,2008-2010), mean values of 2002 and 2007 reports have been used.

### 3-6-5 Kansas Land Use and Land Cover Layer

The Kansas Land Use and Land Cover (LULC) layers have been created by KARS between 2003 and 2012 for this project. The spatial unit of the geolayer is the Common Land Unit (CLU) in accordance with the USDA- Farm Agency Service's (FSA) definition. By FSA definition, CLU is the smallest unit of land that has a "permanent, contiguous boundary, common land cover, common land management, and common owner"(FSA, 2013). CLU boundaries were part of KARS purchase from FarmMarket ID Company". Sub-CLU boundaries, which generally represent a refinement of the CLU boundaries and which provide the minimum map units for the LULC raster time series for 2003-2012, were developed using digitizing and aerial photography"(Kastens, 2015a).

A hybrid, hierarchical classification of multi-temporal, multi-resolution imagery has been used to developed LULC maps of Kansas by KARS. LULC layers for 2006-2012 are based on USDA-NASS-Crop Data Layer (CDL) layers. Due to a lack of irrigation status in the CDL layers, KARS developed MODIS NDVI-based DT (data-trained) models to map irrigation status of the five main crops in the state. In order to develop DT models, the state was divided into two modeling zones; western- central ASDs (10-60), and eastern ASDs (70, 80, 90). The zones were divided according to regional similarities and differences in crop phenologies management practices, and climatic tendencies .The ground reference dataset used for model training was developed using the FSA CLU spatial coverage from 2007 and FSA 578 Compliance data tables. Because it was not enough ground reference data for eastern ASDs, ground reference data from the Center region was included. In order to develop irrigation mask for the DT models, a single, constant irrigation mask that was applied to all 10 years of LULC maps. It was assumed that the set of irrigated fields in Kansas were largely stable during the 10-year study period. Creation and implementation of a hierarchical logical rule set were used for final procedure. Final procedure utilized LULC trajectories, USDA NASS irrigated acreage statistics, and maximum MODI NDVI values from individual fields (Kastens, 2014).

Mapped classes include irrigated and non-irrigated alfalfa, corn, sorghum, soybeans, winter wheat, and double crop rotations. Each CLU boundary has a unique or primary key identifier, which is called 'SCTFS'. The planted area of each crop and irrigation status has been listed for each record in square meters. In order to perform calibration and sensitivity analysis, the KARS LULC training dataset has been used. CLUs with acreage between 120 to 160 acres, which could be a representative area of most center pivot systems in the study region, were

selected. Table 3-3 shows the number of used KARS LULC training dataset per crop and Agricultural District Number (ASD).

**Table 3-3 Number of fields based on geographic distribution and number per crop- KARS LULC training dataset**

| Agricultural District Number (ASD) | Corn | Sorghum | Soybean | Winter Wheat | Alfalfa | Grand Total |
|---|---|---|---|---|---|---|
| **2010** | 265 | 2 | 13 | 11 | 4 | 295 |
| **2020** | 25 | 1 | 2 | 7 | 1 | 36 |
| **2030** | 253 | 8 | 11 | 36 | 82 | 390 |
| **2040** | 18 | 2 | 4 | | 1 | 25 |
| **2050** | 41 | 3 | 8 | 6 | 4 | 62 |
| **2060** | 302 | 3 | 31 | 58 | 53 | 447 |
| **2070** | 4 | | 2 | | | 6 |
| **2080** | 8 | | 2 | | | 10 |
| **Grand Total** | **916** | **19** | **73** | **118** | **145** | **1271** |

### 3-6-6 Annual Irrigated Water-Use Report

The State of Kansas has legally-binding limitations on water-use (referred to as water rights), and it is required that water right holders annually report water-use for individual points of diversion (e.g. ground-water wells and surface water intakes). This data is archived in the Water Right Information System (WRIS). WRIS is an Oracle-based relational database management system (RDBMS) that encompasses over 70 relational tables, and it includes the individual WIMAS and Wizard databases. WRIS includes data on present day water rights, the location of points of diversion, authorized places of use, authorized quantity and rate allocations, and historic reported water usage. In the Figure 3-6, percentage of water from ground or surface water sources by county in 2000 is shown. In the Figure 3-7, percentage of water-use for each county in 2007 is shown.

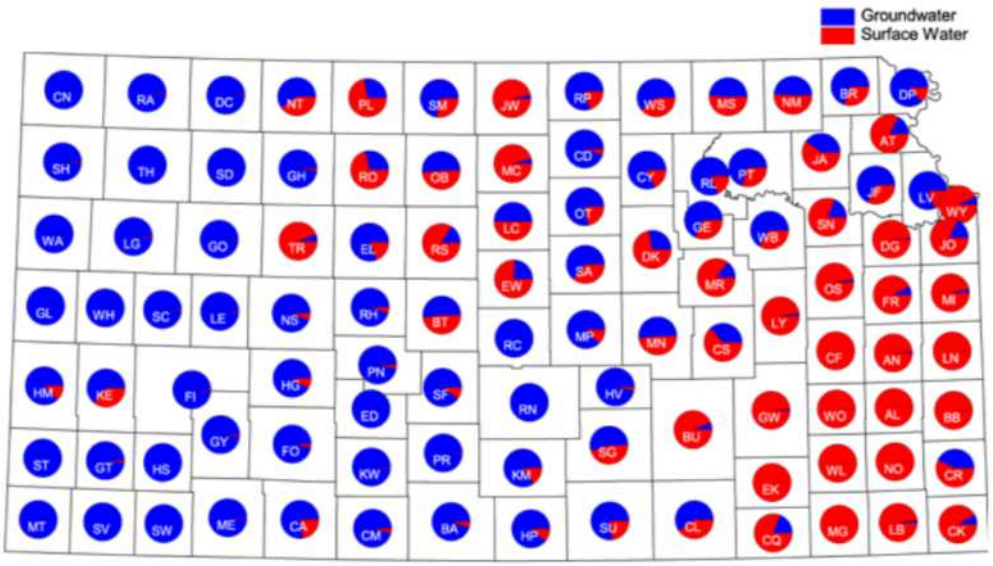


**Figure 3-6 Percentage of water from ground or surface water sources by county in 2000 (Sophocleous et al., 2000c)**

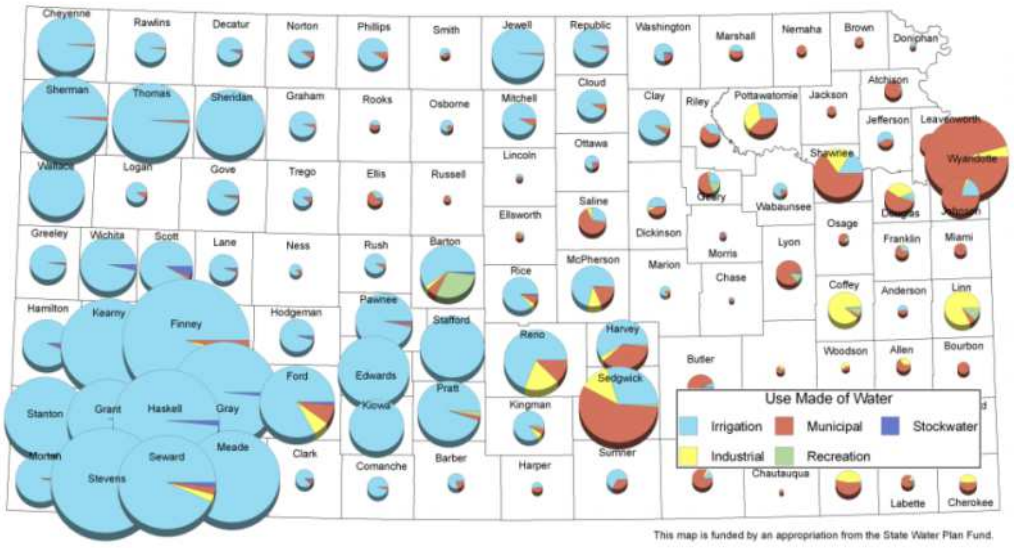


**Figure 3-7 Percentage of water-use for each county in 2007; larger circles mean a larger quantity of water- use (Dermyer, 2011)**

The data accessed by Water Information Management and Analysis System (WIMAS) is one of the most comprehensive and complex data sets for water rights in the United States. Two

ways have been provided to access water rights information: a web-based WIMAS (accesibile at http://hercules.kgs.ku.edu/geohydro/wimas/query_setup.cfm) and a customized ArcGIS project file that can be obtained through an open records request to the Kansas Geological Survey (KGS) via http://hercules.kgs.ku.edu/geohydro/wimas/index.cfm . In this project, the ESRI Geodatabase format was used, since complex queries and advanced geospatial queries were performed.

By Kansas Law, each water right is defined by one or more points of diversion along with one or more places of use (i.e. land upon which the water can be used), regardless of the end use of water (e.g. irrigation, industrial, municipal, etc.) and source (e.g. ground, surface). Therefore, a single water right may contain several points of diversion and many places of use. The WRIS database uses Public Land Survey System (PLSS) descriptions for the place(s) of use (PLU) authorized for water rights. For irrigation-based water rights, the authorized PLU acreage is described to the quarter-quarter section or 40-acre tract level (Wilson et al., 2005). The unit of authorized volume and acreage are acre-feet and acres, respectively. According to the prior appropriation doctrine of water right definition (Peck, 2005), the right to pump or divert water is based on an appropriation date. This doctrine creates two types of water right holders, which are called “senior” and “junior”.

Analyzing water rights geospatially is complicated, primarily because a single point of diversion or a single place of use might have numerous, overlapping water rights. The volume of annual water-use is reported under the senior water right number for overlapping points of diversions. Therefore, extracting any water-use measurement for an individual water right cannot be accurate. In order to ensure an accurate comparison of water-use with authorized quantity, water rights were clustered into a “water right group” in which all points or diversion and places of use were common to that group (i.e. not associated with any other water right outside the

group). For this project, Brownie Wilson (Kansas Geological Survey) coded an ArcGIS Extension tool (the water right grouping tool) for water right grouping that can utilize the WRIS ArcGIS database.

### 3-6-7 Water Right Grouping Tool

The water right grouping tool has three functions: creating water right groups, reporting authorized volume and acreage, and reporting annual water-use at the water right group level. The tool is capable of associating authorized 40-acre tracts defined by each water right group with other polygon-based data layers representing field boundaries or common land units (CLUs). The output of the tool has five fields for each target boundary, including a primary identifier of target boundary, a water right group number, acreage of target boundary, acreage and percentage of intersected water group and target boundary.

For Water Budget validation, water right groups with one point of diversion and one water right were selected because it is possible to associate the water-use from the point of diversion to the irrigated fields within the place(s) of use. In order to select the set, water rights were grouped statewide by the water right grouping tool. Then, the LCLU Layer with field or CLU boundaries were overlapped, and all CLU boundaries that have 95% overlapped area with the associated water right group were selected. This resulted in a validation dataset of 29070 fields.

The schematic of data preparation for validation is shown in Appendix D. It should be noted that the water grouping tool has been used for creating a report at the field-level scale. In order to study the county-level, the aggregated report of annual water-use for each county was extracted manually from WIMAS.

### 3-6-8 Physical Properties of The High Plain Aquifer

Physical properties of the High Plain Aquifer including aquifer base, the aquifer boundary, hydraulic conductivity, Kansas digital elevation model, and specific yield were obtained from USGS in the form of shape files. (http://water.usgs.gov/lookup/getgislist.)

### 3-6-9 Wizard:

For the HPA, DWR measures the depth to water in 1260 wells across Kansas annually in January. This water surface elevation data is archived in the Wizard database (http://www.kgs.ku.edu/Magellan/WaterLevels/). Wizard database has been used for saturated thickness calculation. Figure 3-8 shows Wizard Wells Location.

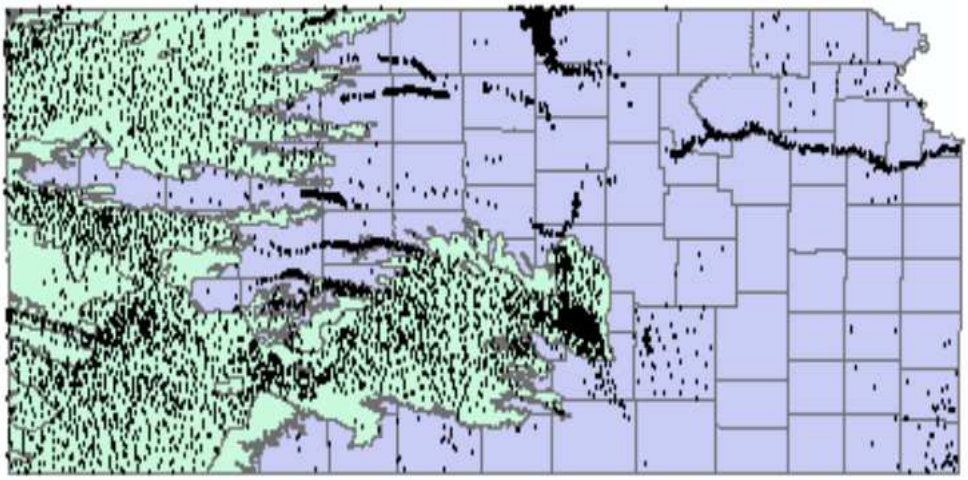

**Figure 3-8 Location of Wizard Wells**

### 3-6-10 Survey Wave

As part of the NSF project, two sets of farmer surveys were conducted. 2318 surveys were mailed to irrigators in the 2012 crop year. Among those, 817 usable surveys were returned.

The average pumping rate was calculated based on these surveys. The statewide pumping rates extracted from Survey Wave has been shown in the Figure 3-9

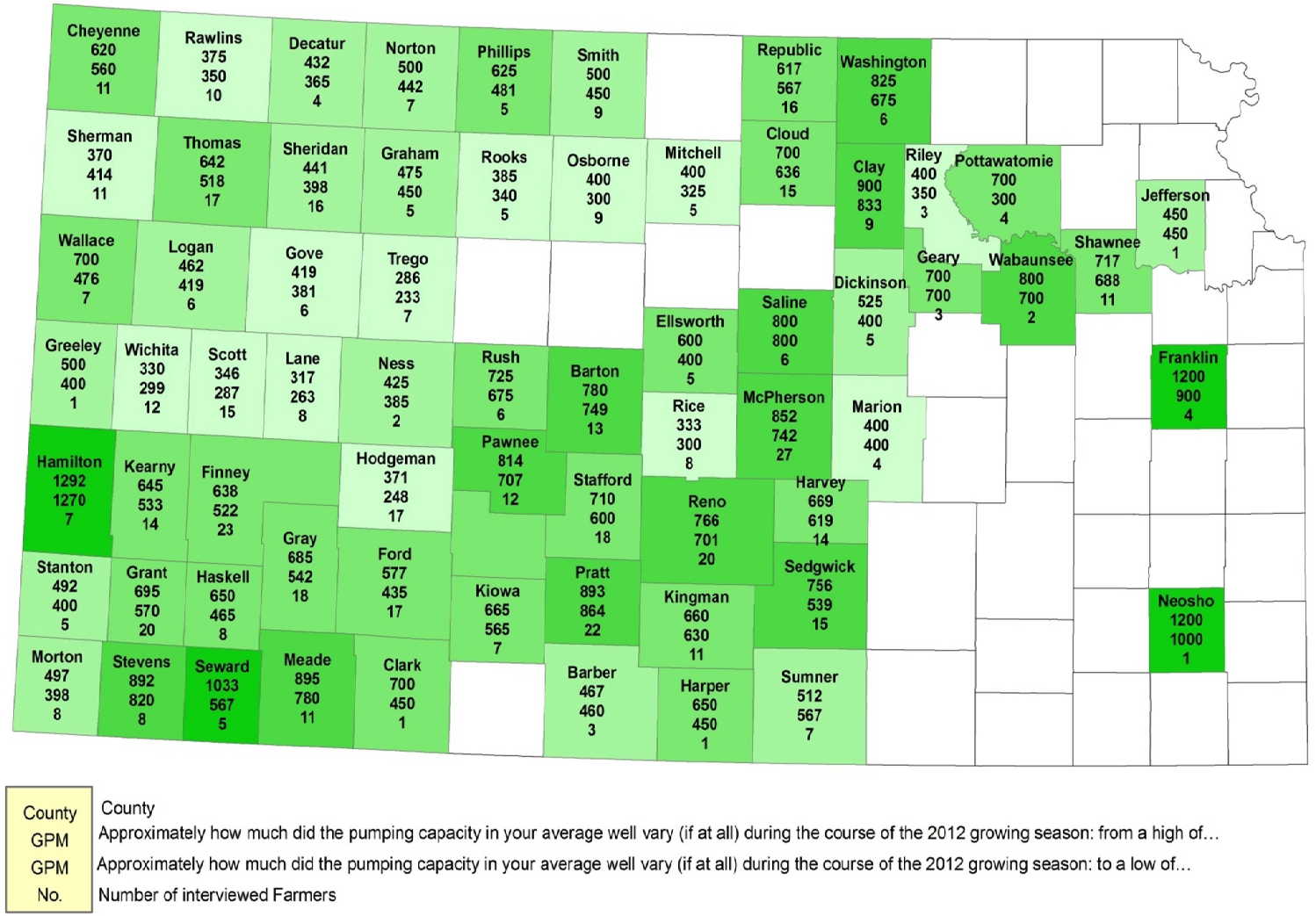


**Figure 3-9 Pumping rates based on the BACC:FLUD Survey Result**

# Chapter 4 : Model Validation

## 4-1 Accuracy and Robustness of The Water Budget Model (Sensitivity analysis)

A sensitivity analysis was performed to identify parameters that are sensitive for simulation. The one-factor-at-a-time sensitivity analysis (OAT) and global sampling methods are two well-known methods (Griensven et al., 2006). OAT involves evaluating the effect of one changing input parameter at a time, while keeping all other input parameters constant. OAT approach confirms that a change in model output is unambiguously attributed to the change in an input parameter. In contrast, global sampling methods cover the entire range of possible input values in a random or systematic way, creating an enormous number of model runs. Prior to manual calibration, sensitivity analysis was implemented using the OAT approach. OAT starts with taking a number of CLUs from the training dataset that are representative of irrigated center pivot-based CLUs for each crop. Then, the input data have been provided for water budget calculation.

For the sensitivity analysis, three main parameters were tested systematically (minimum and maximum soil moisture, and pumping rate). Often farmers save water by eliminating unnecessary irrigation and maintaining soil moisture at lower level (Upendram et al., 2006) . They use a management allowed deficit (MAD) level to cope with water stress. MAD limits are represented by minimum and maximum soil moisture contents. For each CLU, the model calculated irrigation demand for the training dataset boundaries by changing each of the selected parameters one at a time. The method operates by loops and each loop starts with a baseline

value. Around each baseline value, a partial effect $S_{Parameter}^{Partial}$ is calculated for any $J$ value. In the following equation, the $WB_{parameter}$ refers to the WB model function.

$$S_{Paramter}^{Partial} = \frac{WB_{parameter}\,(baseline \pm j)}{WB_{Parameter}(baseline)}$$

The final effect is calculated by averaging the partial effects of each loop for CLUs grouping based on their agricultural statistics district boundary (ASD). Not only the most sensitive parameter can be identified, but the impact of each selected parameter can also be quantified. In the Table 4-1 Initial and final values of the calibration parameters, plus possible ranges Where applicableTable 4-1, initial and final values of the calibration parameters plus possible ranges are shown. Pumping rate varies based on the well yield.

**Table 4-1 Initial and final values of the calibration parameters, plus possible ranges Where applicable**

| Parameter | Initial values | Range | Calibrated values |
|---|---|---|---|
| **Pumping rate** | 800 | 400-1200 | NA |
| **Maximum Soil Moisture Content** | 1.00 | .85-1.00 | .95 |
| **Minimum Soil Moisture Content** | .75 | .50-.90 | .60 |

In Figure 4-1, the result of sensitivity analysis of three parameters on the corn fields is shown for Kansas agricultural district ASD 2010. Figure 4-1 shows that the maximum and minimum soil moisture have the same trend. Also the slope of trend lines of pumping rate and maximum soil moisture shows that maximum and minimum soil moisture limits are most

sensitive to change rather than to the pumping rate. It should be noted that the slope of trend lines of maximum and minimum soil moisture are not the same for all crops. For example, sorghum rate of response is more sensitive to the minimum soil moisture than corn response. Results of sensitivity analysis were used for state-wide model calibration.

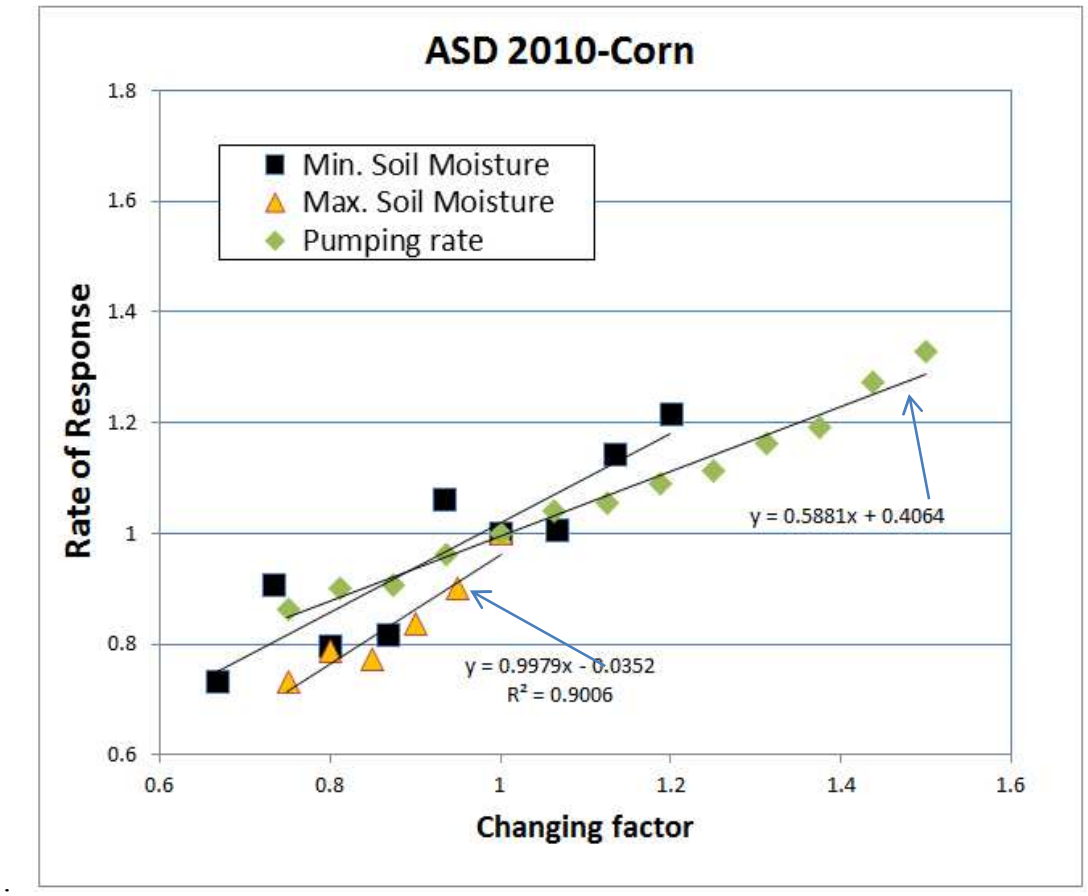


**Figure 4-1 Sensitivity Analysis of selected parameter for ASD 2010 Corn Fields**

## 4-2 Model Calibration and Validation

The goal of model calibration is to adjust model parameters, within applicable ranges, to increase the agreement between observed data and model results. Calibration has been

undertaken by comparing predicted irrigation demand to irrigation water-use records from WIMAS for 2007. For calibration, a trial and error approach was used by changing three sensitive parameters were identified in the sensitivity analysis.

For field-level calibration; it was known that the field-level dataset of irrigated crops had uncertainties caused by the remote sensing classification techniques of irrigated fields. In order to remove these uncertainties from the calibration, a training datasets was used.

In order to calibrate the model, the training data set for land cover/use classification obtained from KARS was used. From this dataset, state-wide irrigated field boundaries from selected water group were chosen for model calibration. The number of fields based on geographic distribution and number per crop were shown in Table 3-3.

In order to evaluate model performance, a ratio of the calculated annual irrigation demand (water budget output) to actual reported water-use (WIMAS database) was calculated.

$$Performance\ Ratio = \frac{[Irrigation\ demand\ (acre - feet)\ ]}{Actual\ reported\ water\ use\ (acre - feet)}$$

The actual reported water-use record was collected from WIMAS using the water right grouping tool. The data was aggregated manually for county-level studies. The annual irrigation demand was calculated by aggregating daily irrigation demand for any water group boundary by the following formula during the calibration and validation period (2007) where irrigation amount is the aggregated daily irrigation demand during the growing season.

$$\begin{bmatrix} Irrigation\ demand \\ (acre-feet) \end{bmatrix} = \left[\frac{Area\ in\ Acres}{Irrigation\ Efficency}\right] * \frac{\begin{bmatrix} Irrigation\ demand \\ (mm) \end{bmatrix}}{25.4\frac{mm}{in} * 12\frac{inch}{ft}}$$

In order to aggregate daily irrigation demand for selected water group boundaries, the crop-specific daily irrigation demand was calculated for the fields within the selected water groups. The irrigation demand for the growing season for all crops within a water group were then aggregated and compared to the water-use reports for the water group.

A one year initialization or start-up period has been used, in order to minimize the impacts of uncertain initial conditions in the model. Because winter wheat has a two-year growing season, the period between 2005 and 2007 has been selected for field-level validation.

Input data for this validation period were obtained as described in the methods section. Briefly, the irrigated acreage was collected from the LULC layer and NASS statistics for field and county-level studies, respectively. Irrigation efficiency is a critical measurement of irrigation performance, which is defined in terms of three factors: " 1) the irrigation system performance, 2) the uniformity of the water application, and 3) the response of the crop to irrigation. These measures vary with scale and time and are interrelated to each other" (Howell, 2003) For center pivot systems, the range of irrigation efficiency is between 70 and 98 percent. The attainable number is a value between 85 and 95 percent (Howell, 2003). In this study, irrigation efficiency was set to 90 percent as the average value for the state for center pivot (Dermyer, 2011). From the sensitivity analysis the assumed pumping rate was known to greatly affect the model results. The statewide farmer survey results were used to inform the pumping rate. The survey had 817 number of irrigating farmer respondents, who responded to the question. One of the survey questions is about their pumping rate in 2012 which was shown in

the Figure 3-9. For model validation, the average value of the statewide pumping rate (600 gallons per minute) was used.

## 4-3 Model Performance

In this study, the aggregated simulated daily irrigation demand against actual water use during the validation periods are shown in a scatter plot. In addition, the performance ratio of the model is shown in crop-specific boxplots.

Figure 4-2 shows the performance ratio of the training dataset for the calibrated model. The model calibrated using soil moisture and irrigation efficiency. According to the calibrated results of 1253 water groups, the optimal values for all crops were obtained when the maximum and minimum soil moisture was adjusted to 95 and 60 percent, respectively. In Figure 4-2, the mean performance ratios for corn, sorghum, soybean, winter wheat, and alfalfa are 1.05, 0.78, 0.75, 0.93, and 1.40, respectively.

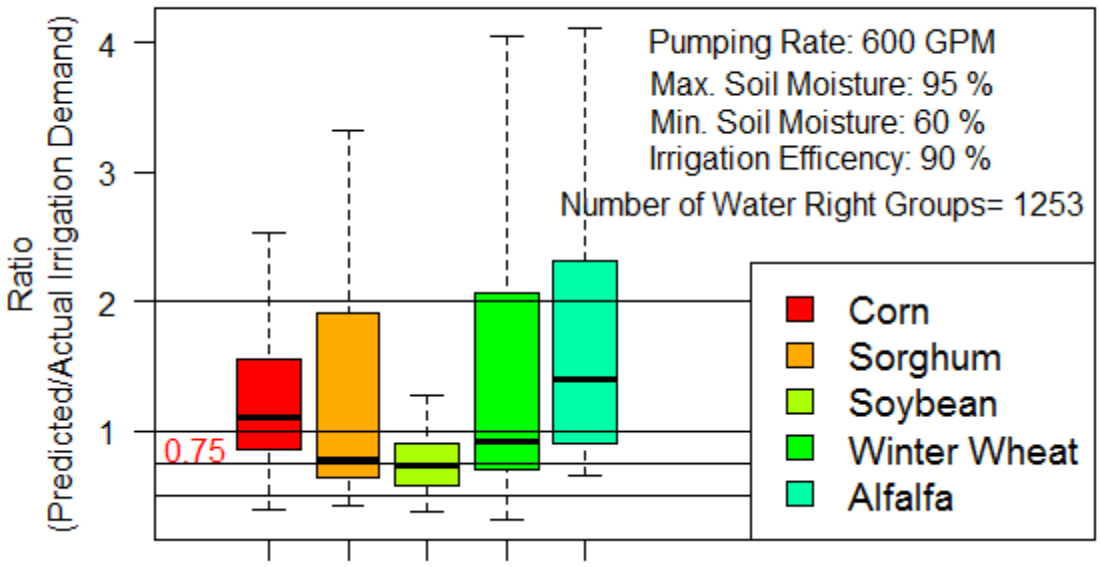


**Figure 4-2 Crop-specific Performance Ratios distribution for each crop**

### 4-3-1 Field Level

After the calibration step, a validation step was performed for a greater number of fields. Among 1,390,000 fields within the 2007 LULC layer, 290,000 were selected within 4544 water right groups. For each water right group and its corresponding fields, irrigation demands were calculated and compared with the actual water-use report from 200. Figure 4-3 shows the correlation of predicted irrigation demands versus actual water-use. The figure shows a high positive correlation between predicted and actual values, with a slope of 0.79 and $R^2$ of 0.51.

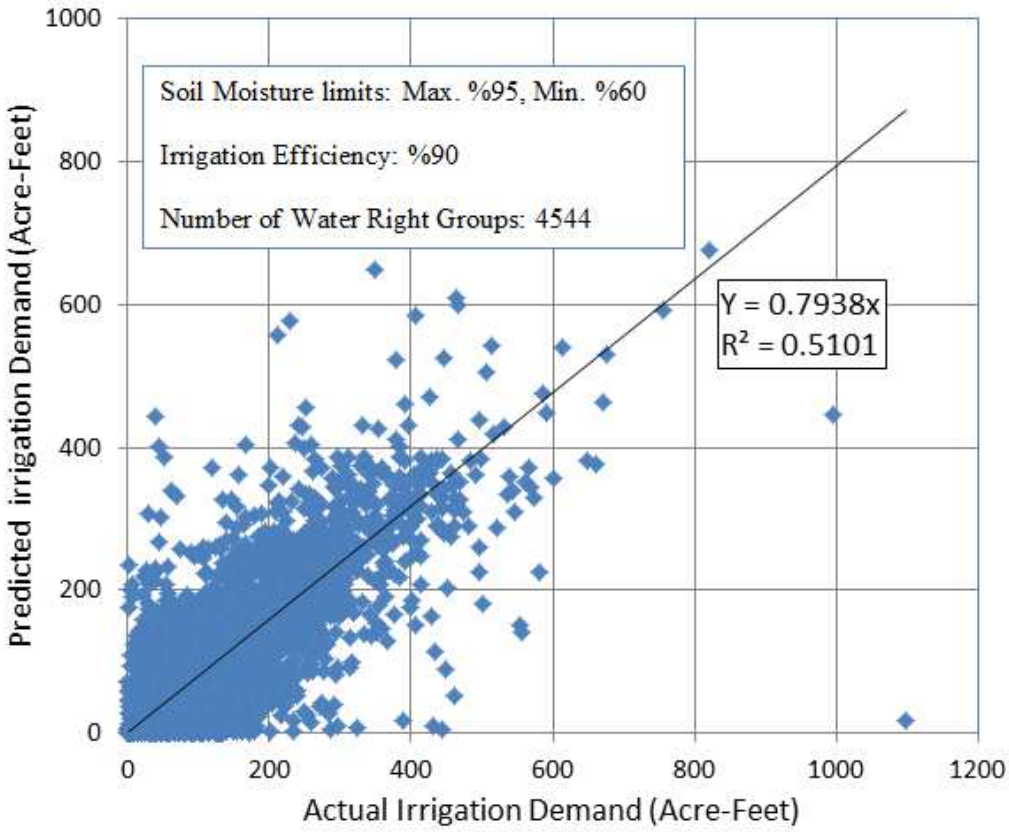


**Figure 4-3 Correlation of Predicted Irrigation Demand to Actual Demand at the Field**

As mentioned before, the WIMAS dataset provides information regarding the specific irrigation system for each water right (although this data element is missing for many water rights). In order to compare the effect of irrigation system on the performance ratio, the water budget results were analyzed for each irrigation system by crop type. The distributions of performance ratio for all irrigation systems and crops are not similar. Center-pivot, center pivot - low energy precision application (LEPA) have similar performance ratio excluding corn.

The mean performance ratios for center-pivot and center pivot LEPA systems are generally similar to the calibrated model. Flood system has similar range and mean performance

ratio for all crops. The following boxplots (Figure 4-4 through Figure 4-6) represent the distribution of performance ratios for each irrigation system for field-level analysis. Figure 4-4 shows the performance ratio for corn fields for each irrigation system; this represents a selection of 353 water groups. A limited number of field performance ratios above 5 are outliers and were removed to depict the plot. The water budget performed best for center pivot and center pivot - LEPA systems, with a mean ratio of 1.05. It should be noted, these two systems are most prevalent system in the study.

Figure 4-5 shows the performance ratio of the water budget for sorghum fields for each irrigation system; this represents a selection of 181 statewide water groups. For sorghum, the center pivot LEPA systems had a mean performance ratio of 0.6. Figure 4-6 shows the performance ratio of the water budget for soybean fields for each irrigation system; this represents a selection of 350 statewide water groups. For soybean, the center pivot LEPA systems had a mean performance ratio of 0.75.

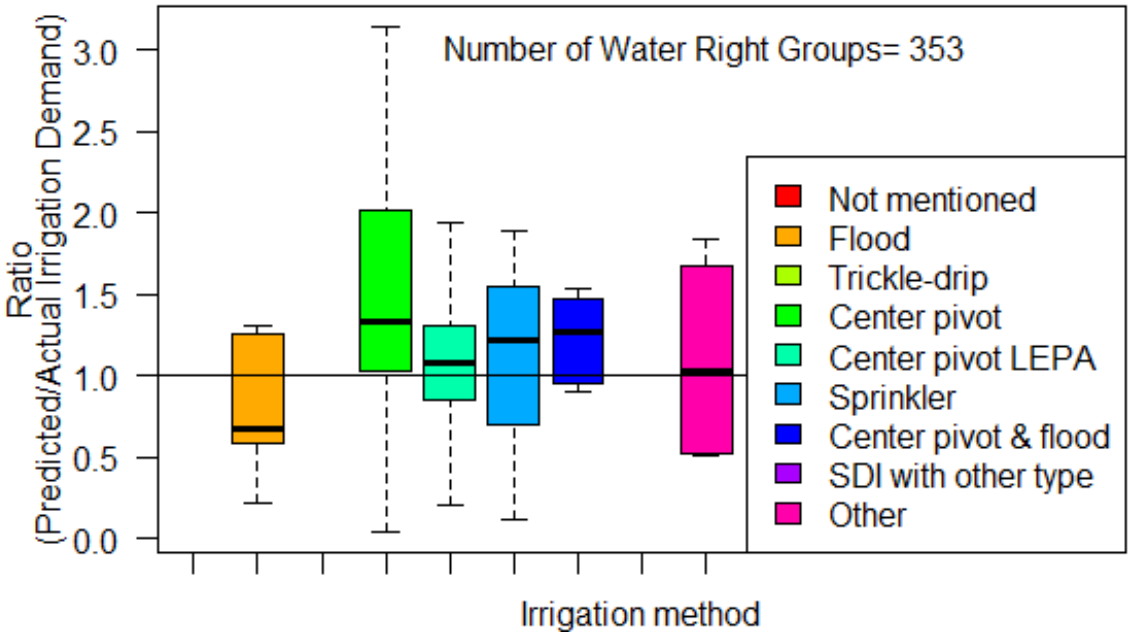


**Figure 4-4 Predicted to Actual Irrigation Ratio for corn-planted fields for each irrigation system (Ratio< 5)**

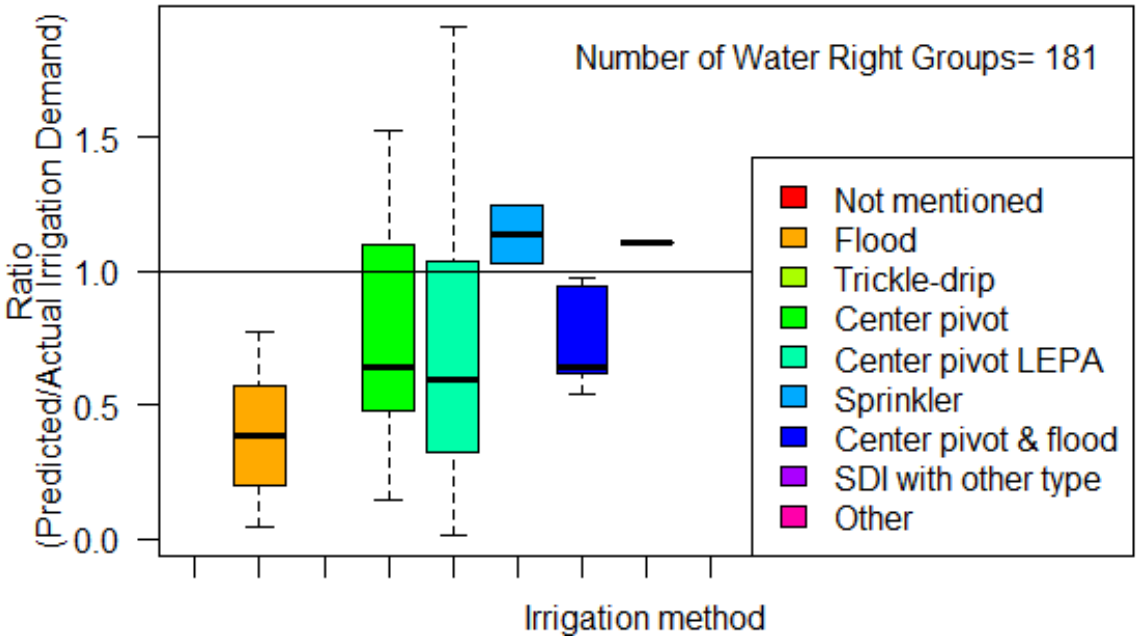


**Figure 4-5 Predicted to Actual Irrigation Ratio for sorghum-planted fields for each irrigation system (Ratio< 5)**

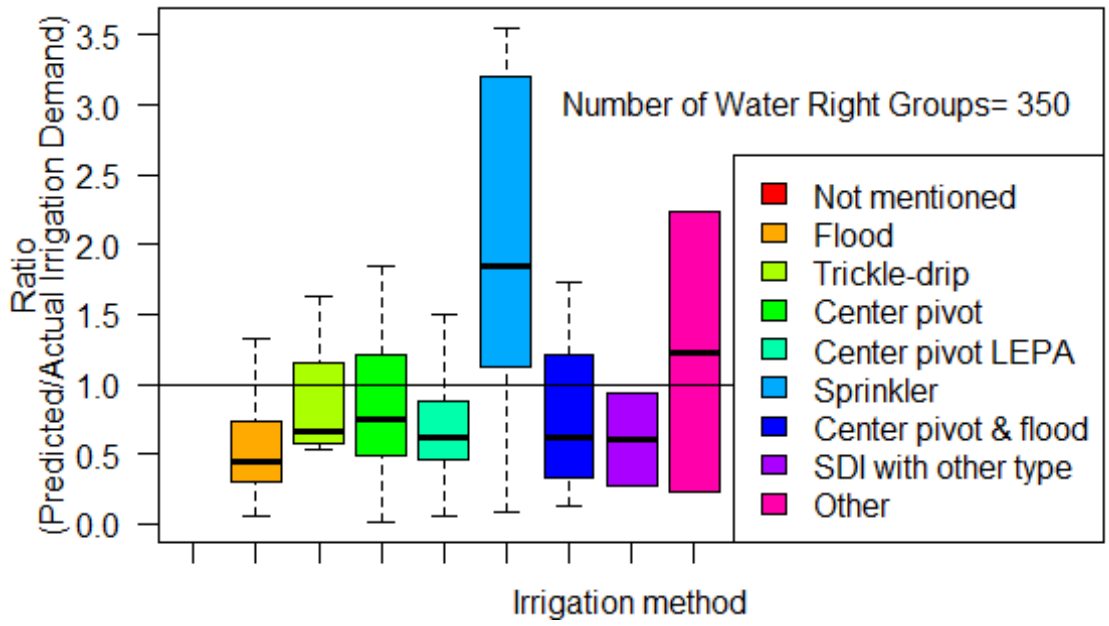


**Figure 4-6 Predicted to Actual Irrigation Ratio for Soybean-planted fields for each irrigation system (Ratio< 5)**

Figure 4-7 shows the performance ratio of the water budget for winter wheat fields for each irrigation system; this represents a selection of 513 statewide water groups. For winter wheat, the center pivot LEPA systems had a mean performance ratio of 0.70.

Figure 4-8 shows the performance ratio of the water budget for alfalfa fields for each irrigation system; this represents a selection of 2638 statewide water groups. For alfalfa, the center pivot LEPA systems had a mean performance ratio of 0.85.

Without exception, the mean performance ratios for all crops irrigated by flood irrigation are less than the other systems. This reflects the inherent inefficiency of flood irrigation, which results in over-use or extraction of water. The mean performance ratios for all crop irrigated by center pivot systems are similar, because systems are prevalent system in the analysis.

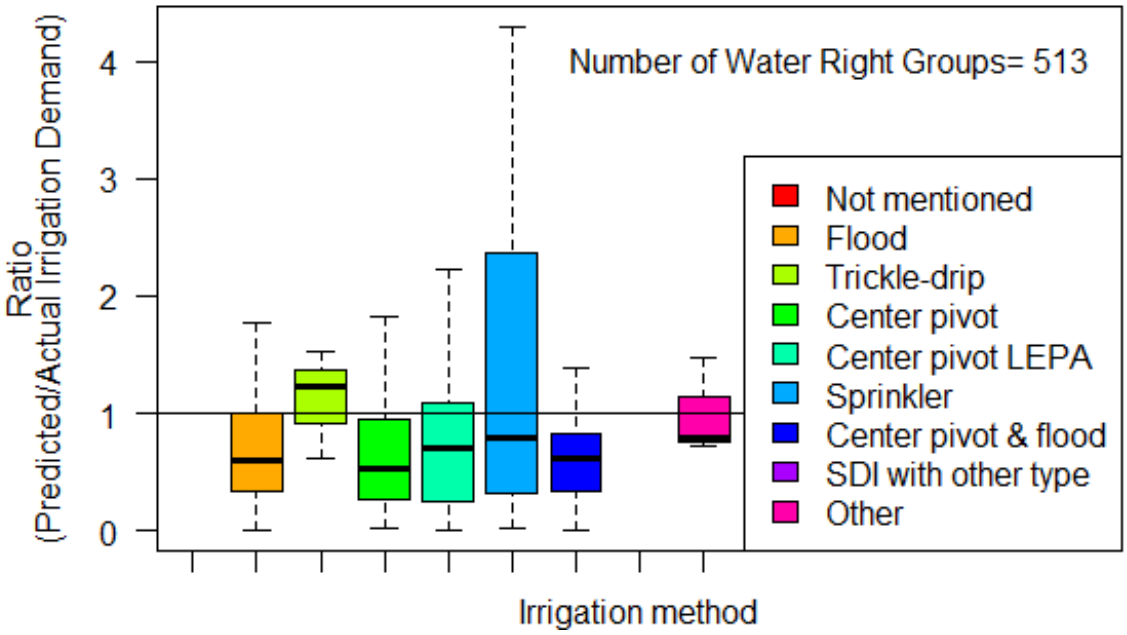


**Figure 4-7 Predicted to Actual Irrigation Ratio for Winter Wheat-planted fields for each irrigation system (Ratio< 5)**

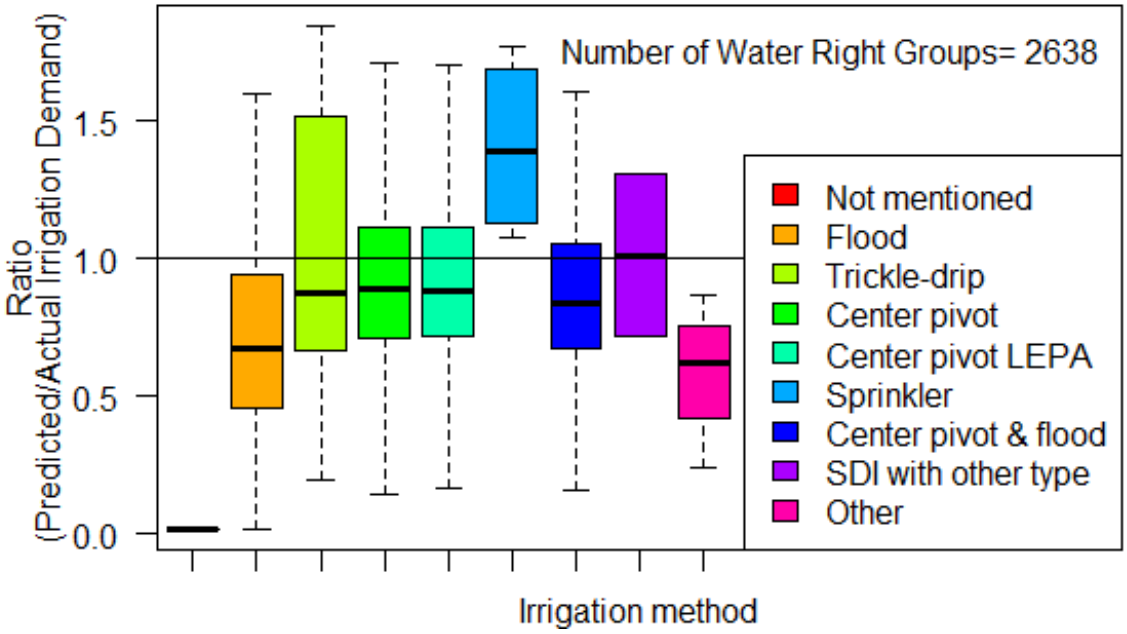


**Figure 4-8 Predicted to Actual Irrigation Ratio for Alfalfa-planted fields for each irrigation system (Ratio< 5)**

### 4-3-2 County-Level Validation

Validation step for water budget was also performed at the county-level. For this, the annual predicated irrigation demands for each county were calculated. The county was defined as the intersection of two ArcGIS layers, the PLU layer and political county boundaries. Based on the centroid of each polygon, weather data was extracted. Soil properties were extracted based on weight average of each polygon. For each county, the water budget was calculated for two scenarios of pumping rate: (1) a fixed pumping rate (600 GPM), and (2) a mean ten-year allowable pumping rate. The ten-year allowable pumping rate was calculated for all counties above the HPA based on the saturated thickness, hydraulic conductivity, and an assumed spacing of neighboring wells (described in detail in the methods chapter).

After running the two scenarios, irrigation demands were calculated and compared to the actual water use report for years 2000-2010. For all years, the irrigated acreage for crops was taken from NASS. Figure 4-9 and Figure 4-10 show the correlation coefficient of irrigation demands versus actual water use. For the eastern parts of Kansas, the ratio is typically higher than 1, whereas for the southwest and western part it is less than one. Counties without any water used or NASS statistics were depicted as empty boundaries. The mean performance ratio of each GMDs was calculated and is shown in Table 4-2. GMDs boundary are shown in Figure 4-11. Among all GMDs, GMD1 and GMD4 have the highest ratio equal to 1 and 0.93, respectively. The mean performance ratios of GMD 2, GMD 3, GMD 5 are not changed by changing the pumping rate from 600 GPM to allowable pumping rate.

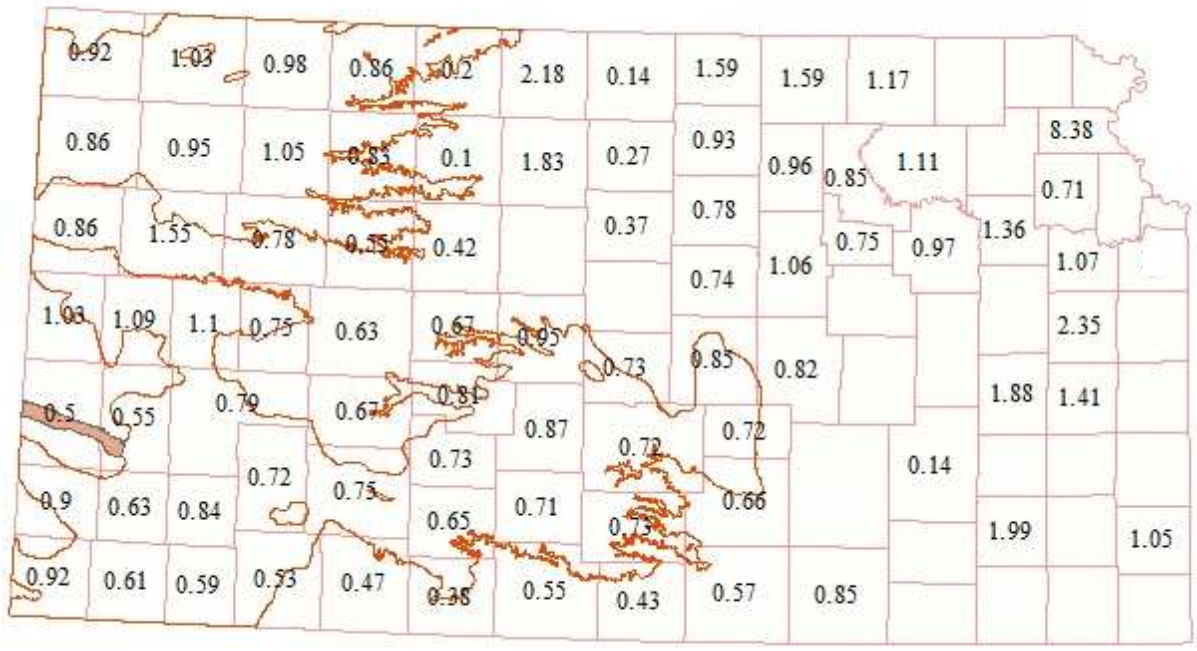


**Figure 4-9 Calculated Predicted to Actual Irrigation Ratios (using a fixed pumping rate of 600 GPM)**

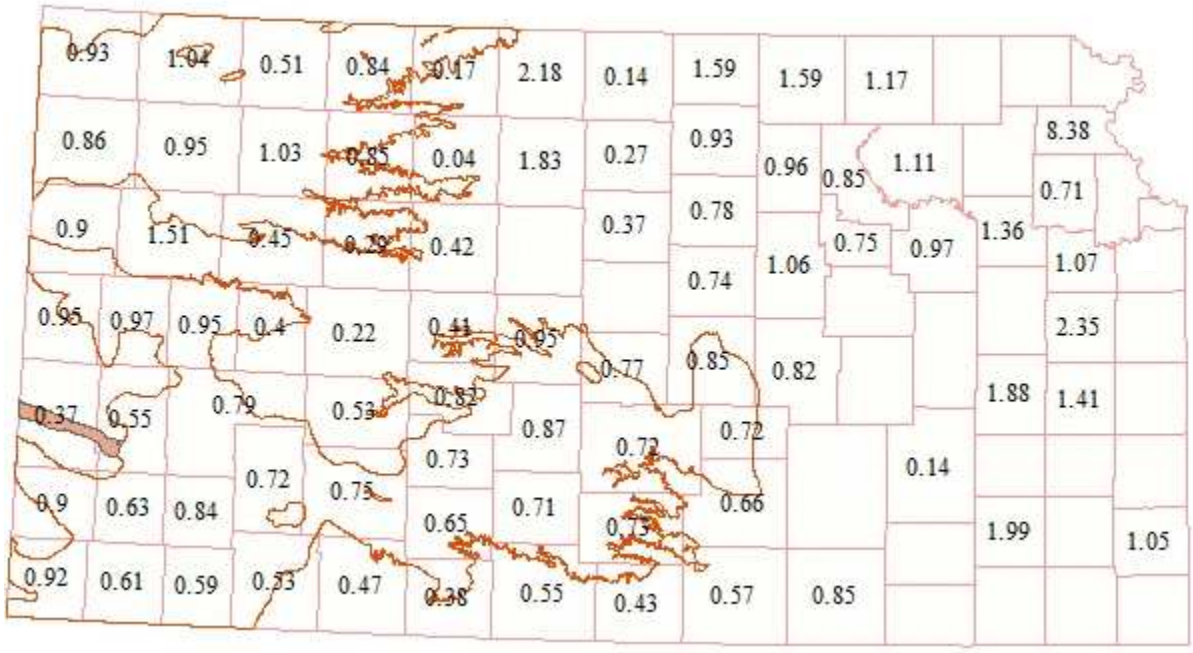


**Figure 4-10 Calculated Predicted to Actual Irrigation Ratios (using a 10-year mean allowable pumping rate)**

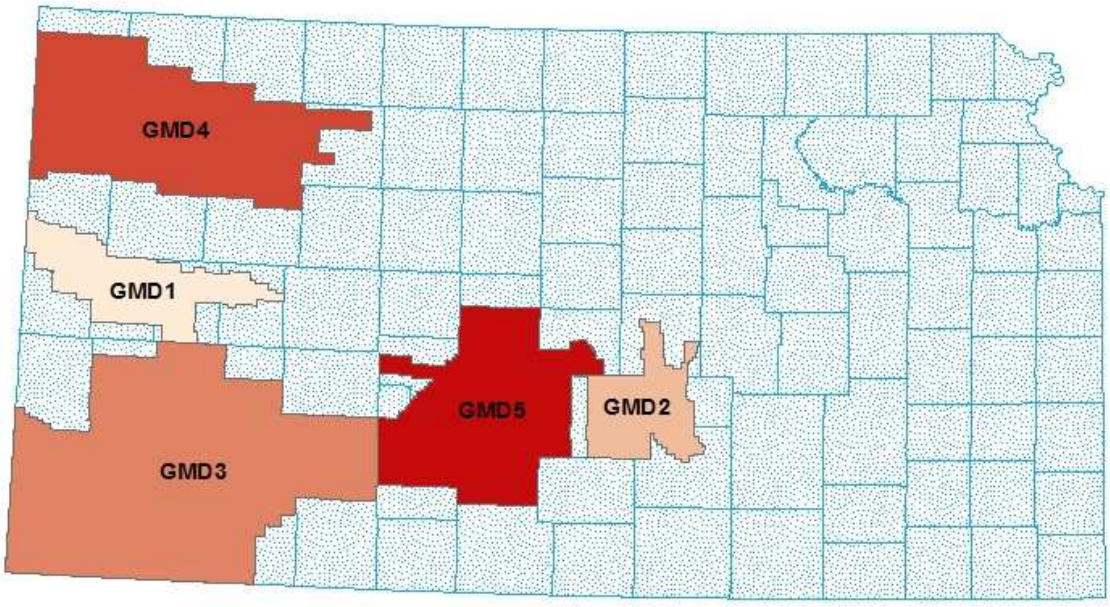


**Figure 4-11 GMDs boundary**

**Table 4-2 Effect of puming rate on the mean ratio( performance ratio) of GMDs. Averages and Standard Deviations (STD) are shown for all counties within each GMD**

| GMD ID | Mean ratio (600 GPM) | STD. ratio (600 GPM) | Mean ratio (Allowable pumping rate) | STD. ratio (Allowable pumping rate) |
|---|---|---|---|---|
| **1** | 1.02 | 0.27 | 0.92 | 0.33 |
| **2** | 0.73 | 0.06 | 0.74 | 0.06 |
| **3** | 0.70 | 0.17 | 0.68 | 0.17 |
| **4** | 0.93 | 0.23 | 0.85 | 0.32 |
| **5** | 0.73 | 0.10 | 0.71 | 0.15 |

## 4-4 Coupling Water Budget with Climate Change Effect

As mentioned in the methodology section, in order to construct a weather dataset showing the effect of climate change, the linear decadal trend was added to the PRISM-based and HPRCC datasets for Lakin weather station. This method of constructing a climate change

scenario has been named the Delta change or Perturbation factor (Hay et al., 2000). In order to test the ability of the weather generator at producing weather data with similar distributions as actual observations, one data set has been obtained from the Lakin HPRCC station from 1900 to 2010, then the weather generation code was used to generate 10 realizations at the same location. The water budget results of the 10 realizations (Delta-WG) were averaged based on the Julian day of the year. The probabilty distrbution function of two data sets is presented in Figure 4-12. Figure 4-12 shows that the weather generator makes weather timeseries consistent with the Lakin historical dataset, but it is not able to cover all trends. It produces milder tempretures than Lakin historical dataset.

For both datasets, the Delta change approach was applied. The "Delta-Lakin" dataset represents the Lakin station weather data with the linear trend of climate change effect applied under the A1b scenario. The "Delta-WG" dataset represents the mean of ten generated weather datatsets with the climate change effect applied under the A1b scenario.

In order to create any climate scenario, a baseline period must be defined. During scenario construction, baseline period is a reference and observed climate period from which the modelled future changes are calculated. According to the IPCC recommendation, the baseline period 1961 to 1990 is usually favored. In this study, baseline scenario was selected from period 1980 to 1989.

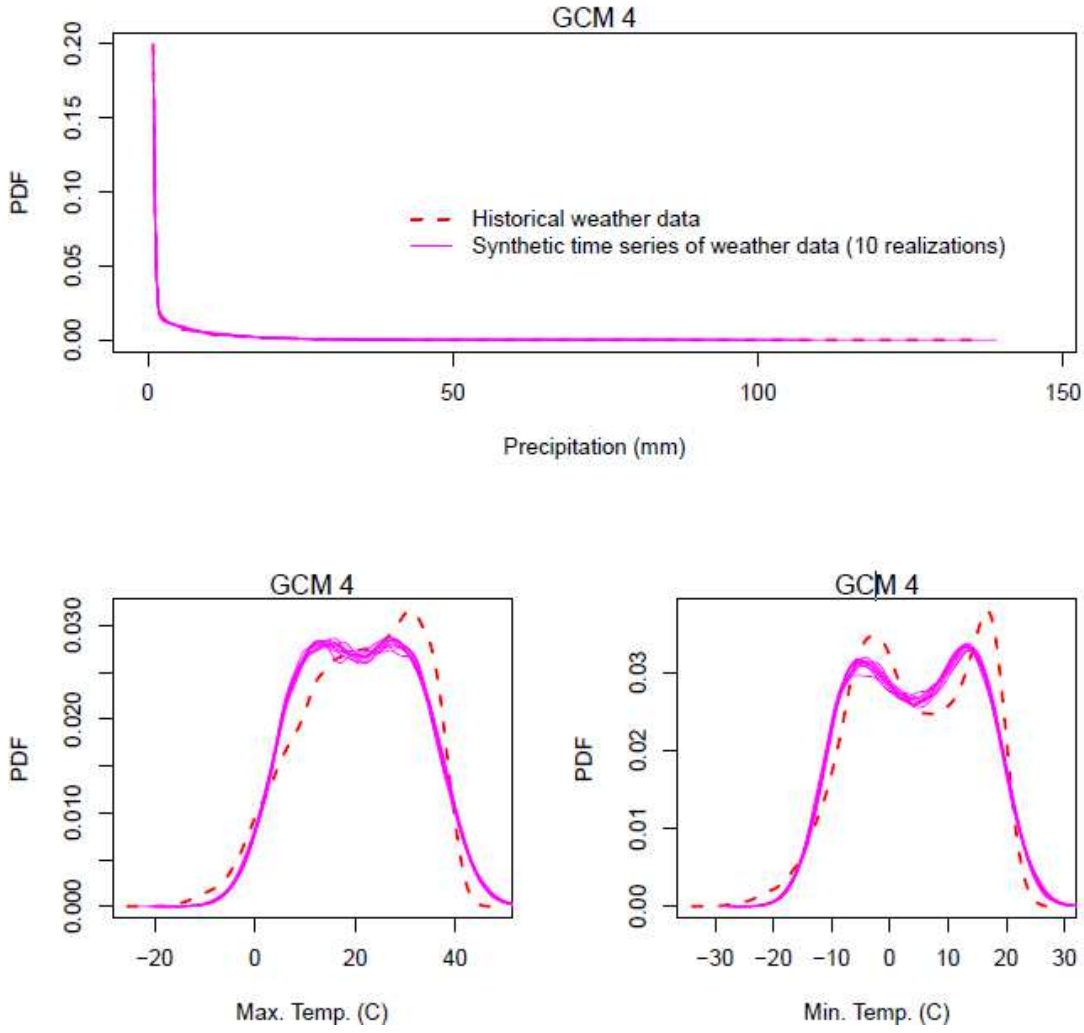


**Figure 4-12 Probability distribution functions (PDF) of maximum and minimum temperature and precipitation for 10 synthetic time series generated from Lakin HPRCC weather station (Historical weather data)**

### 4-4-1 Effect of Climate Change A1b Scenario on the Reference Evapotranspiration

Under the A1b scenario, the average daily increase in the reference evapotranspiration from the baseline scenario (1980-1989) to the period of 2090-2100 will start with an increase of 0.2 millimeters per day in January and intensify through June, reaching a maximum increase of 0.55 millimeters per day. Figure 4-13 shows the effect of climate change on the the reference

evapotranspiration from a baseline scenario for the period of 2090 to 2100. Figure 4-13 shows that the grass reference evapotranspiration will be increased between 0.2 to 0.5 millimeters of water per day on average for period of 2090 to 2100.

In addition to the above, the effect of climate change on the monthly reference evapotranspiration is shown in Figure 4-14. Except November, the minimum amount of increasing monthly reference evapotranspiration is 50 millimeters per month, while the highest is 180 millimeters per month in June. On average, the monthly grass reference evapotranspiration increased around 80 millimeters per month during the growing season. Although Delta-Lakin and Delta-WG show increasing in the monthly potential evapotranspiration, the intensities are not similar. As it was shown in Figure 4-12, the sythetics weather dataset (WG) did not completely generate its source. Therfore less amount of grass reference evapotranspiration is expected for Delta-WG. In terms of trend, declining pattern is similar, mostly after May.

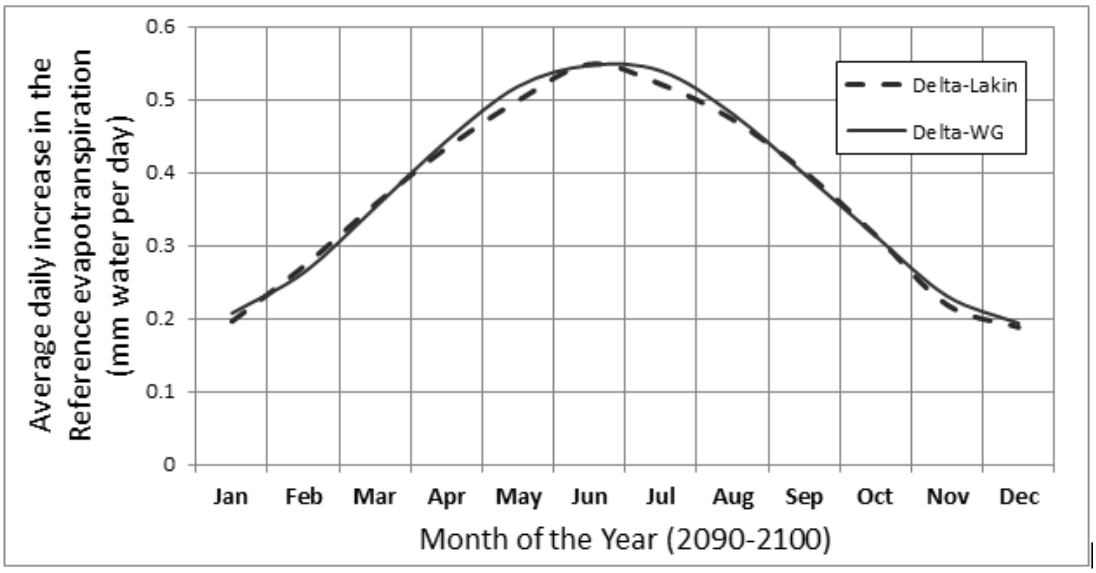


**Figure 4-13 Effect of Climate change on the daily evapotranspiration, A1b IPCC Scenario (2090-2100)**

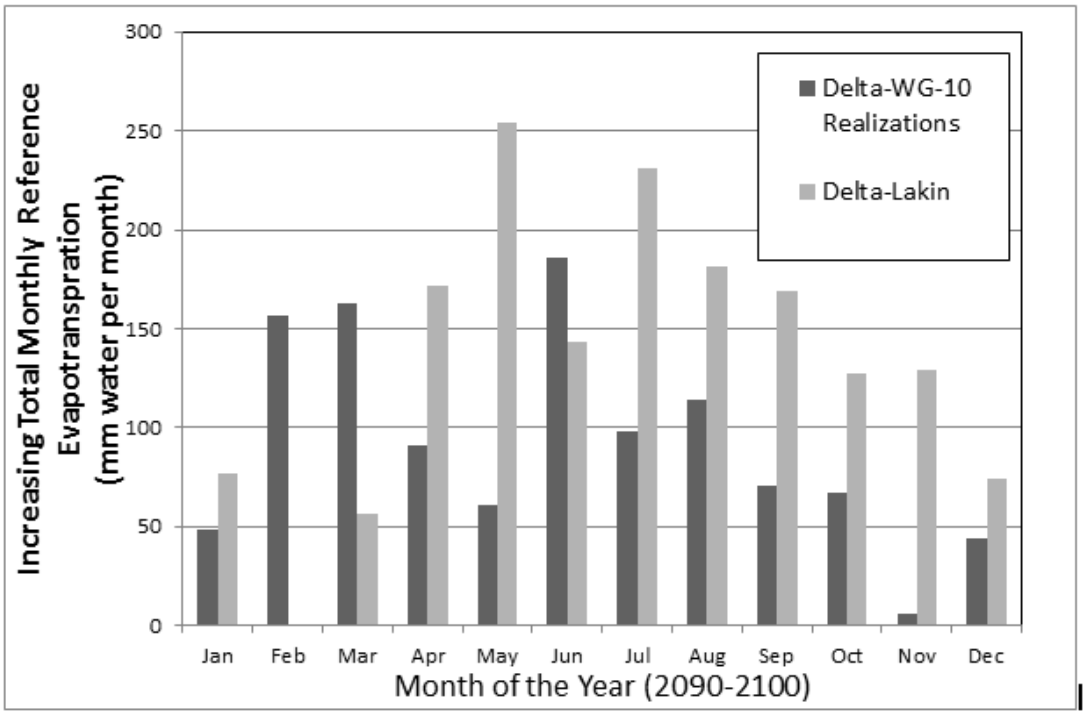


**Figure 4-14 Change in the monthly reference evapotranspiration, using the A1b IPCC Scenario**

### 4-4-2 Effect of Climate Change on the Water Budget

One field nearest to the Lakin HPRCC station was selected to analyze the effect of climate change under the A1b IPCC scenario. The baseline period was between 1980 and 1990, and the target period was between 2090 to 2100. The water holding capacity of the field, along with curve number and other data, were extracted from the ArcGIS data layers, then water budget was calculated with both the Delta-Lakin and Delta-WG for each crop. To compare the irrigation demand, daily irrigation demands were extracted from the output of the model. The figures below show potential evapotranspiration and instantaneous irrigation for Lakin, KS; a baseline average weather data from 1980 to 1990 and a climate change scenario for for two weather datastes 2090 to 2100. Instantaneous irrigation is amount of irrigated water when there is not any limiting rate for pump. Figure 4-15 and Figure 4-16 show potential evapotranspiration and instantaneous irrigation of sorghum. Figure 4-17 and Figure 4-18 show potential evapotranspiration and instantaneous irrigation of Soybean. Figure 4-19 and Figure 4-20 show potential evapotranspiration and instantaneous irrigation of Winter Wheat. As it can be seen in Figure 4-15 and Figure 4-17, potential evapotranspiration is increased by 0.5 millimeter per day for soybean and sorghum during peak time. On the other hand, the amount of potential evapotranspiration for winter wheat decreases under the climate change scenario with 1.5 millimeter of less water per day during peak time.

It can be seen in Figure 4-15, Figure 4-17, and Figure 4-19 the growth season decreases by 20, 25, 30 days for sorghum, soybean, and winter wheat, respectively

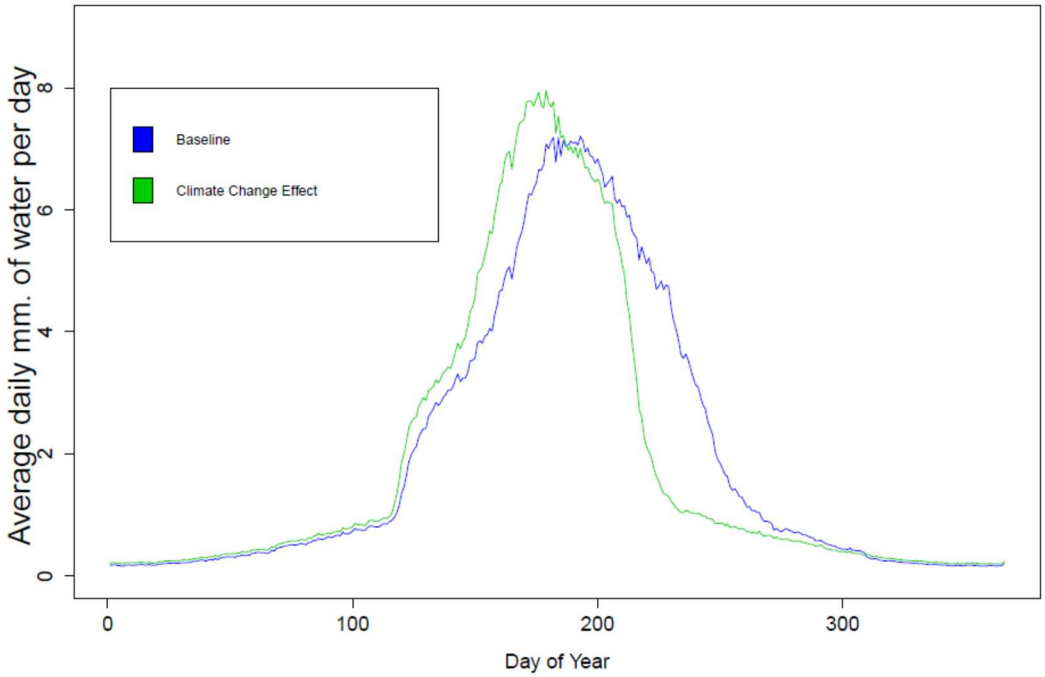


**Figure 4-15 Potential Evapotranspiration of Sorghum for two weather datastes for Lakin, KS: A baseline average weather data from 1980 to 1990 and a climate change scenario for 2090 to 2100.**

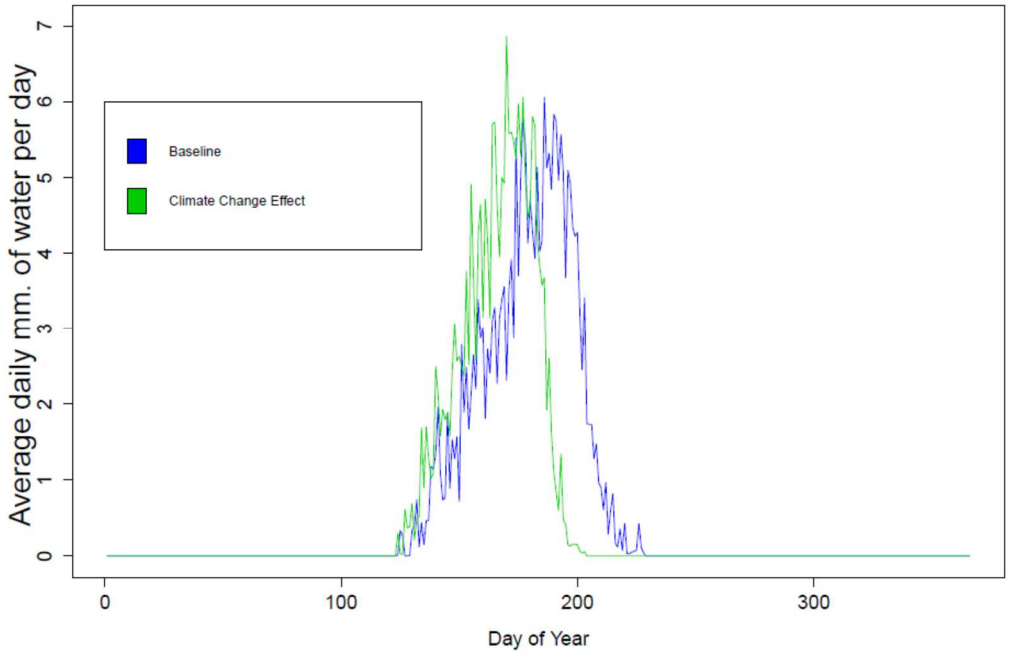


**Figure 4-16 Instantaneous Irrigation of Sorghum of Sorghum for two weather datastes for Lakin, KS: A baseline average weather data from 1980 to 1990 and a climate change scenario for 2090 to 2100**

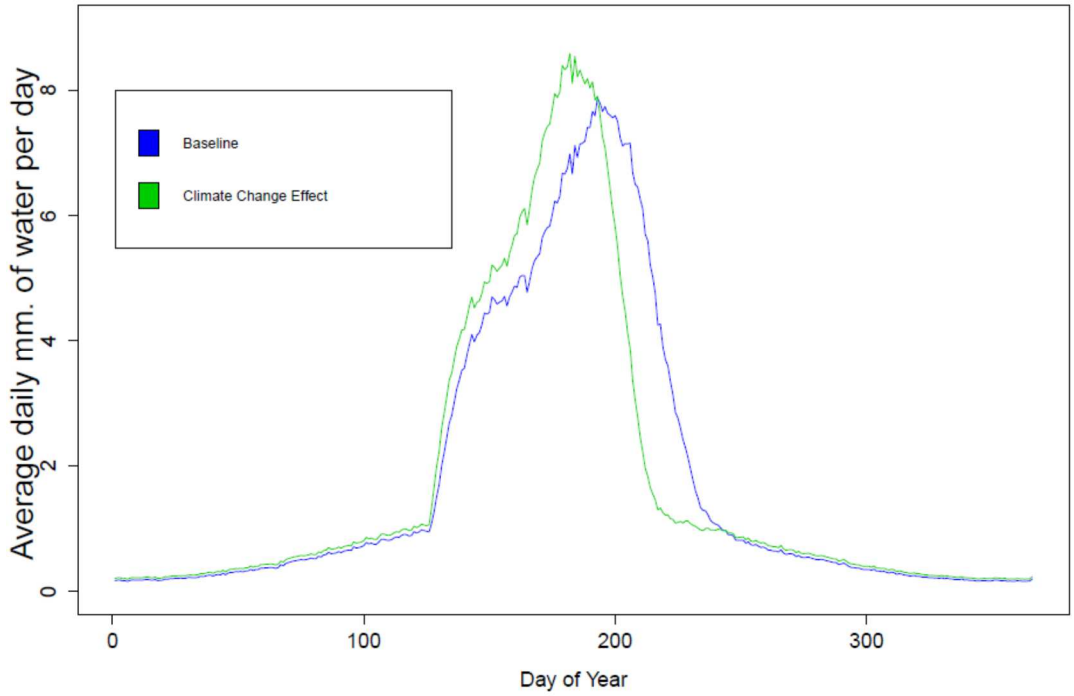


**Figure 4-17 Potential Evapotranspiration of Soybean for two weather datastes for Lakin, KS: A baseline average weather data from 1980 to 1990 and a climate change scenario for 2090 to 2100.**

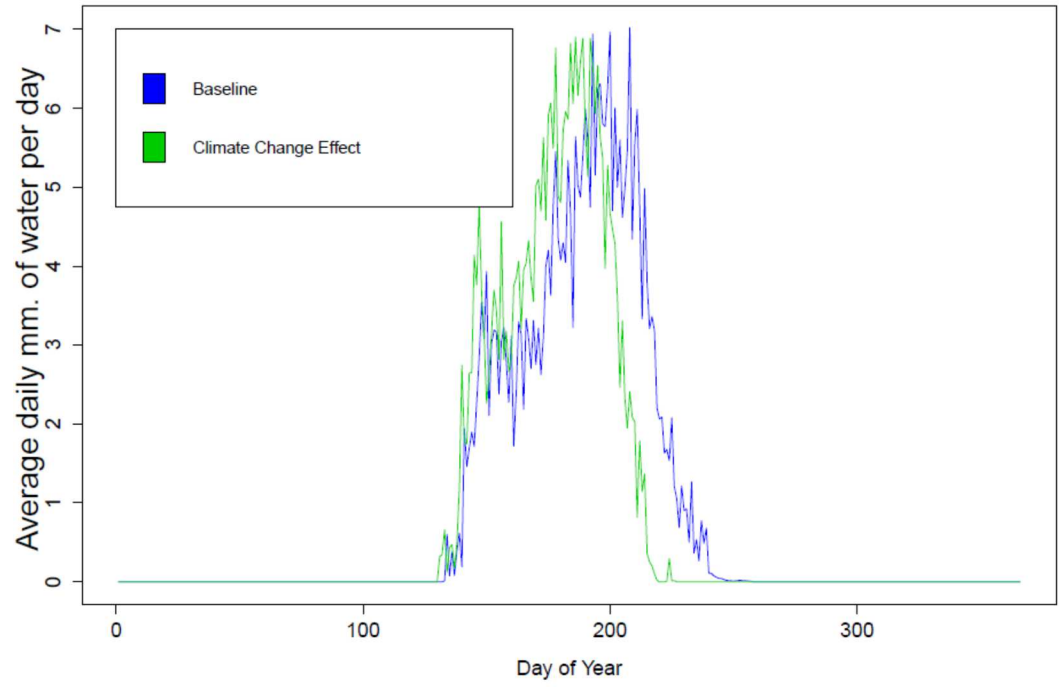


**Figure 4-18 Instantaneous Irrigation of Soybean for two weather datastes for Lakin, KS: A baseline average weather data from 1980 to 1990 and a climate change scenario for 2090 to 2100**

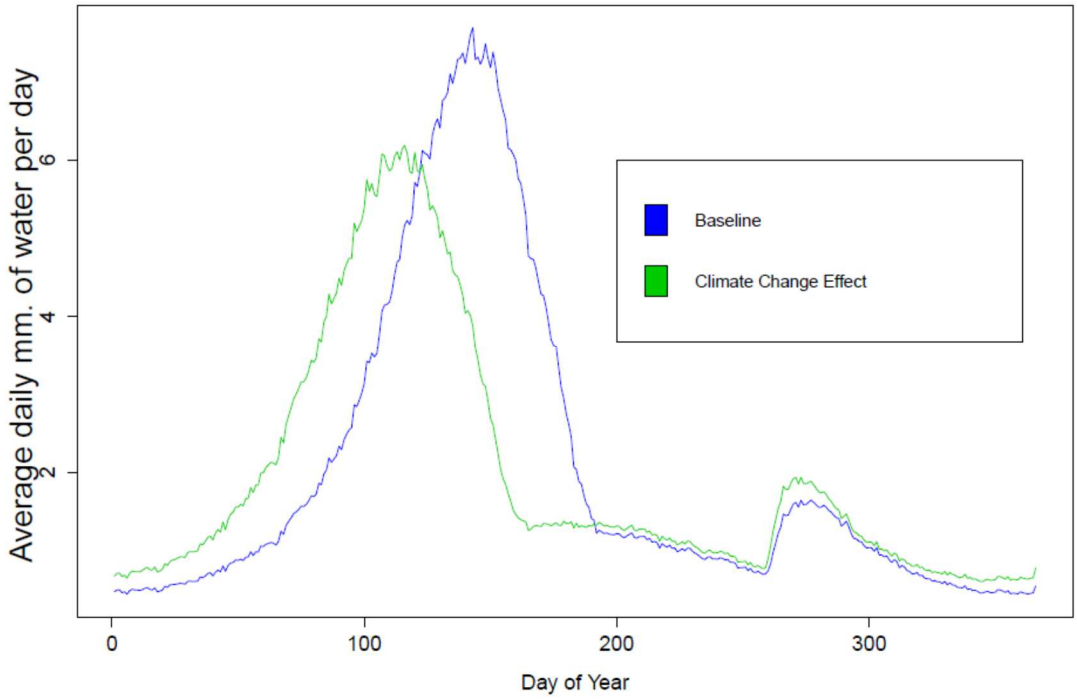


**Figure 4-19 Potential Evapotranspiration of Winter Wheat for two weather datastes for Lakin, KS: A baseline average weather data from 1980 to 1990 and a climate change scenario for 2090 to 2100**

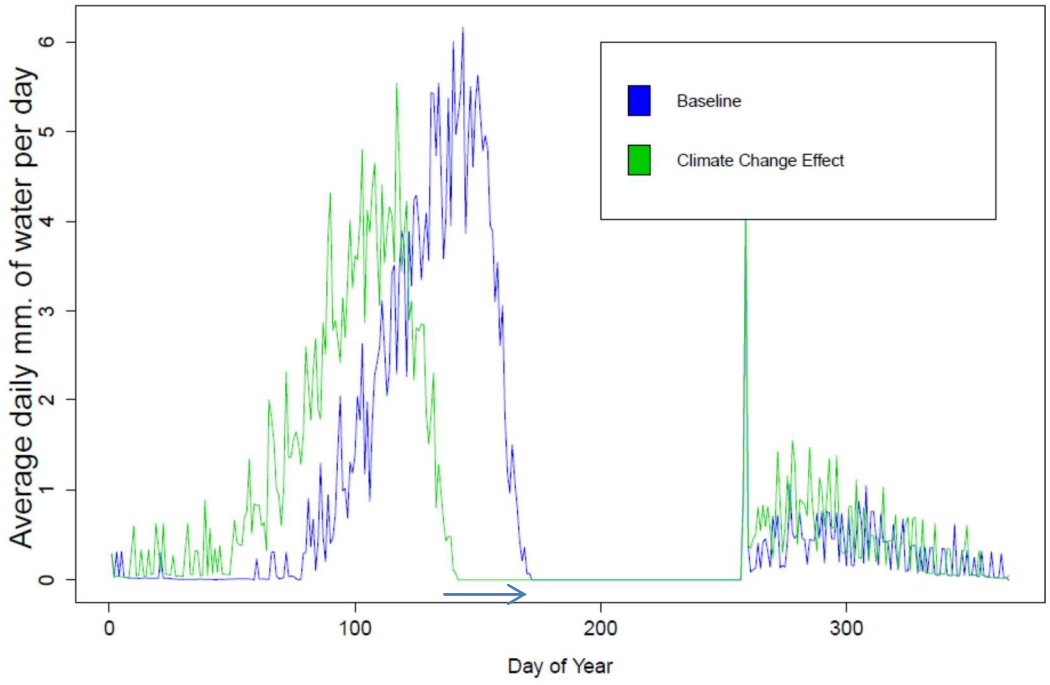


**Figure 4-20 Instantaneous Irrigation of Winter Wheat for two weather datastes for Lakin, KS: A baseline average weather data from 1980 to 1990 and a climate change scenario for 2090 to 2100**

## 4-5 Discussion of Results

The waterbudget model under-predicts irrigation demand compared to reported water-use.The water budget pridicts the minimum water requirement. In reality many factors such as irrigation managemnet practices affect the minimum requirement. Usally the actual water-use is higher than minimum water requirement. As it can bee seen in Figure 4-9 and Figure 4-10, the mean performace ratio in the eastern kansas is higher than 1. Spatially, the mean performance ratios in the west are closer to the performance ratio of field level validation.As it was shown in the Table 3-3, the distribution of used KARS LULC training dataset per crop and Agricultural District Number (ASD) were not homogenous in the study area. More fields belong to the western part of Kansas including ASD10, ASD20, ASD30, and ASD60. Because calibration was undertaken by using KARS LULC training dataset, the model produces better result in the west than east. The number of fields on the ASD 70 (Northeast) and ASD 80 (East Central) and ASD 90 (Southwest) are significantly less than other ASDs.

As it can be seen in Figure 4-10Table 4-2, the mean performance ratio in GMD 2, GMD 5, and GMD 4 are closer to the the performance ratio of field level validation. But the mean performance ratios in GMD 1, GMD 3 are not consistent with the other GMDs (2, 5, and 4). In this study, the reported (not measured) water-use was used for validation and correlation. So the accuracy of water right report could expplain the result of the model in the GMD1, GMD 3. In one study, two sets of regressions were applied for Kansas GMDs (Whittemore et al., 2014). One between groundwater level changes and climate indices, and another one between groundwater level changes and reported pumping. For GMD 2, GMD4, and GMD 5, it was shown that two sets of regressions match well (Whittemore et al., 2014). But for GMD1 and GMD3, it was

shown that climate correlates well just with groundwater level changing, not with reported pumping. The authors reach to this point that in the GMD1 and GMD 3 is greater use of less-accurate meters (Whittemore et al., 2014).

In addition to the water extraction from HPA, five irrigation districts diverting water from five US Bureau of Reclamation reservoirs in Kansas and one U.S. Army Corps of Engineers reservoir in Nebraska. The name of those irrigation districts are Almena, Kirwin, Webster, Kansas Bostwick, Glen Elder, and Lower Smoky Hill. They have surface irrigation systems and water rights. Framers who purchase water from the district will not have their usage listed in WIMAS. The total diverted water is reported under one water right for each irrigation district. For example, The Bostwick irrigation district is located in the lower republican basin. The mean performance ratios of counties in the lower republican basin (near to Bostwick) are higher than one. One explanation is using surface water. But the usage is not reported in an appropriate county or fields.

Evapotranspiration is a useful indicator for linking impacts of climate change on irrigation water demand, but the ET calculation may be limited for future conditions. In this study, it has been assumed that solar radiation will be the same in 2090-2100, without any change in cloudiness. Also, it has been assumed that no plant adaptation has happened in response to climate change. Planting dates and crop scheduling were not changed in the model. One irrigation schedule was used: when soil moisture deficit is below 60 percent, irrigation starts.

In the climate change scenario, crop development is accelerated, and the growth period is modeled as shorter, if irrigation demand is met (as is modeled in the water budget). It can be seen

in Figure 4-15, Figure 4-17, Figure 4-19 the growth season decreases by 20, 25, 30 days for sorghum, soybean, and winter wheat, respectively. In one climate change impact study, it was found that decreasing the growth period has more potential economic benefits due to increasing the land preparation time and cultivating alternative crops before or after the main crop (Gohari et al., 2013). But in other studies, it has been reported that grain yield will decease due to a shortened the life cycle (Islam et al., 2012).

The delta change or perturbation factor that has been used for constructing the climate change scenario ignores the potential changes in future weather time series including atmospheric and (or) oceanic circulation (Islam et al., 2012). Climate can change by numerous natural phenomena related to atmospheric and (or) oceanic circulation. The effect can be local or global. Whereas the North Atlantic Oscillation (NAO) and the El Niño-Southern Oscillation (ENSO) are the best identified Oscillation, others include the Pacific Decadal Oscillation (PDO) and the Atlantic Multidecadal Oscillation (AMO), which have been addressed recently (Kløve et al., 2014). Each of these phenomena could change the yearly climate regionally and seasonally. So, the world could be seasonally warmer or colder in any year (Kløve et al., 2014). The linear trend, which is used for the delta change method, assumes a constant decadal trend that is the decadal average of numerous GCM models. So climate variability could happen in any year. In other words, any year could be warmer or colder or wetter or drier.

For any model, two types of uncertainty can be expected. First, model calibration and parameterization. Second, inherent uncertainties in the model structure (Islam et al., 2012). In order to understand the possible error involved in predicting irrigation demand using the water budget, both types of uncertainties will be discussed.

### 4-5-1 Uncertainty of Model Calibration and Parameterization

For model calibration, constant numbers have been used for four types of parameters including irrigation efficiency, root depth and cutting cycle, crop acreage MAD levels. Among them, the MAD level is highly dependent on human decision-making. Each of these parameters are discussed in detail below.

#### 4-5-1-1 Irrigation Efficiency

Irrigation or water conveyance efficiency is defined as the ratio of the volume of water spread to the volume of water diverted from the source. Irrigation water can be pumped and diverted through canals or pipelines (Howell, 2003). Water loss and seepage in canals are higher than in pipeline conveyance systems. Poor maintenance and material deterioration are two main reasons of declining conveyance efficiency in any kind of system (Howell, 2003).

In addition to the water conveyance efficiency, field irrigation application efficiency depends on the irrigation equipment. It has been shown that the surface irrigation or flood irrigation method has an efficiency between 40 to 70 percent (Howell, 2003). For center pivot systems, the range is between 75 and 98 percent. For sprinkle systems, it is between 60 and 90 percent (Howell, 2003). For micro-irrigation systems, including trickle and subsurface drip irrigation, it is between 75 and 95 percent (Howell, 2003).

According to those numbers, there are wide ranges for irrigation efficiency. As seen in Figure 4-4, Figure 4-6, Figure 4-7, and Figure 4-8, the mean model performance ratios for all crops irrigated by flood irrigation are less than the other systems. In addition, the performance ratio for two types of center pivot irrigation systems is seemingly equal. In this study, the irrigation efficiency was set to 90 percent for center pivot systems. The irrigation efficiency has

been considered equal for all water groups, whereas in reality, the efficiency changes spatially and temporally with the age and type of irrigation system for any individual water.

#### 4-5-1-2 Alfalfa Cutting Cycles:

The uniqness of alfalfa regarding the cutting cycles can explain why mean performance ratio of this crop performs differently than corn, sorghum, soybean, and wheat. In Figure 4-2, the performance ratio for alfalfa is much higher than the other crops with a mean average of 1.4. In the model, three cutting cycles for alfalfa were simulated using a GDD approach, but this may not reflect actual farming practices within Kansas.

#### 4-5-1-3 Remote Sensing Mapping Approach

For field level analysis, KARS extracted irrigated crop acreage from the LULC layer using a hybrid approach between remote sensing and authorized PLU . The remote sensing approach used satellite vegetation index profiling for the irrigated and non-irrigated crops (Peterson et al., 2012). KARS compared the results from its mapping tool with known irrigated crops from the training data set, and the method had a high accuracy (80 - 90%) (Peterson et al., 2012). Mapping irrigated and non-irrigated fields is most difficult for winter wheat and sorghum. In addition, separating irrigated from non-irrigated fields for any crop becomes more difficult as one moves east, in the east rainfall becomes less of a limiting factor for crop development (Kastens, 2015b).

#### 4-5-1-4 Human Factor

Model results indicates that optimal temporal allocation of irrigation water and quantifying the crop responses to water during growing season is feasible. While potential

evapotranspiration calculation and irrigation water requirement, along with a simple rainfall model are deterministic, a farmers' irrigation function remains unquantified.

"The objective function of irrigation could be profit maximization or yield maximization, which defines a set of optimal irrigation policies" (Bras et al., 1981). During water short times, severe water-stress might affect crop yield and profitability. As the result, irrigation timing is very important in individual fields when water is not available. Often farmers save water by eliminating unnecessary irrigation and maintaining soil moisture at lower level (Upendram & Peterson, 2006). Farmers use a MAD level to cope with water stress. MAD is typically an allowed soil-water deficit between 0 and 0.4 from scale 1 (Upendram & Peterson, 2006). A MAD level 0 and .4 equates to a minimum soil moisture level between 100 and 60 percent, respectively. The MAD level can be changed by a farmer during the season to respond to drought conditions and maximize crop yield. Farmers could use a number of managerial decisions affecting water-use which will result in different crop yields. These nuances are not modeled in the water budget presented here.

Crop yield is defined with the following formula based on the FAO definition, where $Y_a$ and $Y_x$ are actual and maximum yields, $ET_a$ and $ET_x$ are the actual and maximum evapotranspiration, and $K_y$ is a yield response factor, which shows the effect of a reduction in evapotranspiration on yield losses (Steduto et al., 2012).

$$\left(1 - \frac{Y_a}{Y_x}\right) = K_y \left(1 - \frac{ET_a}{ET_x}\right)$$

The yield response factor is crop specific and changes during crop growing season. If $K_y > 1$ , it indicates that the crop has a high sensitivity to water deficit, with relatively large yield declines.

On the other hand, if the yield response factor of the crop is less than one, it indicates that the crop has a low sensitivity to water deficit. A low $K_y$ value also indicates that a crop can recover from water-stress with less proportional yield reduction than a crop with a high $K_y$ value. The seasonal yield response factors for alfalfa, sorghum, soybean, and winter wheat are 1.1, 0.90, .85, and 1.05, respectively (Steduto et al., 2012). By definition, sorghum and soybean can tolerate water deficit better than other crops. Farmers are knowledgeable regarding crop sensitivities, and they will selecting MAD levels based on their objective function, the environment, and their risk aversion behavior. In the water budget presented here, a MAD level of 0.60 was modeled for all crops, but it is likely that the actual MAD level differs for crops and farmers. This would explain variance observed in the performance ratios.

### 4-5-2 Uncertainty in the Model Structure- AE method

The Hargreaves–Samani (HS) evapotranspiration equation has been used effectively for on-site irrigation management with limited data inputs for small and midsize farms (Shahidian et al., 2013b). It has been shown that using the standard method of HS can overestimate evapotranspiration in humid zones and underestimate it in arid and windy zones. Based on the county-level results, the model overpredicts on eastern part compared to western part (Ravazzani et al., 2012). In Kansas, the western part contains arid zones, while the eastern part is humid. The known bias of the HS method can explain the overestimation and underestimation of the HS method in both zones. Many studies have been conducted to improve precision of the reference evapotranspiration (ETo) estimates (Ravazzani et al., 2012; Sepaskhah et al., 2009; Shahidian et al., 2013a). As described earlier, the HS equation used for $ET_0$ is

$$ET_0 = 0.0023(T_{max} - T_{min})^2 \, (T_{mean} + 17.8)R_{\alpha}$$

where $ET_0$ in mm/day, $T_{max}$ and $T_{min}$ are maximum and minimum daily temperatures in C°, and $R_\alpha$ is extraterrestrial radiation in $MJ/m^2$ day or equivalent evaporated water depth (mm/day).

However, the original form of the equation is (Samani, 2000):

$$ET_0 = 0.0135\ K_T(T_{max} - T_{min})^2\ (T_{mean} + 17.8)R_\alpha$$

Where $K_T$, radiation adjustment coefficient, is an empirical coefficient that was initially fixed at 0.17 for Salt Lake City, Utah by Samani (Samani, 2000). Assuming a constant value of $K_T$, then 0.0135 $K_T$ is equal to 0.0023. However, $K_T$ could range between 0.16 to 0.24 (Samani, 2000). Samani has shown that this coefficient can take into account the effect of cloudiness and humidity on solar radiation of any desired location. Many efforts have been done to calibrate the radiation adjustment coefficient, such as parametric calibration, linear regression with lysimeter data, altitude, temperature differences. To date, the results are not consistent and are the subject of ongoing research (Shahidian et al., 2013b).

### 4-5-3 Limitation of the Coupling Water Budget Model and Climate Change Effect

In this study, the effects of elevated $CO_2$ were not included in the calculation of reference evapotranspiration. It has been shown that $CO_2$ concentration will affect the reference evapotranspiration, and this is the subject of ongoing research (Cheng et al., 2014; Dijkstra et al., 1999; Twine et al., 2013).

## 4-6 Recommendations

The developed model and methodology can be used as a framework for calculating crop water requirements. By adjusting input parameters (average weather, soil properties, crop

choice), the model can be used as a decision-making tool for farmers and agencies. Also, the soil-water framework is a model that can be used to calculate direct groundwater recharge phenomena (Dripps et al., 2007; Finch et al., 1998). Asdescribed in the methodology section, the soil-water balance model was developed for recharge estimation. Under climate change the pattern and timing of groundwater recharge will be changed (Kløve et al., 2014), so the model could be used to study groundwater recharge under various climate change secnarios.The model provides great flexibility to calculate the temporal and spatial recharge rate in Kansas.

The water budget approach can be performed at multiple spatial scale, from field-level to regional estimates. This can be useful for finding problamatic zones of irrigation water-use at numerous spatial levels and connecting the findings across different administrative levels. The study and method provide an understanding of irrigation requirements with large geographic coverage, across a wide distribution of crops, soil conditions, and climate. Also the method can estimate net irrigation requirements, using numerous irrigation strategies, which can help irrigators to adapt irrigation more specifically to soil and weather conditions along with crop growth.

## References:


Allen, R. (2000). Using the fao-56 dual crop coefficient method over an irrigated region as part of an evapotranspiration intercomparison study. *Journal of Hydrology, 229*(1-2), 27-41.

Allen, R. (2005). *The asce standardized reference evapotranspiration equation*: American Society of Civil Engineers.

Allen, R.G., Pereira, L.S., Raes, D., & Smith, M. (1998). Crop evapotranspiration-guidelines for computing crop water requirements-fao irrigation and drainage paper 56. *FAO, Rome, 300*.

Alley, W.M. (1984). On the treatment of evapotranspiration, soil moisture accounting, and aquifer recharge in monthly water balance models. *Water Resources Research, 20*(8), 1137-1149. doi: 10.1029/WR020i008p01137

Bras, R.L., & Cordova, J.R. (1981). Intraseasonal water allocation in deficit irrigation. *Water Resources Research, 17*(4), 866-874. doi: 10.1029/WR017i004p00866

Brian D Wardlow, S.L.E., Jude H Kastens. (2007). Analysis of time-series modis 250 m vegetation index data for crop classification in the u.S. Central great plains. *Remote Sensing of Environment, 108*(3), 290-310. doi: 10.1016/j.rse.2006.11.021

Brian D. Wardlow, J.H.K., and Stephen L. Egbert. (2006). Using usda crop progress data for the evaluation of greenup onset date calculated from modis 250-meter data. *Photogrammetric Engineering & Remote Sensing, 72*(11).

Brown, D.G., Walker, R., Manson, S., & Seto, K. (2004). Modeling land use and land cover change *Land change science* (pp. 395-409): Springer.

Bruce M. McEnroe, P.G. (2003). Storm duration and antecedent moisture conditions for flood discharge estimation *Report No. K-TRAN: KU-02-4*. University of Kansas.

Brunsell, N.A., Jones, A.R., Jackson, T.L., & Feddema, J.J. (2010). Seasonal trends in air temperature and precipitation in ipcc ar4 gcm output for kansas, USA: Evaluation and implications. *International Journal of Climatology, 30*(8), 1178-1193.

Buchanan, R.C., Buddemeier, R.R., & Wilson, B.B. (2009). Public information circular 18 - the high plains aquifer. Lawrence: Kansas Geological Survey.

Cheng, L., Zhang, L., Wang, Y.-P., Yu, Q., Eamus, D., O'Grady, A., . . . O'Grady, A. (2014). Impacts of elevated co2, climate change and their interactions on water budgets in four different catchments in australia. *Journal of Hydrology, 519*, 1350-1361. doi: 10.1016/j.jhydrol.2014.09.020

Colaizzi, P., Gowda, P., Marek, T., & Porter, D. (2009). Irrigation in the texas high plains: A brief history and potential reductions in demand. *Irrigation and Drainage, 58*(3), 257-274.

Danny H. Rogers, G.M.P., and Kerri Ebert. (2013). Water primer, part 5: Water law: Kansas State University.

Dennehy, K., Litke, D., & McMahon, P. (2002). The high plains aquifer, USA: Groundwater development and sustainability. *Geological Society, London, Special Publications, 193*(1), 99.

Dennehy, K.F., & US Geological Survey. (2000). *High plains regional ground-water study*: US Department of the Interior.

Dermyer, R. (2011). *Modeling the high plains aquifer's response to land use and climate change.* (M.S.), University of Kansas.

Dijkstra, P., Schapendonk, A., Groenwold, K., Jansen, M., Van de Geijn, S.C., Dijkstra, P., . . . Van de Geijn, S.C. (1999). Seasonal changes in the response of winter wheat to elevated atmospheric co2 concentration grown in open-top chambers and field tracking enclosures. *Glob. Change Biol., 5*(5), 563-576.

Douglas G. Goodin, J.E.M., Mary C. Knapp, Raymond E. Bivens. (1995). *Climate and weather atlas of kansas-an introduction*

Dridi, C., Khanna, M., Dridi, C., & Khanna, M. (2005). Irrigation technology adoption and gains from water trading under asymmetric information. *American Journal of Agricultural Economics, 87*(2), 289-301. doi: 10.1111/j.1467-8276.2005.00722.x

Dripps, W., Bradbury, K., Dripps, W., & Bradbury, K. (2007). A simple daily soil-water balance model for estimating the spatial and temporal distribution of groundwater recharge in temperate humid areas. *Hydrogeol. J., 15*(3), 433-444. doi: 10.1007/s10040-007-0160-6

Finch, J.W., & Finch, J.W. (1998). Estimating direct groundwater recharge using a simple water balance model – sensitivity to land surface parameters. *Journal of Hydrology, 211*(1), 112-125. doi: 10.1016/S0022-1694(98)00225-X

Flora, S.D. (1988). *Climate of kansas*. Retrieved 285, LXVII, Retrieved from http://www.ksre.ksu.edu/wdl/climate/cok/indexcopy.asp?page=i

Fraser, E., Stringer, L.C., Fraser, E., & Stringer, L.C. (2009). Explaining agricultural collapse: Macro-forces, micro-crises and the emergence of land use vulnerability in southern romania. *Glob. Environ. Change-Human Policy Dimens., 19*(1), 45-53. doi: 10.1016/j.gloenvcha.2008.11.001

FSA. (2013). *Common land unit (clu)*. Retrieved from: http://www.fsa.usda.gov/FSA/apfoapp?area=home&subject=prod&topic=clu

Furrer, E., & Katz, R. (2007). Generalized linear modeling approach to stochastic weather generators. *Climate Research, 34*, 129-144. doi: 10.3354/cr034129

Gohari, A., Eslamian, S., Abedi-Koupaei, J., Bavani, A.M., Wang, D., Madani, K., . . . Madani, K. (2013). Climate change impacts on crop production in iran's zayandeh-rud river basin. *The Science of the Total Environment, 442*, 405.

Griensven, A.V., Meixner, T., Grunwald, S., Bishop, T., & M Diluzio, R.S. (2006). A global sensitivity analysis tool for the parameters of multi-variable catchment models. *Journal of hydrology, 324*(1), 10-23. doi: 10.1016/j.jhydrol.2005.09.008

Gutentag, E.D., Heimes, F.J., Krothe, N.C., Luckey, R.R., & Weeks, J.B. (1984). *Geohydrology of the high plains aquifer in parts of colorado, kansas, nebraska, new mexico, oklahoma, south dakota, texas, and wyoming*. (U.S. Geological Survey Professional Paper 1400-B). Washington: United States Government Printing Office.

Hamon, W. (1963). Computation of direct runoff amounts from storm rainfall.

Hansen, C.V. (1991). Estimates of freshwater storage and potential natural recharge for principal aquifers in kansas. *Available from Books and Open File Report Section, USGS, Box 25425, Denver, CO 80225. USGS Water-Resources Investigations Report 87-4230, 1991. 100 p, 19 fig, 4 tab, 66 ref. USGS Project*.

Hargreaves, G., & Samani, Z. (1984). Economic considerations of deficit irrigation. *Journal of Irrigation and Drainage Engineering, 110*(4), 343-358. doi: 10.1061/(ASCE)0733-9437(1984)110:4(343)

Hay, L.E., Wilby, R.L., & Leavesley, G.H. (2000). A comparison of delta change and downscaled gcm scenarios for three mounfainous basins in the united states1. *JAWRA*

*Journal of the American Water Resources Association, 36*(2), 387-397. doi: 10.1111/j.1752-1688.2000.tb04276.x
Hecox, G.R., Macfarlane, P.A., & Wilson, B.B. (2002). Calculation of yield for high plains wells: Relationship between saturated thickness and well yield: KGS.
Hock, R. (2003). Temperature index melt modelling in mountain areas. *Journal of Hydrology, 282*(1), 104-115. doi: 10.1016/S0022-1694(03)00257-9
Howell, T.A. (2003). Irrigation efficiency *Encyclopedia of Water Science* (pp. 467-472). New York: Marcel Dekker.
Howell, T.A., & Evett, S.R. (2004). The penman-monteith method.
HPRCC. 2015/01/15/01:11:39). *Automated weather data network - high plains regional climate center*. Retrieved from http://www.hprcc.unl.edu/awdn/et/
IPSR. (2012). *Biofuels and climate change: Farmers' land use decisions*. 2015, Retrieved from http://www.ipsr.ku.edu/CEP/BACC/
Islam, A., Ahuja, L.R., Garcia, L.A., Ma, L., Saseendran, A.S., & Trout, T.J. (2012). Modeling the impacts of climate change on irrigated corn production in the central great plains. *Agricultural Water Management, 110*, 94-108. doi: 10.1016/j.agwat.2012.04.004
Jensen, M., Burman, R., & Allen, R. (1990). *Evapotranspiration and irrigation water requirements*.
Kastens, J. (2015a, 23/1/2015). [Clu boundary ].
Kastens, J.E. (2015b, 1/23/2015). [Separating irrigated from non-irrigated fields ].
Kastens, J.H. (2014). [Description of lulc dataset].
Kløve, B., Ala-Aho, P., Bertrand, G., Gurdak, J.J., Kupfersberger, H., Kværner, J., . . . Pulido-Velazquez, M. (2014). Climate change impacts on groundwater and dependent ecosystems. *Journal of Hydrology, 518*, 250-266. doi: 10.1016/j.jhydrol.2013.06.037
Konikow, L.F. (2013). Groundwater depletion in the united states (1900–2008) (2013 ed.): U.S. Department of the Interior,U.S. Geological Survey.
Kranz, W.L., Martin, D.L., Irmak, S., Donk, S.J.v., & Yonts, C.D. (2008). *Minimum center pivot design capacities in nebraska*: Cooperative Extension, Institute of Agriculture and Natural Resources, University of Nebraska-Lincoln.
Mair, A., Hagedorn, B., Tillery, S., El-Kadi, A.I., Westenbroek, S., Ha, K., & Koh, G.-W. (2013). Temporal and spatial variability of groundwater recharge on jeju island, korea. *Journal of Hydrology, 501*, 213-226. doi: 10.1016/j.jhydrol.2013.08.015
McGuire, V.L. (2007). *Water-level changes in the high plains aquifer, predevelopment to 2005 and 2003 to 2005*.
McGuire, V.L. (2009). *Water-level changes in the high plains aquifer, predevelopment to 2007, 2005-06, and 2006-07*. (Scientific Investigations Report 2009-5019). Reston, Virginia: U.S. Geological Survey,.
McMaster, G.S., & Wilhelm, W.W. (1997). Growing degree-days: One equation, two interpretations. *Agricultural and Forest Meteorology, 87*(4), 291-300.
Mesinger, F., DiMego, G., Kalnay, E., Mitchell, K., Shafran, P.C., Ebisuzaki, W., . . . Shi, W. (2006). North american regional reanalysis.(author abstract). *Bulletin of the American Meteorological Society, 87*(3), 343.
NRCS. (2004). *Soil survey geographic (ssurgo) database for kansas*. Washington, DC: Retrieved from http://soildatamart.nrcs.usda.gov.
Peck, J.C. (2002). Property rights in groundwater--some lessons from the kansas experience. *The Kansas Journal of Law & Public Policy*.

Peck, J.C. (2005). Groundwater management in kansas: A brief history and assessment. *Kansas Journal of Law and Public Policy, 15*, 441.

Perry, C.A. (2006). Effects of irrigation practices on water use in the groundwater management districts within the kansas high plains, 1991–2003 *Scientific Investigations Report 2006–5069*.

Peterson, D., Whistler, J., Bishop, C., & Kastens, J. (2012). *Mapping irrigated cropland in kansas*. University of Kansas-KARS. Retrieved from http://www.magicgis.org/magic/symposiums/2012/SympPresentations/Peterson_MAG399.pdf

Peterson, J.M. (2014). *Motivations and impediments underlying irrigation decisions.* Paper presented at the Kansas Water Symposium University of Kansas

Peterson, J.M., & Ding, Y. (2005). Economic adjustments to groundwater depletion in the high plains: Do water-saving irrigation systems save water? *American Journal of Agricultural Economics, 87*(1), 147-159. doi: 10.1111/j.0002-9092.2005.00708.x

Piccinni, G., Ko, J., Wentz, A., Leskovar, D., Marek, T., & Howell, T. (2007). Determination of crop coefficients (kc) for irrigation management of crops. *28th Annual International Irrigation Show, San Diego, CA, December*, 9–12.

Ravazzani, G., Corbari, C., Morella, S., Gianoli, P., & Mancini, M. (2012). Modified hargreaves-samani equation for the assessment of reference evapotranspiration in alpine river basins. *Journal of Irrigation and Drainage Engineering, 138*(7), 592-599. doi: 10.1061/(ASCE)IR.1943-4774.0000453

Rogers, D.H. (1995). *Using evapotranspiration reports for center pivot irrigation scheduling*: Cooperative Extension Service, Kansas State University.

Rogers, D.H., & Koelliker, J.K. (2011). *Evaluating center pivot, nozzle-package performance.* Paper presented at the Central Plains Irrigation Conference, Burlington, CO.

Rogers, D.H., & Service, K.S.U.C.E. (1997). *Efficiencies and water losses of irrigation systems*: Cooperative Extension Service, Kansas State University.

Samani, Z. (2000). Estimating solar radiation and evapotranspiration using minimum climatological data.(statistical data included). *Journal of Irrigation and Drainage Engineering, 126*(4), 265.

Schlenker, W. (2014). Daily weather data: Original vs knock-off. Retrieved from http://www.g-feed.com/2014/04/daily-weather-data-original-vs-knock-off.html

Sepaskhah, A.R., & Razzaghi, F. (2009). Evaluation of the adjusted thornthwaite and hargreaves-samani methods for estimation of daily evapotranspiration in a semi-arid region of iran. *Archives of Agronomy and Soil Science, 55*(1), 51-66. doi: 10.1080/03650340802383148

Serneels, S., Lambin, E., Serneels, S., & Lambin, E. (2001). Proximate causes of land-use change in narok district, kenya: A spatial statistical model. *Agric. Ecosyst. Environ., 85*(1-3), 65-81.

Shahidian, S., Serralheiro, R.P., Serrano, J., & Teixeira, J.L. (2013a). Parametric calibration of the hargreaves-samani equation for use at new locations: Calibration of the hargreaves equation. *Hydrological Processes, 27*(4), 605-616. doi: 10.1002/hyp.9277

Shahidian, S., Serralheiro, R.p., Serrano, J., & Teixeira, J.l. (2013b). Parametric calibration of the hargreaves–samani equation for use at new locations. *Hydrological Processes, 27*(4), 605-616. doi: 10.1002/hyp.9277

Sik, H., Jeonju, C.a., & Korea, S. (2014). A stochastic model for options and strategiesfor the spanish agricultural sector under climate change *Reports on Earth System Science*. Hamburg.
Sophocleous, M. (2005). Groundwater recharge and sustainability in the high plains aquifer in kansas, USA. *Hydrogeology Journal, 13*(2), 351-365.
Sophocleous, M., & Perkins, S.P. (2000a). Methodology and application of combined watershed and ground-water models in kansas. *Journal of Hydrology, 236*(3-4), 185-201.
Sophocleous, M., & Schloss, J.A. (2000b). Estimated annual groundwater recharge *An Atlas of the Kansas High Plains Aquifer*.
Sophocleous, M.A., & Wilson, B.B. (2000c). *Surface water in kansas and its interactions with groundwater*. *An Atlas of the Kansas High Plains Aquifer.* Retrieved from http://www.kgs.ku.edu/HighPlains/atlas/atswqn.htm
Steduto, P., Food, & Agriculture Organization of the United, N. (2012). *Crop yield response to water*. Rome: Food and Agriculture Organization of the United Nations.
Steward, D.R., Bruss, P.J., Yang, X., Staggenborg, S.A., Welch, S.M., & Apley, M.D. (2013). Tapping unsustainable groundwater stores for agricultural production in the high plains aquifer of kansas, projections to 2110. *Proceedings of the National Academy of Sciences, 110*(37), E3477-E3486. doi: 10.1073/pnas.1220351110
Thornthwaite, C.W. (1948). *An approach toward a rational classification of climate*: American Geographical Society.
Twine, T., Bryant, J., Richter, K., Bernacchi, C.J., McConnaughay, K., Morris, S.J., . . . Leakey, A. (2013). Impacts of elevated co2 concentration on the productivity and surface energy budget of the soybean and maize agroecosystem in the midwest USA. *Glob. Change Biol., 19*(9), 2838-2852. doi: 10.1111/gcb.12270
U.S. Geological Survey. (2010). *High plains water-level monitoring study*. Retrieved May 25, 2011, Retrieved from http://ne.water.usgs.gov/ogw/hpwlms/
Upendram, S., & Peterson, J.M. (2006). Optimal irrigation schedules and estimation of corn yield under varying well capacities and soil moisture levels in western kansas: AgEcon Search.
USDA-NRCS. (1986). Urban hydrology for small watersheds.
Verburg, P., Schot, P., Dijst, M., & Veldkamp, A. (2004a). Land use change modelling: Current practice and research priorities. *GeoJournal, 61*(4), 309-324. doi: 10.1007/s10708-004-4946-y
Verburg, P.H., Schot, P.P.D., & Martin J., V., A. (2004b). Land use change modelling: Current practice and research priorities. *GeoJournal, 61*(4), 309-324. doi: http://dx.doi.org/10.1007/s10708-004-4946-y
Westenbroek, S.M., Kelson, V.A., Dripps, W.R., Hunt, R.J., & Bradbury, K.R. (2012). Swb—a modified thornthwaite-mather soil-water-balance code for estimating groundwater recharge (pp. 60): .S. Geological Survey Techniques and Methods 6–A31, .
White, S.S., & Selfa, T. (2013). Shifting lands: Exploring kansas farmer decision-making in an era of climate change and biofuels production. *Environmental Management, 51*(2), 379-391. doi: 10.1007/s00267-012-9991-6
Whittemore, D.O., Butler, J.J., Wilson, B.B., Whittemore, D.O., Butler, J.J., & Wilson, B.B. (2014). Assessing the major drivers of water-level declines: New insights into the future of heavily stressed aquifers. *Hydrological Sciences Journal*. doi: 10.1080/02626667.2014.959958

Wilks, D.s., & Wilby, R.l. (1999). The weather generation game: A review of stochastic weather models. *Progress in Physical Geography, 23*(3), 329-357.
Wilson, B., Bartley, J., Emmons, K., Bagley, J., Wason, J., & Stankiewicz, S. (2005). Kgs ofr 2005-30: Water information management and analysis system (wimas), version 5, for the web. User manual. *KGS Open-file Report*.

# Appendix

## Appendix A: Weather Datasets Comparisons

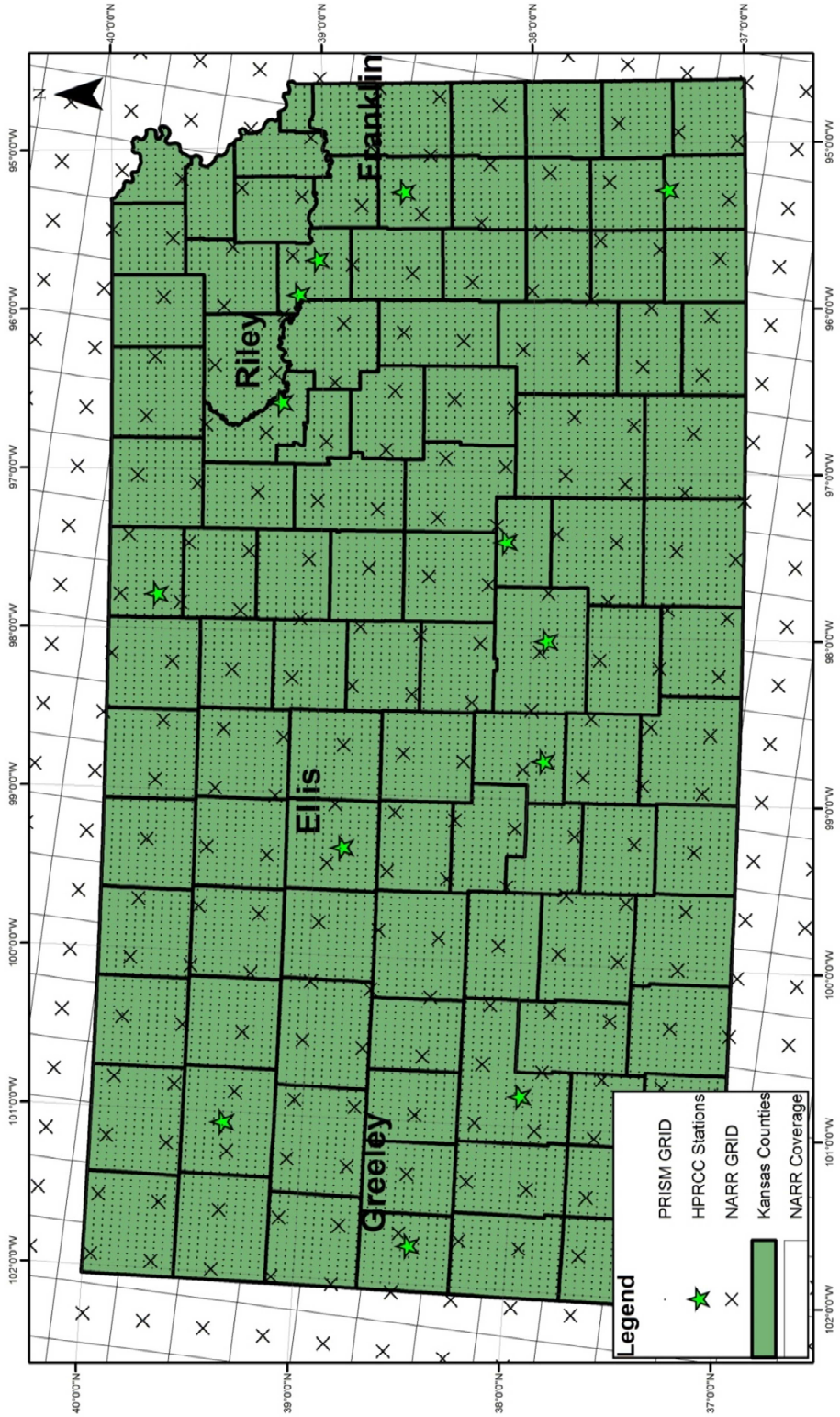


Spatial Coverage of HPRCC stations, NARR, PRISM grid

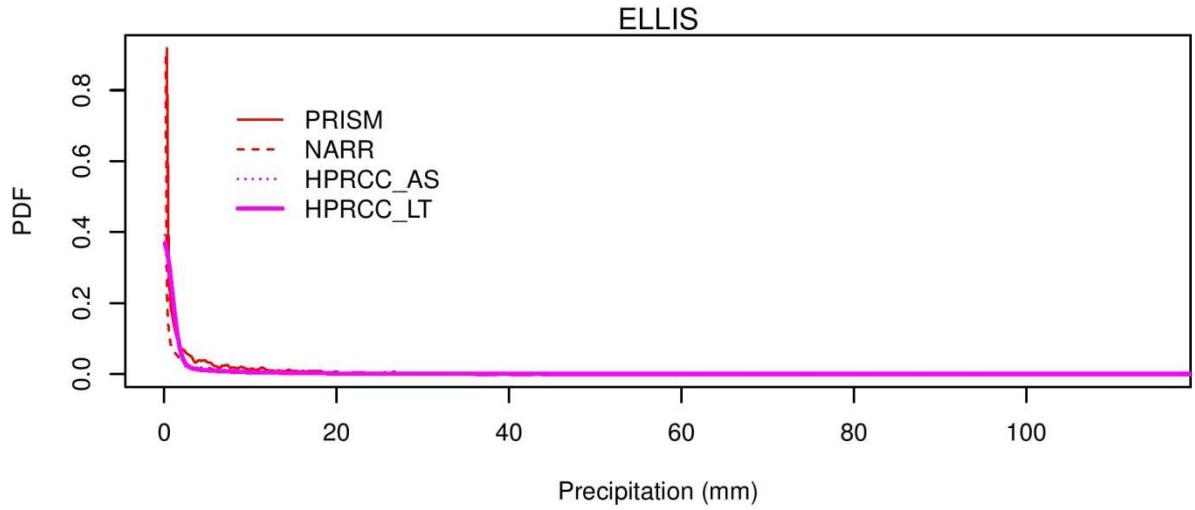


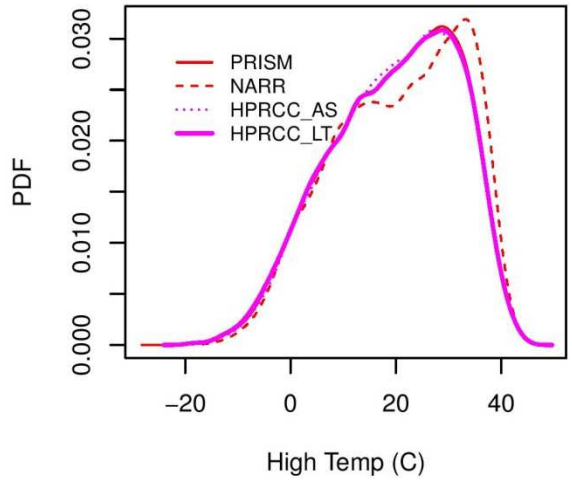


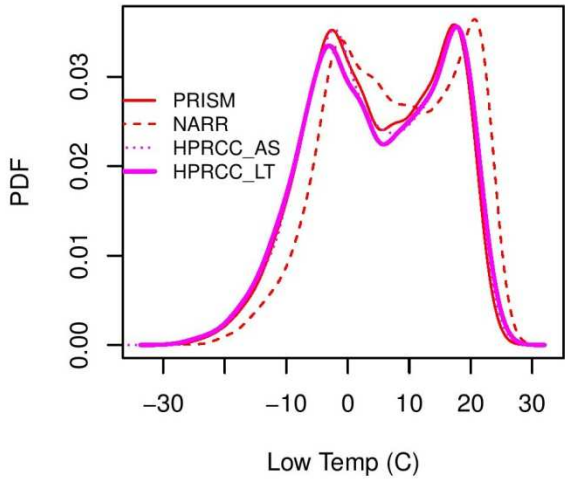


Probability distribution functions (PDF) of maximum and minimum temperature and precipitation for PRISM, NARR, and HPRCC datasets for Ellis

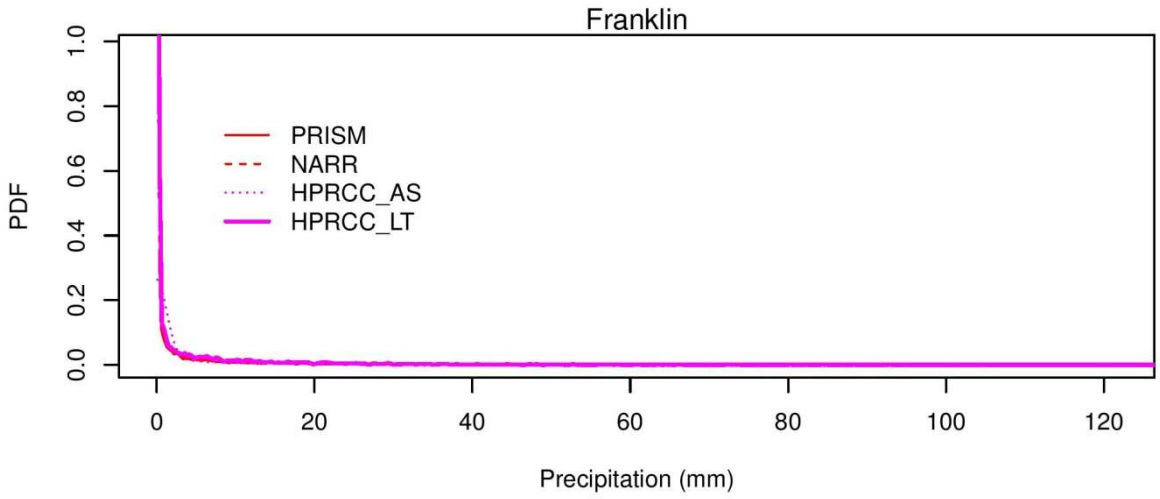


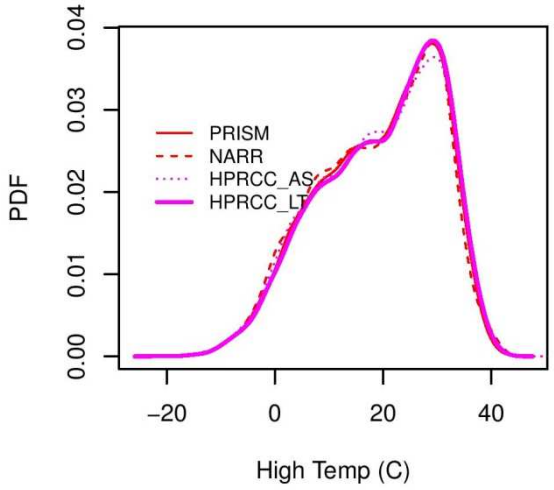


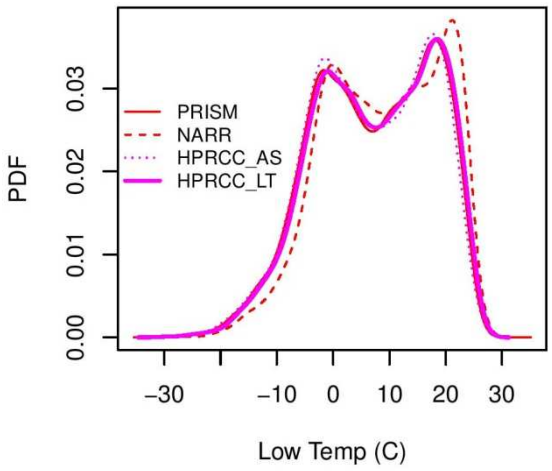


Probability distribution functions (PDF) of maximum and minimum temperature and precipitation for PRISM, NARR, and HPRCC datasets for Franklin

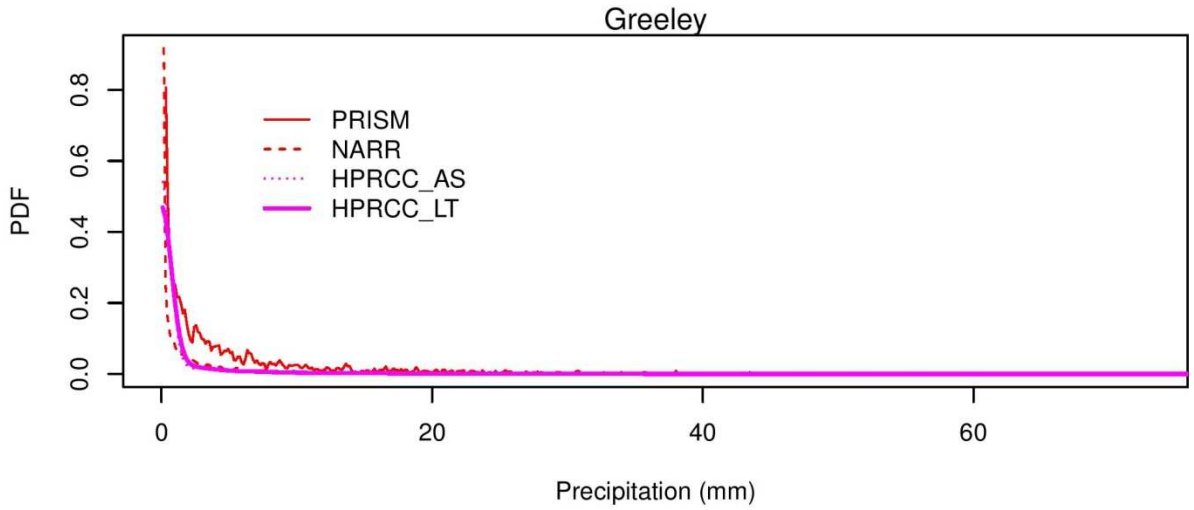


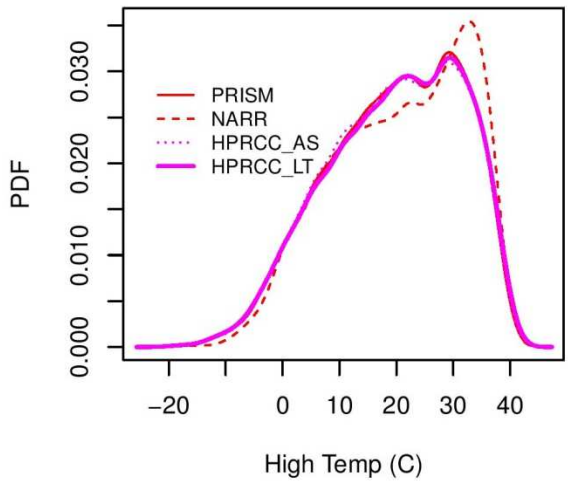


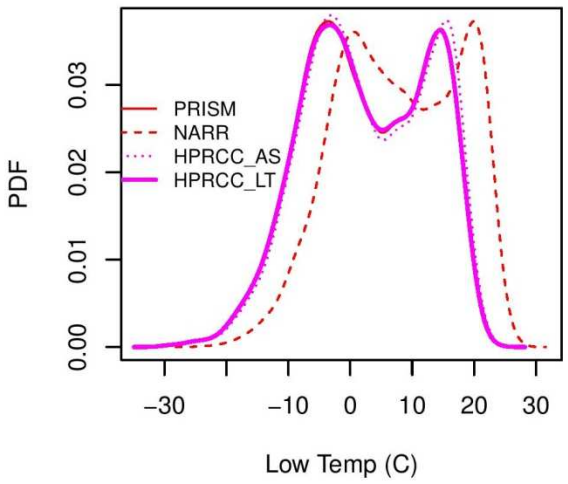


Probability distribution functions (PDF) of maximum and minimum temperature and precipitation for PRISM, NARR, and HPRCC datasets for Greely

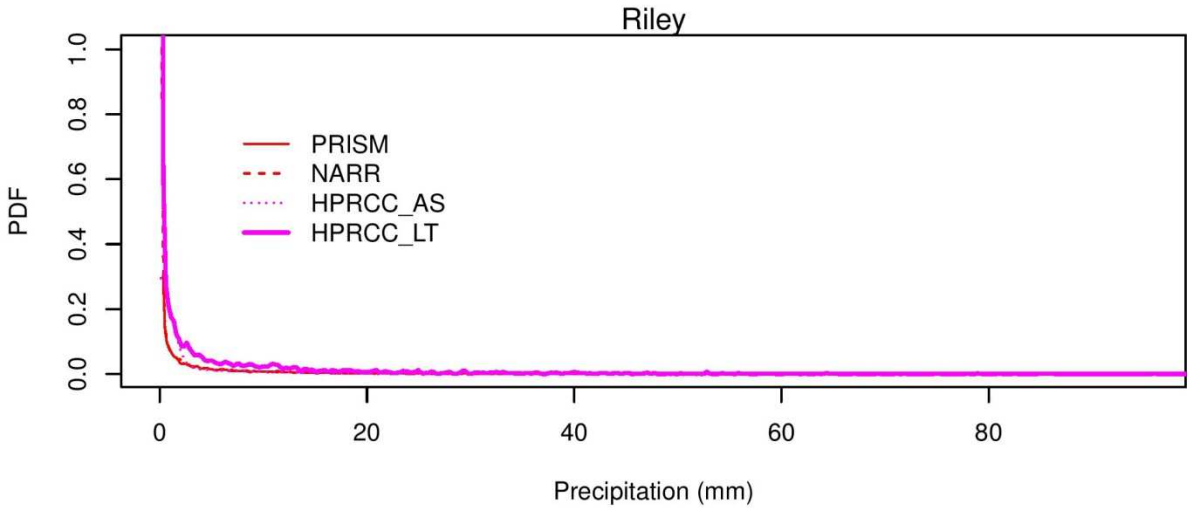


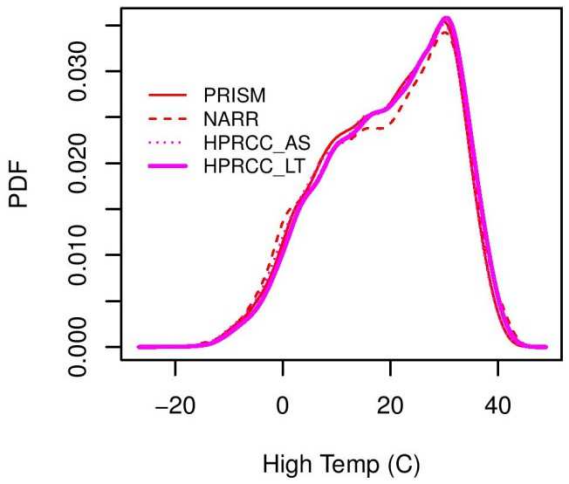


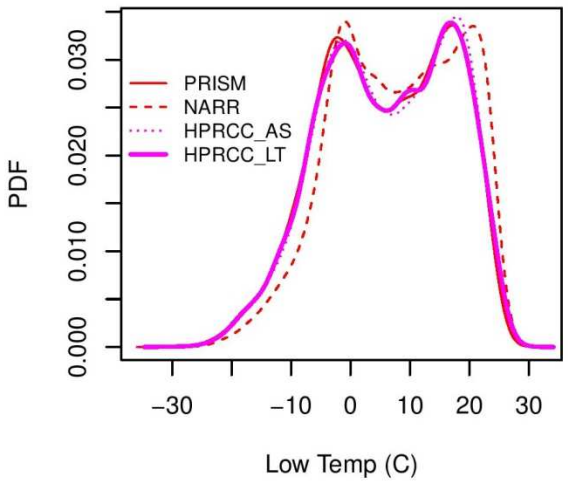


Probability distribution functions (PDF) of maximum and minimum temperature and precipitation for PRISM, NARR, and HPRCC datasets for Riley

## Appendix B: Seasonal Trends in Air Temperature and Precipitation in IPCC AR4 GCM Output for Kansas

Figure 1 and table III and IV have been used from Brunsell, N. A., Jones, A. R., Jackson, T. L. and Feddema, J. J. (2010), Seasonal trends in air temperature and precipitation in IPCC AR4 GCM output for Kansas, USA: evaluation and implications. Int. J. Climatol., 30: 1178–1193. doi: 10.1002/joc.1958

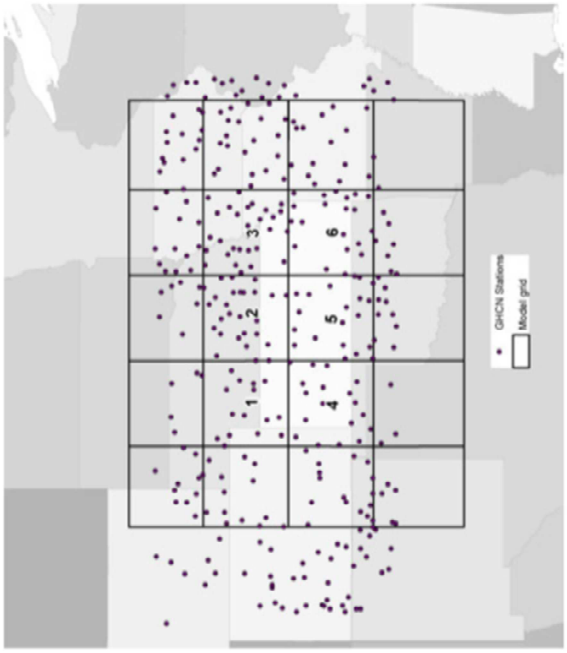


Figure 1. Depiction of global climate model grid cells and Global Historical Climate Network station locations used in this analysis. This figure is available in colour online at www.interscience.wiley.com/ioc

Table III. Linear precipitation trends (mm/year) and associated $r^2$ values.

| Grid Cell | Decadal | | Winter | | Spring | | Summer | | Fall | |
|---|---|---|---|---|---|---|---|---|---|---|
| | Trend | $r^2$ | Trend | $r^2$ | Trend | $r^2$ | Trend | $r^2$ | Trend | $r^2$ |
| GHCN (1950–2000) | | | | | | | | | | |
| 1 | 8.54E-2 | 0.00 | 5.86E-2 | 0.02 | 2.37E-2 | 0.00 | 1.38E-1 | 0.01 | 1.22E-1 | 0.02 |
| 2 | 5.47E-2 | 0.00 | −9.18E-2 | 0.02 | 1.76E-1 | 0.01 | −2.74E-2 | 0.00 | 1.62E-1 | 0.01 |
| 3 | −1.22E-1 | 0.00 | −3.37E-2 | 0.00 | −4.28E-2 | 0.00 | −4.94E-1 | 0.04 | 8.20E-2 | 0.00 |
| 4 | 1.86E-1 | 0.01 | 8.74E-2 | 0.04 | 1.94E-1 | 0.02 | 2.68E-1 | 0.02 | 1.97E-1 | 0.05 |
| 5 | 3.11E-1 | 0.02 | **2.27E-1** | **0.09** | **6.09E-1** | **0.10** | 1.39E-1 | 0.00 | 2.69E-1 | 0.03 |
| 6 | 4.33E-1 | 0.04 | **4.18E-1** | **0.11** | **6.54E-1** | **0.09** | 4.31E-2 | 0.00 | 6.16E-1 | 0.05 |
| GCM (1950–2000) | | | | | | | | | | |
| 1 | 1.86E-2 | 0.00 | 3.32E-3 | 0.01 | 1.70E-2 | 0.05 | 1.20E-1 | 0.27 | 2.00E-2 | 0.04 |
| 2 | 1.34E-2 | 0.00 | −1.36E-3 | 0.00 | 2.63E-2 | 0.15 | 9.08E-2 | 0.26 | 2.45E-2 | 0.20 |
| 3 | 1.20E-2 | 0.00 | 7.88E-4 | 0.00 | 5.32E-2 | 0.45 | 5.82E-2 | 0.12 | 2.44E-2 | 0.22 |
| 4 | −2.58E-2 | 0.00 | 2.36E-3 | 0.01 | −4.34E-2 | 0.17 | −4.94E-2 | 0.46 | 1.31E-2 | 0.03 |
| 5 | −2.45E-2 | 0.00 | −5.53E-3 | 0.02 | −2.12E-2 | 0.04 | 9.47E-5 | 0.00 | 8.16E-3 | 0.02 |
| 6 | −2.54E-2 | 0.00 | 8.71E-3 | 0.03 | 9.22E-3 | 0.01 | 1.23E-2 | 0.01 | 4.04E-3 | 0.01 |
| GCM (2010–2100) | | | | | | | | | | |
| 1 | −1.11E-8 | 0.17 | **3.41E-2** | **0.74** | −1.56E-3 | 0.00 | **−7.34E-2** | **0.65** | **−4.38E-2** | **0.65** |
| 2 | −9.08E-9 | 0.16 | **2.38E-2** | **0.52** | **3.60E-2** | **0.46** | **−7.18E-2** | **0.62** | **−4.76E-2** | **0.72** |
| 3 | −4.99E-9 | 0.12 | **2.37E-2** | **0.70** | **7.48E-2** | **0.82** | **−6.05E-2** | **0.53** | **−4.05E-2** | **0.46** |
| 4 | −1.69E-8 | 0.22 | 1.46E-2 | 0.28 | **−6.06E-2** | **0.59** | −8.44E-2 | 0.44 | **−4.79E-2** | **0.84** |
| 5 | −1.69E-8 | 0.23 | 3.56E-3 | 0.02 | −9.68E-3 | 0.03 | **−8.88E-2** | **0.61** | **−6.08E-2** | **0.81** |
| 6 | −1.70E-8 | 0.24 | −6.16E-3 | 0.04 | 2.03E-2 | 0.06 | **−8.64E-2** | **0.57** | **−5.49E-2** | **0.61** |

GHCN, Global Historical Climate Network; GCM, global climate model.

Table IV. Linear temperature trends (°C/year) and associated $r^2$ values.

| Grid Cell | Decadal | | Winter | | Spring | | Summer | | Fall | |
|---|---|---|---|---|---|---|---|---|---|---|
| | Trend | $r^2$ | Trend | $r^2$ | Trend | $r^2$ | Trend | $r^2$ | Trend | $r^2$ |
| GHCN (1950–2000) | | | | | | | | | | |
| 1 | 4.48E-3 | 0.00 | 6.92E-3 | 0.00 | 2.19E-2 | 0.07 | −1.13E-3 | 0.00 | −9.83E-3 | 0.02 |
| 2 | −1.54E-2 | 0.00 | −6.47E-3 | 0.00 | −2.51E-3 | 0.00 | **−2.18E-2** | **0.09** | **−3.08E-2** | **0.14** |
| 3 | 2.93E-3 | 0.00 | 7.11E-3 | 0.00 | 1.78E-2 | 0.04 | −1.26E-4 | 0.00 | −1.31E-2 | 0.03 |
| 4 | 1.29E-2 | 0.00 | 5.24E-3 | 0.00 | **3.21E-2** | **0.13** | −1.77E-3 | 0.00 | 1.60E-2 | 0.04 |
| 5 | 2.64E-3 | 0.00 | 3.63E-3 | 0.00 | 1.79E-2 | 0.04 | −8.60E-3 | 0.02 | −2.37E-3 | 0.00 |
| 6 | 4.59E-3 | 0.00 | 5.35E-3 | 0.00 | 1.37E-2 | 0.03 | 2.19E-3 | 0.00 | −2.88E-3 | 0.00 |
| GCM (1950–2000) | | | | | | | | | | |
| 1 | 2.99E-2 | 0.067 | **1.61E-2** | **0.88** | **1.53E-2** | **0.705** | **1.93E-2** | **0.852** | **2.03E-2** | **0.81** |
| 2 | 3.15E-2 | 0.067 | **1.66E-2** | **0.817** | **1.53E-2** | **0.639** | **1.86E-2** | **0.861** | **2.09E-2** | **0.78** |
| 3 | 3.37E-2 | 0.067 | **1.79E-2** | **0.828** | **1.55E-2** | **0.626** | **1.89E-2** | **0.882** | **2.18E-2** | **0.77** |
| 4 | 2.97E-2 | 0.066 | **1.48E-2** | **0.836** | **1.75E-2** | **0.774** | **2.22E-2** | **0.862** | **2.09E-2** | **0.82** |
| 5 | 3.05E-2 | 0.065 | **1.50E-2** | **0.78** | **1.64E-2** | **0.702** | **2.03E-2** | **0.854** | **2.12E-2** | **0.79** |
| 6 | 3.13E-2 | 0.065 | **1.56E-2** | **0.779** | **1.53E-2** | **0.666** | **1.92E-2** | **0.849** | **2.10E-2** | **0.76** |
| GCM (2010–2100) | | | | | | | | | | |
| 1 | 4.03E-2 | 0.131 | **3.59E-2** | **0.995** | **3.49E-2** | **0.985** | **4.67E-2** | **0.981** | **4.27E-2** | **0.984** |
| 2 | 4.16E-2 | 0.128 | **3.82E-2** | **0.995** | **3.53E-2** | **0.986** | **4.73E-2** | **0.979** | **4.31E-2** | **0.983** |
| 3 | 4.30E-2 | 0.125 | **4.07E-2** | **0.994** | **3.62E-2** | **0.987** | **4.75E-2** | **0.978** | **4.35E-2** | **0.982** |
| 4 | 4.06E-2 | 0.13 | **3.44E-2** | **0.995** | **3.79E-2** | **0.982** | **4.77E-2** | **0.981** | **4.39E-2** | **0.985** |
| 5 | 4.14E-2 | 0.128 | **3.57E-2** | **0.995** | **3.67E-2** | **0.982** | **4.86E-2** | **0.978** | **4.42E-2** | **0.983** |
| 6 | 4.18E-2 | 0.126 | **3.64E-2** | **0.995** | **3.55E-2** | **0.985** | **4.89E-2** | **0.979** | **4.37E-2** | **0.983** |

Bold indicates significant at $p < 0.05$

## Appendix C Weather Extraction R Code:

```
# Coded by Babak MardanDoost, final revised 7/9/2013
# Extracting Weather set from Netcdf files
# Input:
library(FNN)
library(ncdf)
library(foreign)
# reading the main coordinates of PRISM grid Cells
t<-read.csv("Weather_e_input\\XX-yy.csv", header = TRUE, sep = ",",  dec=".")
tgrid<-matrix(t[,1], nrow=179,ncol=73)
tfips<-matrix(t[,2], nrow=179,ncol=73)
tx<-matrix(t[,6], nrow=179,ncol=73)
ty<-matrix(t[,7], nrow=179,ncol=73)
ttx<-as.vector(tx)
tty<-as.vector(ty)
coor<-data.frame(ttx,tty)
# reading the target coordinates
counties<-read.dbf("Weather_e_input\\counties.dbf")
namet<-counties[,5]
name<- as.matrix(namet)
X<-counties[,10]
y<-counties[,11]
c_target<-cbind(X,y)
dayno=1
filename_tmin="Weather_e_input\\tmin_n.nc"
filename_date="Weather_e_input\\tmin_new.nc"
filename_prec="Weather_e_input\\prec_n.nc"
```

```
filename_tmax="Weather_e_input\\tmax_n.nc"
fdate <- open.ncdf(filename_date)
Time = get.var.ncdf( fdate, "Time")
Lat = get.var.ncdf( fdate, "Lat")
Lon = get.var.ncdf( fdate, "Lon")
ftmin <- open.ncdf(filename_tmin)
ftmax <- open.ncdf(filename_tmax)
fprec <- open.ncdf(filename_prec)
for (i in 1:105) {
lat_s<-c_target[i,1]
lon_s<-c_target[i,2]
## nn.index  an n x k matrix for the nearest neighbor indice.
## nn.dist  an n x k matrix for the nearest neighbor Euclidean distances.
## K=1, first nearest
 index<-get.knnx(coor,data.frame(lat_s,lon_s), k=1)$nn.index
 distance<-get.knnx(coor,data.frame(lat_s,lon_s), k=1)$nn.dist
 Vcol<-index%%179
 Vrow<-(index%/%179)+1
 Vcol<-((1-sign(index%%179))*179)+(sign(index%%179)*index%%179)
 Vrow<-((1-sign(index%%179))*(index%/%179))+(sign(index%%179)*((index%/%179)+1))
  N_Vrow<-Vrow #Vrow
gridid <-tgrid[Vcol,N_Vrow]
fipsid<-tfips[Vcol,N_Vrow]
info<-cbind(gridid,name[i],counties[i,],fipsid,Lat[74-N_Vrow],Lon[Vcol])
# IF using old PRISM data, use N_Vrow<-Vrow
# IF using Vesion2 PRISM data, use N_Vrow<-74-Vrow
tmin=get.var.ncdf(nc=ftmin,start = c(Vcol,74-N_Vrow, dayno),  count = c(1,1,14975))
tmax=get.var.ncdf(nc=ftmax,start = c(Vcol,74-N_Vrow, dayno),  count = c(1,1,14975))
prec=get.var.ncdf(nc=fprec,start = c( Vcol,74-N_Vrow, dayno),  count = c(1,1,14975))
# filter to zero all pec. below 1mm
```

```
prec_filter<-ifelse(prec<.99999,0,prec)
Weather<-cbind(Time,tmin,tmax,prec_filter)
fileinfo<-paste(getwd(),"/weather_e_output/",name[i],"_info",".csv",sep="")
filen<-paste(getwd(),"/weather_e_output/",name[i],".csv",sep="")
write.csv(Weather, file = filen)
write.csv(info,file=fileinfo)
print(filen)
}
close.ncdf(fdate)
close.ncdf(ftmin)
close.ncdf(ftmax)
close.ncdf(fprec)
```

## Appendix D Schematic of data preparation by water grouping tool

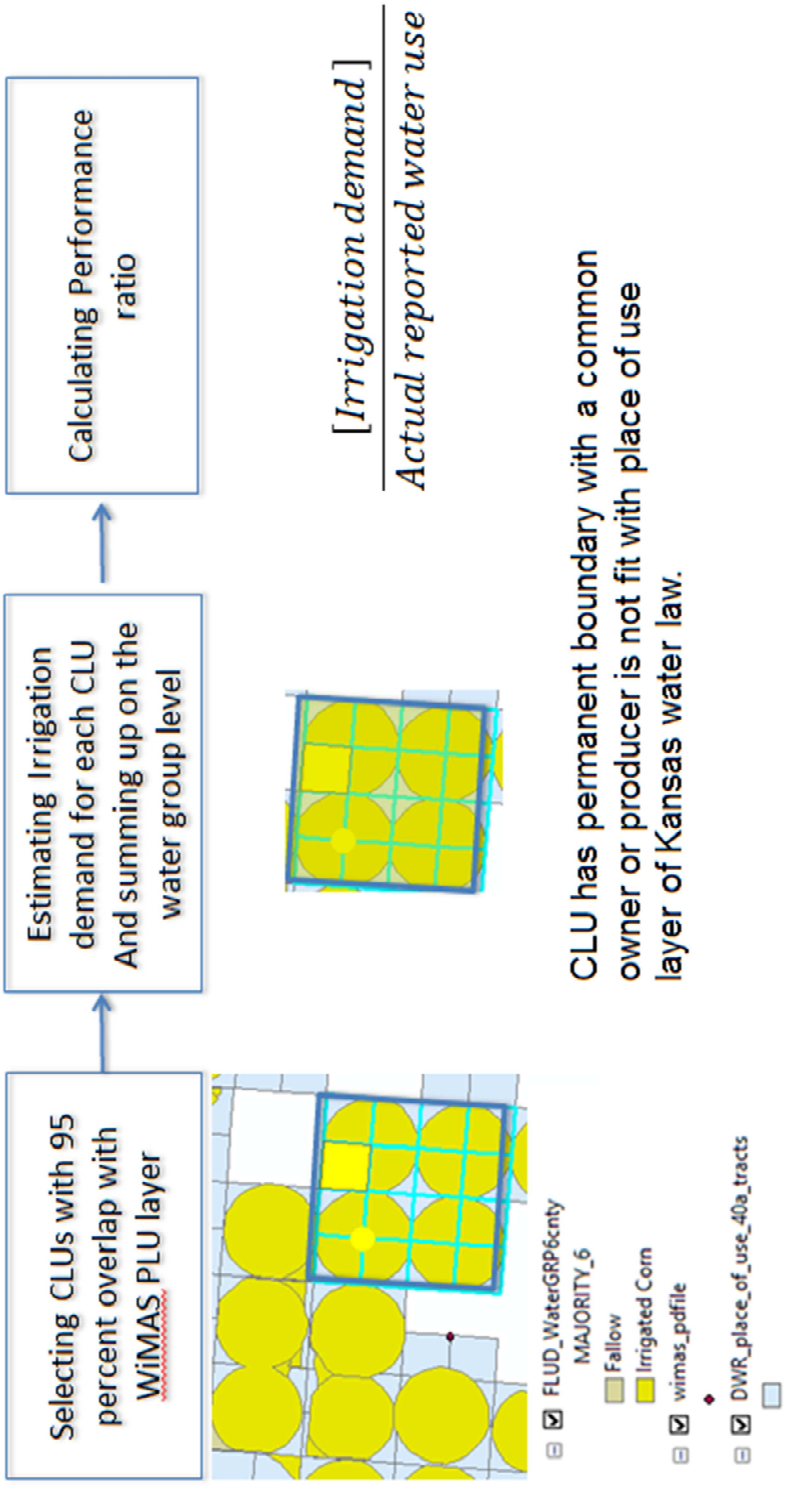

| OBJECTID_1 * | OBJECTID | sctfs | WR_GROUP | GRP_ACRES | TRGT_ACRES | OVLP_ACRES | OVLP_PCT | GRP_WR_CNT | GRP_PDIV_C |
|---|---|---|---|---|---|---|---|---|---|
| 20114 | 20114 | 20047000061100130 5 | 7741 | 160 | 128.850777 | 0.091125 | 0.000707 | 1 | 1 |
| 29222 | 29222 | 20047000061100130 5 | 11321 | 160 | 128.850777 | 128.759652 | 0.999293 | 1 | 1 |